Design, Synthesis, and Evaluation of Site-Specific Hsp90 Inhibitors

By:

Matthew J. Axtman

Submitted to the graduate degree program in Department of Medicinal Chemistry and the Graduate Faculty of the University of Kansas in partial fulfillment of the requirements for the degree of Master's of Science

Committee Members:

_____

Chairperson: Brian S. J. Blagg Ph.D.

_____

Dr. Michael Rafferty Ph.D.

_____

Dr. Paul Hanson Ph.D.

Date Defended: May 24, 2011

The Thesis Committee for Matthew J. Axtman certifies that

This is the approved version of the following dissertation:

Design, Synthesis, and Evaluation of Site-Specific Hsp90 Inhibitors

_____

Chairperson: Brian S. J. Blagg, Ph.D.

Date Approved: June 6, 2011

Design, Synthesis, and Evaluation of Site-Specific Hsp90 Inhibitors

Abstract

The heat shock protein 90 (Hsp90) family of molecular chaperones is responsible for the conformational maturation of nascent polypeptides and refolding of denatured proteins. Hsp90 is known to play an important role in the regulation of cell signaling, survival and proliferation, transforming it into a promising target for the treatment of several diseases, including cancer. Proteins associated with all six hallmarks of cancer, as described by Weinberg, are Hsp90 clients. Since these proteins depend upon Hsp90, its inhibition has the potential to simultaneously disrupt all six and halt the malignant progression using a single small molecule. Hsp90 is abundantly expressed in the cell and accounts for 1-2% of the total cellular protein, making itone of the most prevalent proteins in eukaryotic cells. The Hsp90 isoforms are responsible for the conformational maintenance of greater than 150 proteins. There are four distinct isoforms, including Hsp90α, Hsp90β, GRP94 and TRAP1. Hsp90α and β are located in the cytoplasm; Hsp90α is the major inducible form, while Hsp90β is the constitutively active form. In contrast, GRP94 is found in the endoplasmic reticulum and TRAP1 is located in the mitochondrial matrix.

Hsp90 exists as a homodimer consisting of an N- and C-terminal domain, connected by a middle domain. The Hsp90 N-terminus contains an ATP binding site, responsible for the ATPase activity of the chaperone associated with folding of clients. Small molecules that preferentially bind to this nucleotide binding site inhibit the ability of Hsp90 to properly fold polypeptides, ultimately tagging them for degradation through the ubiquitin-proteasome pathway. Natural product inhibitors of the N-terminal ATP binding site include the ansamycin antibiotic geldanamycin (GDA) and the macrocyclic lactone radicicol (RDC). Blagg and co-workers have previously reported the chimeric N-terminal inhibitor radamide, which combines the resorcinol

portion of RDC and the quinone portion of GDA through a flexible linker. Radamide manifests a slightly greater binding affinity for GRP94 (Kd = 0.52 μM) versus cytosolic Hsp90 (Kd = 0.87 μM). This phenomenon is elucidated by examining the unique binding conformations adopted by radamide when crystal structures of were obtained using each isoform. When bound to Hsp90, radamide exhibits a linear conformation, while when bound to GRP94 the quinone portion is bent towards a pocket that is not accessible in Hsp90α or β. By employing conformational constraint, it was proposed that the quinone portion of radamide could exhibit the bent conformation seen in the natural products and result in increased affinity for Hsp90 as well as selective binding to the cytosolic isoforms.

In contrast to radamide, a recent paper by Gasiewicz and co-workers examined the effects of flavones and (-)-Epigallocatechin-3-Gallate (EGCG), the major polyphenolic catechin found in green tea, on the aryl hydrocarbon receptor (AHR). Due to its diverse medicinal properties, EGCG has been proposed as a potential treatment for several diseases. The study by Gasiewicz revealed that EGCG functions through a different mechanism of action than the known flavone antagonists, interacting with the Hsp90 C-terminus rather than the AHR. It was confirmed that EGCG binds specifically to the C-terminal nucleotide binding site, either within or proximal to the site where the natural product novobiocin is thought to bind. Previous studies have determined that EGCG manifests an IC50 of ~150 μM against MCF-7 cells. Upon examination of an overlay of EGCG and novobiocin, the structural similarities of the coumarin and the catechin cores become apparent. It was proposed that design of molecules based on the structure–activity relationships established for novobiocin may result in Hsp90-specific inhibitors based upon the EGCG scaffold.

Acknowledgements

There are several people that I would like to thank for their support and guidance during my years in graduate school. Throughout the good and bad times, these people have provided me with great advice and discussed possible solutions to the problems I have encountered.

Firstly, I would like to thank my family for their support and encouragement. I would like to thank my mom and dad for helping me through the difficult times during graduate school. I would not have succeeded without your unwavering support. Also, I would like to thank my brother Nathan for helping me rise above adversity and cope when times were tough. Finally, I would like to thank Alison for all of your advice and help with everything for the past few years, you have helped me more than you know.

I would also like to thank my advisor, Dr. Blagg, for the patience, guidance and freedom that you have provided me. You offered me the ability to be creative when approaching problems, ultimately allowing me to expand my horizons.

I am also very grateful to many current and former Blagg lab members. Former co-workers James, Donna, Jared, and Geraldine provided friendship and were instrumental in teaching me various lab techniques and engaging in helpful discussions. Additionally, current co-workers Alison, Gary, Teather, Laura, and Adam have been good friends and I have enjoyed countless discussions and collaborative projects with these individuals during my graduate school years. I hope to remain close friends with many of you as we go our separate ways.

Outside of the Blagg lab, I would like to thank my committee members Dr. Rafferty and Dr. Hanson for their suggestions and guidance during my graduate school career. I would also like to thank Dr. Prisinzano, Dr. Timmermann, and Dr. Dutta for being great mentors and

List of Sections:

<div align="center">

Chapter 1

Hsp90 Background

</div>

Chapter 2

Cyclopropyl Derivatives of Radamide

Chapter 3

Development of (-)-Epigallocatechin 3-gallate (EGCG) as an Hsp90 Inhibitor

List of Figures:

Chapter 1

Hsp90 Background

Chapter 2

Cyclopropyl Derivatives of Radamide

Chapter 3

Development of (-)-Epigallocatechin 3-gallate (EGCG) as an Hsp90 Inhibitor

List of Schemes:

<div align="center">

Chapter 2

Cyclopropyl Derivatives of Radamide

</div>

<div align="center">

Chapter 3

Development of (-)-Epigallocatechin 3-gallate (EGCG) as an Hsp90 Inhibitor

</div>

List of Tables:

Chapter 1

Hsp90 Background

Chapter 2

Cyclopropyl Derivatives of Radamide

Chapter 3

Development of (-)-Epigallocatechin 3-gallate (EGCG) as an Hsp90 Inhibitor

Chapter 1

Hsp90 Background

I.   Introduction

The heat shock protein 90 (Hsp90) family of molecular chaperones is responsible for the maturation of nascent polypeptides and the refolding of denatured proteins. Hsp90 is known to play an essential role in regulation of cell signaling, proliferation and survival, which has transformed it into a promising target for the treatment of several diseases, including cancer.[1-3] Hanahan and Weinberg defined the six hallmarks of cancer as causative factors in developing malignancy. These hallmarks include: 1) self-sufficiency in growth signals, 2) insensitivity to antigrowth signals, 3) evasion of apoptosis, 4) limitless replicative potential, 5) sustained angiogenesis, and 6) tissue invasion/metastasis.[4] Hsp90 inhibitors allow for a first-in-class approach toward cancer by enlisting a single agent to functionally disrupt all six of these hallmarks through the targeting of a single Hsp90 protein.[5] Natural product inhibitors of Hsp90, including geldanamycin (GDA), radicicol (RDC), novobiocin, and epigallocatechin-3-gallate (EGCG), represent lead compound that are under investigation for drug development.

II.   Structure of Hsp90

The Hsp90 monomer consists of three distinct domains; the 12kDa C-terminal binding domain, 35 kDa middle domain connected through a charged linker to a 25 kDa N-terminal binding domain. The crystal structure of the yeast Hsp90 homodimer is shown in Figure 1.[6] In eukaryotic cells, Hsp90 is functional as a homodimer and each domain is responsible for distinct functions.[7-8] The C-terminus is responsible for through a bundle of four α-helixes.[9-10]

Additionally, it was discovered that the C-terminus contains a nucleotide binding site that exhibits non-ATPase functions, such as coordinating the exchange of N-terminal nucleotides in an allosteric manner. Novobiocin, EGCG, and taxol are natural products known to bind the C-terminal nucleotide binding site and prevent the binding of ATP to the N-terminus, resulting in inhibition of Hsp90. The C-terminus is also responsible for the coordination of partner proteins, most notably the Hsp70-Hsp90 organizing protein (HOP). Additionally, several Hsp90-associated partner proteins contain a tetratricopeptide repeat (TPR), that bind the Hsp90 C-terminal motif, MVEED, and mediate protein–protein interactions during the protein folding process.[11-12]
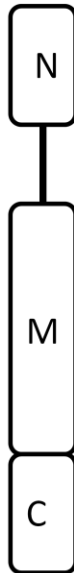
Figure 1 - Crystal structure of Hsp90

In contrast to the C-terminus, more is known about the Hsp90 N-terminus. Unlike the C-terminal nucleotide binding site, a co-crystal structure of the yeast Hsp90 N-terminus bound to ADP has been solved.[13] Nucleotide binding to this site revealed a unique bent conformation, which is only found in related enzymes. Members of this family include DNA gyrase, histidine kinase and MutL, which are members of the GHKL superfamily of proteins. The N-terminal ATP/ADP binding pocket contains a Bergerat fold, characterized by four mixed β-sheets and three α-helices, aligned to sandwich a β-sheet between the α-helices. The ATP binding site is formed by the amino acids on the conserved loops connecting the helices and sheets.[14] The

natural products GDA and RDC have been shown to compete with ATP for binding to this pocket and have been studied extensively as Hsp90 inhibitors.

Finally, the middle domain is a highly charged region that has been identified to associate with the majority of client proteins. This region is also the least conserved amongst species and isoforms.[15-16] Consistent with other members of the GHKL superfamily, Hsp90 has catalytic loop, which contains a key arginine residue (Arg 380) located in the middle domain that is essential for the ATPase activity *in vitro*. This conserved arginine residue functions by polarizing the β-γ-phosphodiester bond of ATP bound to the N-terminus, facilitating the hydrolysis of ATP to ADP.[10]

III.   Hsp90 Functions as a Molecular Chaperone

Molecular chaperones serve many important functions in eukaryotic cells. Chaperones prevent proteins from aggregating and can resolubilize aggregates as well. Moreover, they assist in the folding of nascent polypeptides and can also function in the refolding of damaged proteins.[17] Chaperones utilize an ATP-driven cycle of conformational changes, which are used to fold their targets.[18] Eukaryotic Hsp90 comprises approximately 1-2% of the total protein found in the cytoplasm during normal conditions, and can become significantly overexpressed during cellular stress.[5,19] Cellular stress can be defined as conditions that result in the accumulation of midfolded proteins resulting from elevated temperature, variation in pH, or nutrient deprivation, leading to induction of the heat shock response to fold those misfolded proteins.[1]

As the ribosome synthesizes single-stranded polypeptides, the amino acids have the propensity to spontaneously aggregate. Molecular chaperones are responsible for preventing this aggregation and folding these polypeptide strands into their tertiary and quaternary structures.

The folding process begins with Hsp70 in complex with ATP, and Hsp40 bound to the developing polypeptide. ATP is hydrolyzed to ADP, clamping Hsp70 to the polypeptide substrate to provide
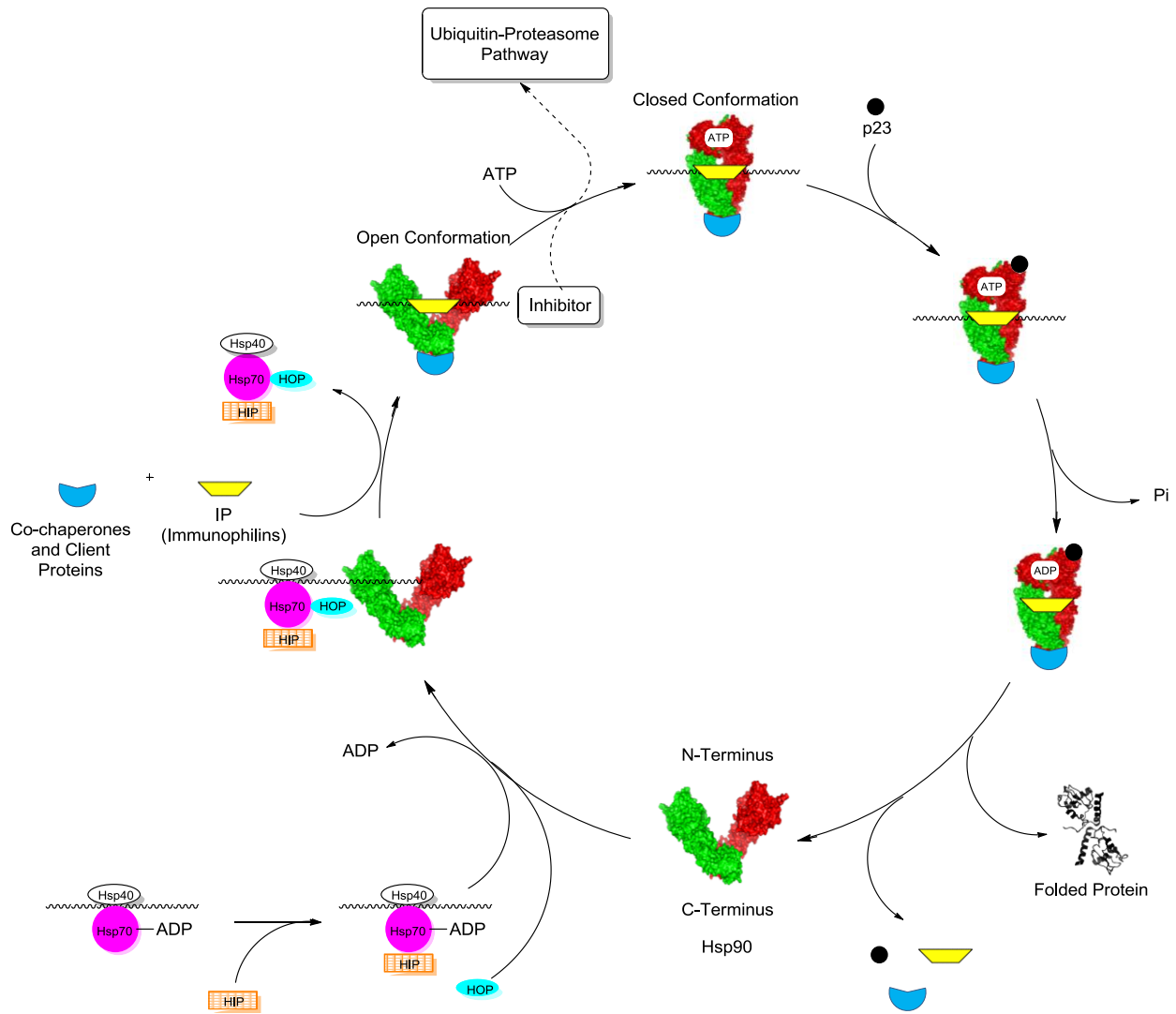
Figure 2 - Hsp90 folding process

stability and prevent aggregation.[17] Hsp70 interacting protein (HIP), binds to this complex and promotes interactions between Hsp70 and Hsp90 to facilitate peptide transfer to the Hsp90 homodimer. Bcl2-associatied athanogene (BAG) can promote dissociation of Hsp70/client

protein complexes through the exchange of ATP for ADP, resulting in polypeptide release from the complex.[20-21] Hsp90-Hsp70 organizing protein (HOP) recognizes Hsp90 through a TPR region and coordinates binding of the polypeptide-Hsp70 complex to Hsp90 forming a heteroprotein complex in the open conformation.[22] This promotes transfer of the unfolded substrate to Hsp90 and the dissociation of Hsp70, HIP and HOP.[23-24] Immunophilins and cochaperones bind to the binary complex, providing ATP the opportunity to occupy the N-terminus, promoting Hsp90 into the closed-clamped conformation around the polypeptide substrate.[25] Competitive inhibitors bind to the N-terminus and prevent Hsp90 from obtaining its closed conformation, ultimately destabilizing the protein complex, which leads to degradation via the ubiquitin-proteasome pathway. In the absence of an inhibitor and in the presence of ATP the protein folding cycle continues through binding of cochaperone p23 to the ATP bound complex, which stimulates the hydrolysis to ADP. The protein complex then folds the linear polypeptide into its intact three dimensional structure, through an uncharacterized process, which is ultimately released. Dissociation of the cochaperones and immunophilins allows the N-terminus to open and allows the cycle to repeat. Figure 2 represents a simplified paradigm for the protein folding cycle, highlighting the central interactions described above.

IV.   Applications for Hsp90 Inhibitors

Hsp90's primary function as a molecular chaperone is to properly fold polypeptides or proteins that are misfolded and unable to function properly. This mechanism can be exploited for development of drugs targeting multiple disease states.[26] Hsp90 is responsible for folding nascent polypeptides, in addition to assisting in the solubilization and refolding of aggregated or denatured proteins. Through development of small molecules possessing a cytotoxic profile, a

blockage of the intact Hsp90-client protein complex ensues, preventing the maturation of bound polypeptides. This blockade disrupts the folding cycle and ultimately targets the protein complex for ubiquitin-proteasome degradation.[27-28] A compound that exhibits a cytotoxic profile possesses the potential for the treatment of cancer through disruption of multiple signaling pathways.[29] In contrast, non-toxic molecules that induce Hsp90 provide increased levels of chaperones, allowing for the refolding of aggregated and denatured proteins.[30-31] Molecules possessing these non-toxic activities belong to a class of molecules that may be used for the treatment of neurodegenerative diseases.

A. Cancer Therapeutics

Traditional therapeutic strategies for cancer have focused on the inhibition of specific oncogenic receptors and enzymes. In 2000, Hanahan and Weinberg defined the six hallmarks that need to be manifested through cellular proteins, enzymes and receptors that can
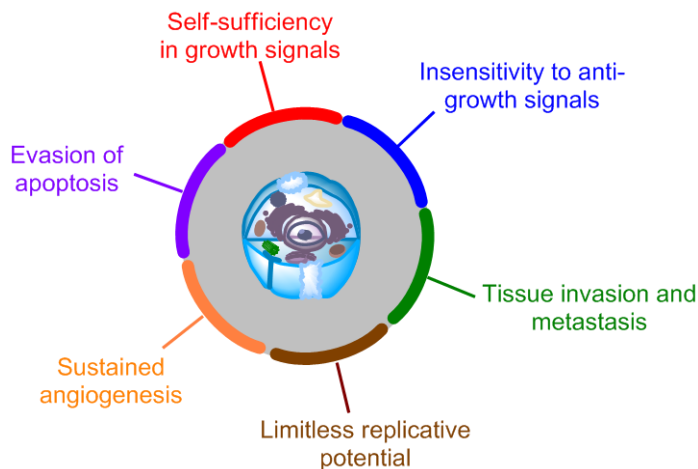
Figure 3 - The six hallmarks of cancer

become hijacked by malignant cells to be classified as cancerous (Figure. 3).[4] Many cancer therapeutics have been successfully developed to target a specific protein or enzyme associated with the hallmarks of cancer, however none have demonstrated the ability to inhibit all six simultaneously. The Hsp90 protein folding machinery has been shown to be critical for the manifestation of all six hallmarks (Table 1), which allows for a single Hsp90 inhibitor to simultaneously disrupt all six hallmarks.[5,32] To date, no other cellular target has exhibited the

ability to inhibit all six hallmarks simultaneously, which has allowed Hsp90 to become one of the most sought after cancer targets yet identified.

Table 1 - Hsp90 client proteins that are associated with the six hallmarks of cancer

Hallmark	Client Protein(s)
Self-sufficiency in growth signals	Raf-1, AKT, Her2, MEK, Bcr-Abl
Insensitivity to anti-growth signals	Plk, Wee1, Myt1, CDK4, CDK6
Evasion of apoptosis	RIP, AKT, mutant p53, c-MET, Apaf-1, survivin
Limitless replicative potential	Telomerase (h-Tert)
Sustained angiogenesis	FAK, AKT, Hif-1α, VEGFR, Flt-3
Tissue invasion/metastasis	c-MET

Hsp90 inhibitors have shown significant differential selectivity toward malignant cells compared to normal cells at concentrations that are nontoxic to animals.[33-35] There are currently three mechanisms that have been postulated to explain the selectivity of Hsp90 inhibitors for transformed cells. First, the over-expression of Hsp90 is directly related to malignant cells attempting to compensate for the upregulated amount of client proteins required for constant growth.[36-37] The second mechanism is based on an idea by researchers at Conforma Therapeutics, wherein the intact Hsp90 homodimer's affinity for ATP compared to the individual monomers. Malignant cells overproduce mutated and overexpressed proteins and force Hsp90 to maintain its intact homodimer form. In contrast, Hsp90 in normal cells shows a higher affinity to maintain the monomer form. Inhibitors are able to bind Hsp90 with greater affinity than ATP thus allowing for selective binding to malignant cells over normal cells.[2] The final mechanism is based on a physiochemical explanation, where lysosomal pH under normal

conditions is around 4 or 5. Traditionally, Hsp90 inhibitors possess basic nitrogens, which are protonated in the lysosome of a cell, and through a process known as pH partitioning these protonated molecules can either be released to the cytoplasm or sequestered in the lysosome.[38] By trapping the inhibitors in the lysosome, inhibitors cannot bind Hsp90 which is found predominately in the cytosol. The lysosome of a malignant cell's pH is neutral which does not protonate basic nitrogens and results in distribution into the cytosol at higher concentrations, allowing the inhibitor to target Hsp90.[39-40]

B. Neuroprotective Agents

The accumulation of misfolded proteins can lead to neurodegenerative diseases such as Alzheimer's, Parkinson's, and Huntington's which can be characterized by plaque formation.[41-42] The function of molecular chaperones can be exploited for the treatment of various neurodegenerative diseases, where these plaques may be removed or disaggregated. Alzheimer's disease is caused through formation of β-amyloid (Aβ) plaques and hyperphosphorylation of the Tau protein, which leads to the aggregation of neurofibrillary tangles.[43]
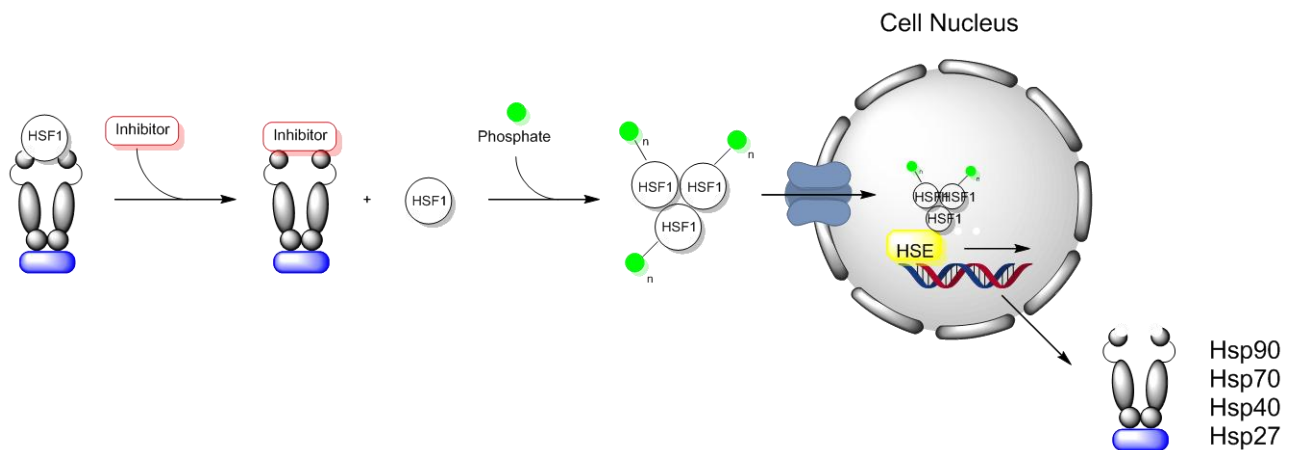
Figure 4 - Hsp90 inhibitors function for treatment of neurodegenerative diseases

Through inhibition of Hsp90, Heat Shock Factor-1 (HSF-1) is released from the intact multiprotein complex, wherein it trimerizes, becomes hyperphosphorylated and translocates to the nucleus and binds to multiple heat shock elements (Figure 4).[44-46] Binding of these heat shock elements, results in the translocation of Hsp90, Hsp70, Hsp40 and Hsp27, producing the heat shock response. This effect allows for modulation of Hsp90 to be used as a potential target for the treatment of neurodegenerative diseases.[47] A study conducted by Dou and coworkers showed that the N-terminal inhibitor, GDA, manifested increased levels of soluble phosphorylated tau and a decrease in aggregated tau tangles.[48] Studies have also demonstrated that using GDA for treatment of neurodegenerative diseases exhibits minimal toxicities, which has been a limiting factor in the development of GDA as an anti-cancer drug.[47,49]
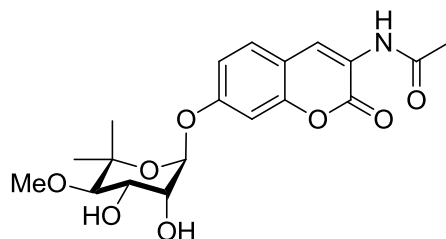
Figure 5 - Neuroprotective novobiocin analogue A4

The use of GDA for a treatment for neurodegenerative diseases remains a tool for researchers, because GDA exhibits a cytotoxic profile with a small therapeutic window. This allows efforts to be focused on the development of other Hsp90 modulators that eliminate the toxicity from the drug profile. The novobiocin analogue A4 (Figure 5), developed in the Blagg Laboratory, has shown great promise as a neuroprotective agent and does not manifest cytotoxicity in assays up to 100 μM.[50] Hsp90 provides a novel target for neuroprotection, through the induction of the heat response, and appears able to slow/halt/reverse the progression some of these diseases.

V.   Natural Product Inhibitors of Hsp90

Targeting ATP binding sites is a common practice for medicinal chemists and has lead to the development of many therapeutics.[51] As stated above, ATP binds the N-terminus of Hsp90 in a unique bent conformation that is present in the GHKL superfamily of proteins. This unique binding site allows for selective structural features to be designed into Hsp90 inhibitors. Clinical trials for select Hsp90 inhibitors have shown potency, but the toxicities and side effects from the compounds have become a limiting factor. Dose dependant hepatotoxicity and gastrointestinal toxicities are hindering preclinical development of GDA and associated analogues.[52] Natural selection and stresses placed on organisms require they develop a defense to these stresses, resulting in an organism developing highly specific and effacious compounds. These compounds show a vast variation of scaffolds but still bind to a specific binding site, which allows for medicinal chemists a diverse set of tools for development of Hsp90 inhibitiors.[53]

A. Geldanamycin and Derivatives

GDA   17-AAG   17-DMAG
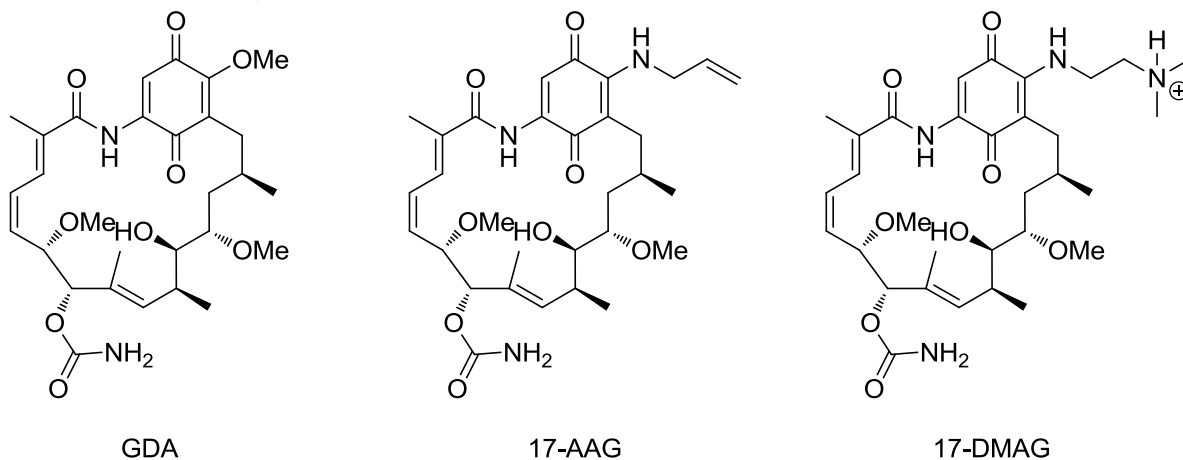
Figure 6 - Geldanamycin and related analogues

Geldanamycin (Figure 6), a naturally occurring ansamycin was originally discovered in 1970. Although fermentation of *Streptomyces hygroscopicus*, allows GDA to be produced in

multigram quantities the first total synthesis was not accomplished until 2002.[54-55] This work produced by Andrus and coworkers yielded a mixture GDA and (-)-*o*-Quinogeldanamycin in low yields.[56] GDA was initially evaluated in various antimicrobial assays and it showed good activity against *Alternizaria, Pythium, Botrytis* and *Penicillium* with a minimal inhibitory concentration (MIC) of 2mg/mL against *Tetrahymena pyriformis*.[54] Further testing demonstrated GDA expressed anti-proliferative activity against a wide range of tumor cell lines.[57] It was originally believed that GDA's anti-proliferative activity was manifested through direct inhibition of a tyrosine kinase, v-Src, which modulates general signaling pathways that regulate the growth and proliferation of cancer cells.[58] Upon further evaluation it was determined that GDA was inactive against purified v-Src protein, suggesting that it was manifesting its activity through an alternate mechanism.[59] Whitesell and Neckers determined that GDA binds Hsp90 through affinity purification and determined that the effects observed for v-Src was the result of downstream properties manifested through inhibition of Hsp90.[60]

The first co-crystal structure of GDA to Hsp90 was reported by Stebbins and coworkers wherein GDA was thought to bind to client protein binding site.[61] Fortunately, additional studies revealed that upon GDA binding to Hsp90 directly affects ATPase activity, suggesting to competitive inhibition of the ATP binding pocket. A second co-crystal structure published in 1997, correctly identified GDA binding to the ATP binding pocket.[13] Interestingly, this structure identified two key features that have become significant in the drug discovery efforts to determine structure-activity relationships (SAR). The first key feature was that GDA binds Hsp90 in a unique bent conformation and contains a *cis*-amide bond, which has been isomerized from the *trans*-conformation present in its native structure.[62] This changes the shape of GDA from the less rigid, flat conformation to the conformationally rigid bent conformation observed

in the co-crystal structure. The second key feature is that GDA binds Hsp90 in such a manner that allows the quinone moiety to project towards the surface of the protein, which allows for modifications to the 17-position without the loss of inhibitory activity.[13,62]

Further *in vivo* studies with GDA have shown that the quinone ring appears to be directly associated with some of the toxicity associated with the molecule. The quinone participates in redox cycling, allowing for the release of superoxide and semiquinone radicals upon exposure to cytochrome P450 reductase.[63] Additionally, the labile nature of the methoxy substituent at the 17-position of GDA has been implicated in the hepatotoxicity.[64] The 17-position projects away from the binding pocket, allowing substitution at this location without effecting GDA's affinity for Hsp90.[13,65] Therefore, analogues were designed to incorporate electron rich substituents at the 17-position that decrease the electron deficient nature of the quinone, which allows for an increased stability.[66] The most potent analogue identified was 17-(allylamino)-17-demethoxygeldanamycin 17-AAG (Figure 6). Although 17-AAG showed an improvement over GDA, 17-AAG exhibited poor solubility, suggesting additional analogues were needed to improve aqueous solubility. In 2004, Kosan Biosciences reported 17-DMAG (Figure 6), through incorporation of a tertiary ammonium group. The ammonium group is protonated at physiological pH, which increases solubility and allows for the potential of oral administration.[52,67]

B. Radicicol and Related Analogues
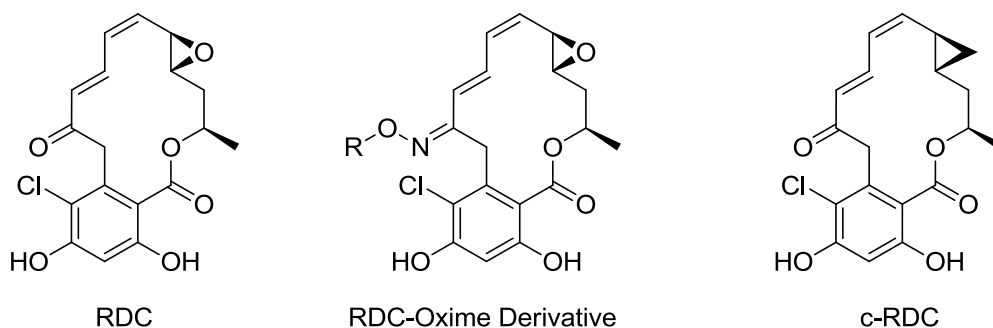
Figure 7 - Radicicol and related analogues

Radicicol (RDC) is a 14 membered macrolide originally isolated in 1953 from *Monosporium bonorden* and used as an antifungal agent (Figure 7).[68] In similar fashion to GDA, RDC was believed to bind v-Src specifically, although further studies showed its ability to suppress the transformation of oncogenes.[69] Additionally, RDC has been shown to be the most potent natural product inhibitor of Hsp90, functioning as a competitive inhibitor of the N-terminal ATP binding pocket.[65] In 1998, Nakano and coworkers demonstrated the ability of radicicol analogues to bind Ras and Src transformed cells, which relates directly to Hsp90 inhibition, and suppression of the ATPase activity.[70]

A co-crystal structure of RDC bound to Hsp90 shows a similar conformation to the native structure of RDC alone, which is an inflexible ring system that allows for binding to both the activated and unactivated forms of Hsp90 with equal affinity.[65] Although RDC exhibits a strong affinity for Hsp90 against purified protein, manifesting an IC_{50} of 23 nM, it unfortunately does not manifest any activity *in vivo*. RDC's activity *in vivo* is a consequence of the $\alpha,\beta,\gamma,\delta$-unsaturated carbonyl and electrophilic epoxide ring, which will be converted to various inactive metabolites.[71] Further investigation of the crystal structure shows the resorcinol ring to bind deep into the ATP binding pocket, establishing essential hydrogen bonding interactions. The phenol at

the 3-position provides a hydrogen bond with Asp79 and a water molecule that mimics the key interactions observed in the co-crystal structure with adenine. Additionally, the phenol at the 5-position forms a hydrogen bond with Leu34 and the chlorine appears to partially fill a hydrophobic cavity.[65,72]

SAR studies have shown through synthetic modification that the *in vivo* metabolism can be minimized through reduction of its electrophilic nature. The synthesis of compounds that replace the α,β,γ,δ-carbonyl for an oxime maintain potent anti-proliferative activities, and continue to induce degradation of Hsp90 dependent client proteins (Figure 7).[73-75] Danishefsky and coworkers developed a synthesis that allowed for the preparation of multiple analogues, which led to the first SAR studies between Hsp90 and RDC. This study identified that the orientation of the macrocycle needs to maintain the conformation observed in the natural product for inhibitory activity.[76] Removal of the electrophilic epoxide for a structurally similar cyclopropyl resulted in retention of activity, highlighting the conformation of the macrocycle is more important than hydrogen bonds formed by the epoxide shown in figure. 7.[76]

C. Novobiocin and Analogues
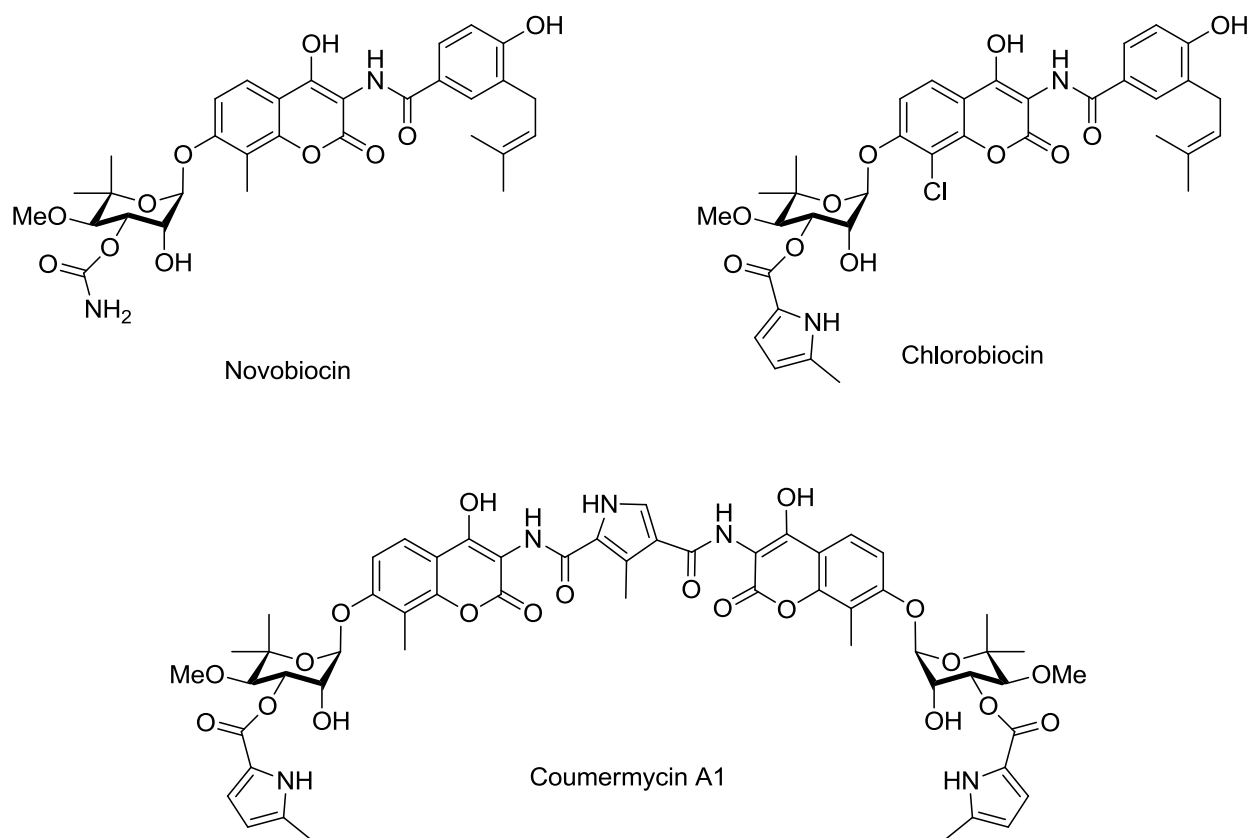
Figure 8 - Novobiocin and various natural product inhibitors of Hsp90 C-terminus

The coumermycin family of antibiotics has been used for their ability to inhibit type II topoisomerases including DNA gyrase, which is a member of the GHKL superfamily.[14] The coumermycin antibiotic family includes novobiocin, chlorobiocin and coumermycin A1 (figure 8), all of which have been isolated from various strains of *spreptomyces*.[77-80] Neckers and co-workers identified novobiocin to bind a previously unidentified C-terminal binding pocket, although the affinity was relatively weak, and inducing the degradation of the Hsp90 client proteins at ~700 μM in SKBr3 cells.[81-82]

Novobiocin is composed of three distinct regions: the benzamide side chain, the coumarin core, and the noviose sugar. Each of these regions can be modified chemically, which allows for the development of analogues to probe for specific SAR at each location. Initial SAR studies conducted by the Blagg Laboratory revealed several structural features that are critical for manifesting the observed activities. The synthesis of A4 (Figure 5) showed that truncation of the benzamide side chain, removal of the 4-hydroxy substituent, and modification to the noviose sugar results in a 70 increase in activity.[83] This result led to the development of an additional set of natural products, DHN1 and DHN2, which confirmed that lacking the compounds 4-hydroxyl group and 3'carbamate facilitate Hsp90 inhibition.[84] Further SAR studies showed the benzamide side chain is required for cytotoxicity, and that a hydrogen bond acceptor in the *meta* or *para* positions, or an aryl side chain were the most effective.[85] These studies also showed that incorporation of a heterocyclic side chain is well tolerated and can actually be used to increase solubility.[85] To date the Blagg laboratory has produced many compounds that manifest IC_{50} values in the low to mid nanomolar range.

D. Epigallocatechin-3-gallate (EGCG)
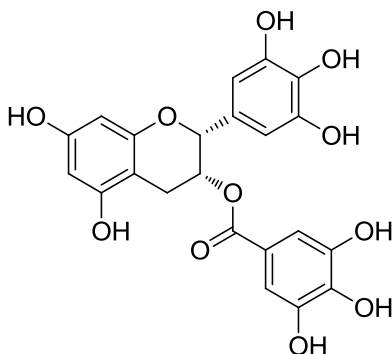
Figure 9 - Structure of Epigallocatechin-3-gallate

EGCG (Figure 9), is the main polyphenolic compound extracted from green tea.[86-87] In 2003 Palermo and coworkers attributed the anticancer effects of EGCG to the Aryl Hydrocarbon Receptor (AhR). AhR is a ligand-activated transcription factor, which upon binding translocates to the nucleus, dimerizes with the AhR nuclear translocator protein (ARNT) and promotes transcription.[86,88-89] Follow-up studies using affinity chromatography showed that EGCG did not directly inhibit AhR, instead they determined that EGCG binds the Hsp90.[90] Truncation of Hsp90 showed that the C-terminus binds to immobilized EGCG, suggesting that binding occurs in the ATP binding site similar to novobiocin.[7,90]

EGCG is composed of three distinct regions: the catechin core, the gallate side chain, and the aryl linked side chain. The majority of the SAR developed for the EGCG scaffold has focused on removal of various the various phenols, resulting in modest changes in biological activity.[91-93] These studies elucidated that removing phenols generally decreases the anti-proliferative activity against several biological targets.[93] A more thorough study that investigates significant modifications to other structural moieties is required to better define SAR for the EGCG core. It is proposed that studies of this type will transform EGCG into a lead structure for development of anti-cancer therapeutics.

Chapter 2

Cyclopropyl Derivatives of Radamide

I.   Introduction

The development of N-terminal Hsp90 inhibitors has been facilitated by rational drug design, which enables the observation of interactions that natural product inhibitors make with the protein.[94] There are currently several research groups targeting the Hsp90 N-terminus using small molecule inhibitors.[95-97] As discussed in Chapter 1, examination of the binding orientation of the endogenous ligand, ATP, and natural product inhibitors, GDA and RDC, reveals that they bind in a similar, but unique, bent conformation. This bent conformation is specific to the GHKL superfamily of proteins, which is comprised of DNA Gyrase, Histidine kinase, Hsp90, and MutL.

Key hydrogen bonding interactions are made by known inhibitors with distinct areas of the ATP binding pocket. For example, the majority of contacts made by GDA are due to the quinone occupying the same space as of the phosphate group of ATP. In contrast, the resorcinol of RDC binds deep into the ATP binding pocket and mimics the purine core. It was hypothesized that fusion of the active moieties of GDA and radicicol into one chimeric molecule would allow for an increase in Hsp90 affinity due to capitalization of both sets of interactions. This hypothesis was tested by Clevenger and co-workers through the development of radamide (figure 14), a hybridized small molecule that demonstrated low micromolar anti-proliferative activity due to Hsp90 inhibition. The co-crystal structure of radamide bound to Hsp90 demonstrated that the flexible linker maintained a linear conformation, thus preventing the quinone to rotate into the phosphate pocket. The use of conformational constraint to insert a predisposed bent conformation into the molecule through incorporation of a *cis*-cyclopropyl linker was proposed

to achieve this goal. It was hypothesized that biasing the linker with this structural modification would orient the quinone of radamide directly into the phosphate pocket.

The majority of research in the Hsp90 field has focused on development of inhibitors that target Hsp90, without any focus on the differences among the various protein isoforms. Emerging research that explored the unique binding pockets of Hsp90α and β in direct comparison to Grp94 has allowed for the development of isoform-specific inhibitors. Examination of the various binding pockets has shown that the movement of a lysine residue enables access to a new hydrophobic pocket in Grp94 by us. In contrast, the phosphate binding pocket of Hsp90α, which is larger and less exclusive, the corresponding pocket in Grp94 is constricted, which restricts binding to this pocket. The *cis*-cyclopropyl radamide analogues take advantage of differences between the phosphate binding pockets, allowing for binding to the α-isoform selectively and development of first-in -class Hsp90β-selective inhibitors. The design, synthesis and evaluation of radamide-based inhibitors containing a *cis*-cyclopropyl linkage are discussed herein.

II.   Comparison of Hsp90 Crystal Structures

Co-crystal structures of several natural product inhibitors of the Hsp90 N-terminus bound to Hsp90 have been solved. The co-crystal structure of ADP bound to Hsp90 shows the conformation of the ligand in the binding pocket and can be used to develop small molecule inhibitors that capitalize on those interactions. As shown in Figure 10, the N-terminal binding pocket is comprised of two distinct subpockets, one that binds the purine base and the other, which is the phosphate binding region.
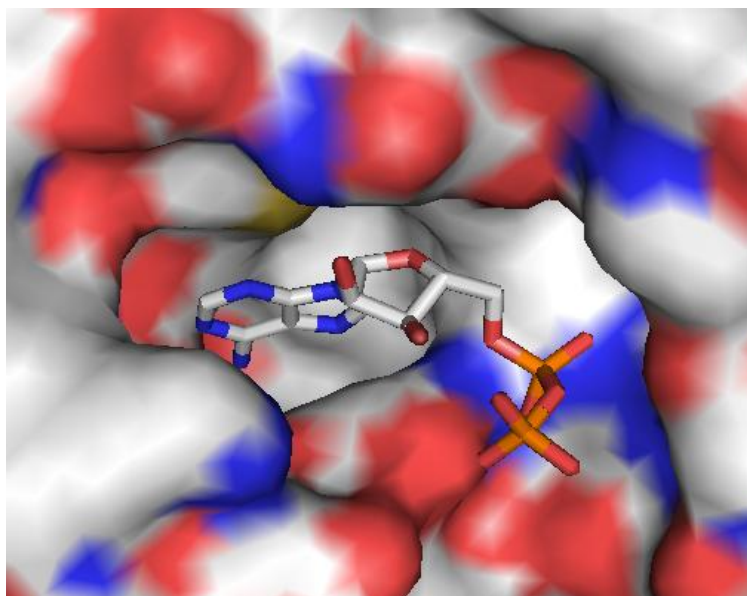
Figure 10 - Identification of the Hsp90 N-terminal ATP binding site

As described in Chapter 1, this ATP binding site contains a Bergerat fold, which forms a pocket behind the α-helix and allows the purine base of ADP to bind within this cavity. The second pocket is an extended purine pocket, but is located on top of α-helix. This region is oriented to accommodate the unique bent conformation of inhibitors, enabling them to bind Hsp90 with high affinity and establish interactions with the purine pocket and the α-helix.[62,65] Additionally, co-crystal structures highlight specific interactions made between the protein and ligand. The natural products GDA and RDC exhibit good affinity for Hsp90, manifesting K_D values of 1215 μM and 19 μM, respectively.[60,69-70]

A. Hsp90 Co-crystal Structure with ADP

In 1998 Obermann and co-workers reported the co-crystallization of Hsp90 in the presence of ATPγS, which yielded the structure of ADP bound to the N-terminal domain of human Hsp90. This structure identified two key features about the N-terminus. First, it was

determined that ADP shares a binding pocket with GDA, indicating a conserved ATP binding site. Second, solving this co-crystal structure confirmed that ADP, rather than ATP, was bound to the active site, indicating that the γ-phosphate is hydrolyzed.[98]
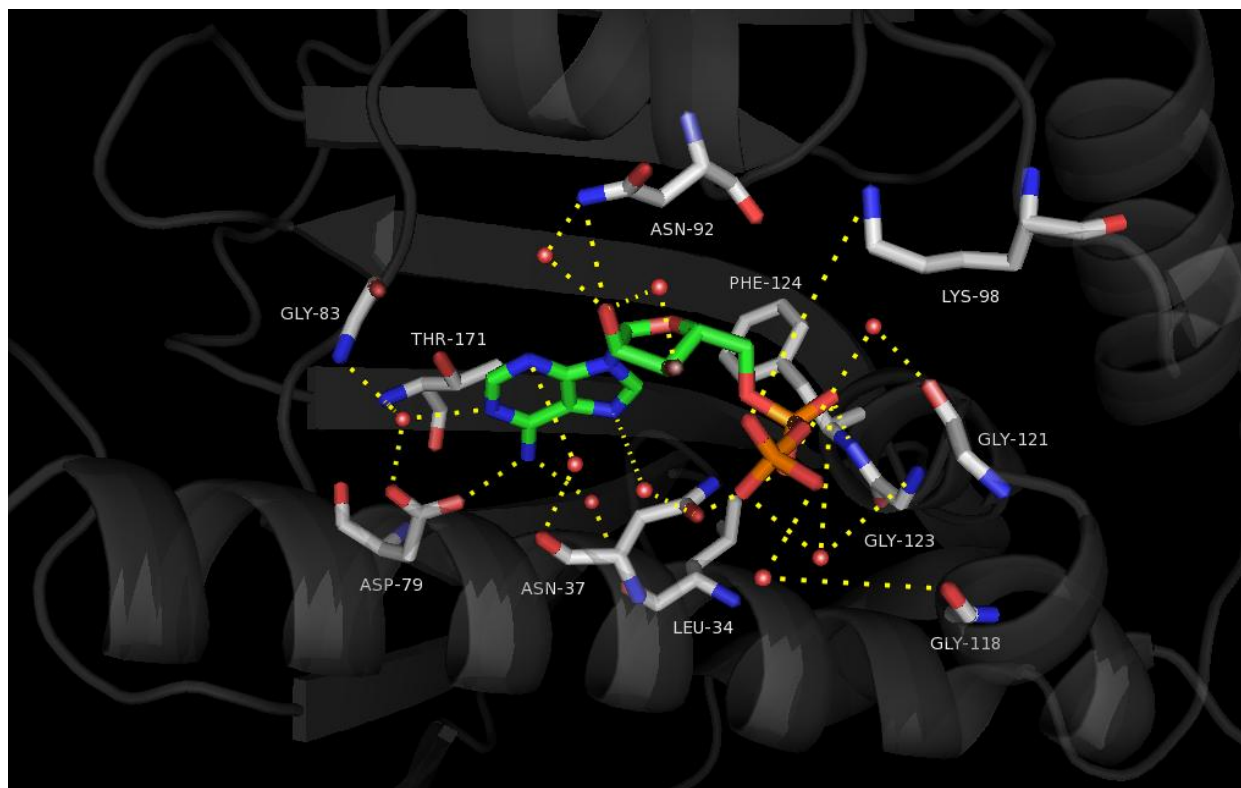
Figure 11 - Key hydrogen bonds made between ADP and Hsp90

As seen in Figure 11, the purine base binds deep into the N-terminal ATP pocket. Adenosine interacts with yeast Hsp90 through an intricate network of hydrogen bonds, both directly and indirectly through water-mediated interactions. Key interactions of adenosine with Hsp90 are made by the nitrogen at the 1-position bonding through a conserved water molecule to Gly83, Asp79 and Thr 171. Moreover, the nitrogen at the 6-position exhibits a direct hydrogen bond with Asp93, in addition to water-mediated hydrogen bonds with the backbone of Leu34. The 7-position of the adenine ring also forms water-mediated hydrogen bonds directly with the

Hsp90 backbone at Asn92.[65,98-99] While the adenosine base projects down into the pocket, the sugar and phosphate portion of ADP project outward into a solvent-exposed region of the protein. The hydroxyl group at the 2-position on the ribose sugar interacts directly with Asn37, while the hydrogen on the 3-position hydroxyl group bonds through a conserved water molecule. Finally, the phosphate region of ADP binds to a small groove found in the phosphate binding region along the α-helix of Hsp90. The α-phosphate interacts directly with Phe124, while Gly121 and Gly 123 interact through a conserved water molecule. The β-phosphate interacts directly with Lys96 and Asp40, while also interacting through water-mediated hydrogen bonds to Gly123 and Gly118.[98-99]

Investigation into the binding orientation of ADP shows that it displays the unique bent conformations previously described. The adenine base binds deep into the pocket, which allows the phosphate region to curl around top of the α-helix. As discussed in Chapter 1, this binding orientation mimics that adopted by other members of the GHKL superfamily and N-terminal inhibitors.[14]

B. Hsp90 Co-crystal Structure with Geldanamycin
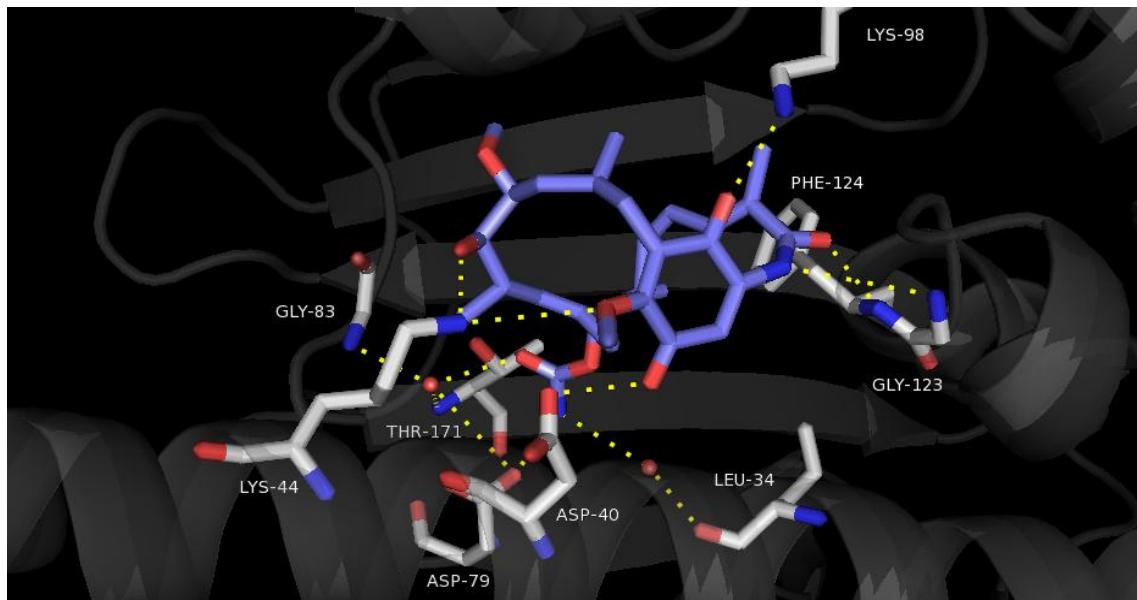
Figure 12 - Hydrogen bonds made between GDA and Hsp90

In 1997, Stebbins and co-workers were able to solve the co-crystal structure of GDA bound to yeast Hsp90. As seen in Figure 12, GDA binds within the N-terminal Hsp90 binding site in a similar manner to ADP, wherein the carbamate binds in the purine pocket. Although, it does not bind as deeply within the pocket, it maintains many of the same interactions as ADP. Specifically, the amino portion of the carbamate interacts directly with Asp79 and, through a conserved water molecule, with Leu34. Moreover, the carbonyl oxygen indirectly interacts with Asp79, Gly83 and Thr171 through a single conserved water molecule.[61,99] Upon binding, the orientation of the GDA amide bond rotates from *trans* to *cis*, which allows GDA to adopt a higher affinity, bent conformation.[62] The new orient[100]ation places the quinone on top of the α-helix, mimicking the phosphate tail of ADP and allowing the quinone to make many of the same interactions as the phosphate region of ADP. Specifically, the amide interacts through both the

carbonyl oxygen and nitrogen directly with Phe124 and Gly123, respectively. The quinone is able to interact with Asp40 and Lys98 through both of the carbonyl oxygens, while the methoxy group at the 17-position interacts directly with Lys44.[61,99]

Analysis of Hsp90 binding to either the endogenous ligand, ADP or to GDA highlights one prominent difference amongst the co-crystal structures. While the aromatic quinone portion of GDA maintains many of interactions as the phosphate tail of ADP, the macrocyclic portion does not appear to maintain these interactions.

C. Hsp90 Co-crystal Structure with Radicicol
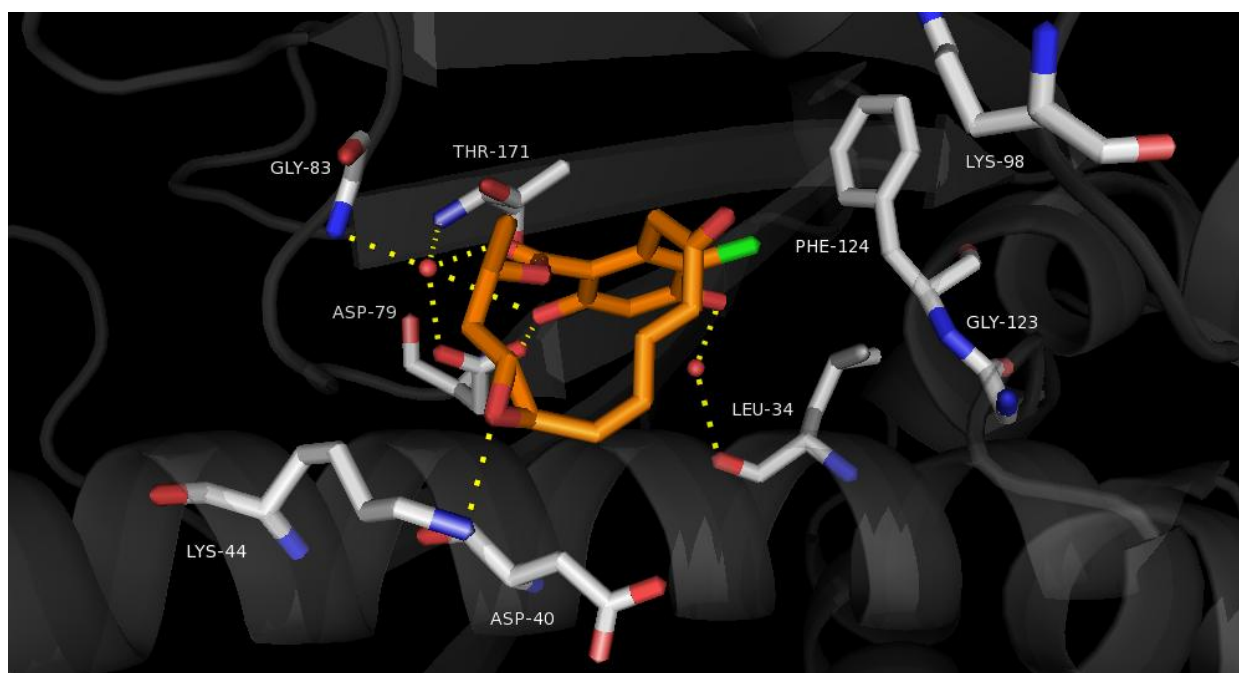
Figure 13 - Hydrogen bonds made between RDC and Hsp90

In 1999 Roe and co-workers solved the co-crystal structure of RDC bound to the N-terminal ATP binding site. Figure 13 shows that, unlike GDA, the macrocycle of RDC does not bind within the purine portion of the binding pocket. Instead, the resorcinol ring binds deep into

the pocket in a manner similar to the purine base, maintaining many of the same interactions with Hsp90 as ADP.[65] Interactions of the resorcinol with Hsp90 are shown in Figure 13. One key interaction involves a hydrogen bond between the phenol *ortho* to the methyl ester and Asp79. This phenol, in addition to the carbonyl oxygen of the methyl ester, interacts through a conserved water molecule with Asp79, Gly83, and Thr171, similar to ADP. Moreover, the phenol in the *para* position makes an interaction with Leu34 through a conserved water molecule.[99] Orientation of the resorcinol ring allows the chlorine to interact through van der Waals forces with the Phe124, strengthening the binding orientation.[65] RDC naturally exhibits a bent orientation in solution, which allows the macrocycle to bend on top of the α-helix.[65] Despite this predisposed bent conformation, the macrocyclic portion of RDC does not maintain many interactions with the protein and only the epoxide oxygen interacts directly with Lys44.

Analysis of Hsp90 interactions with RDC as compared with ADP reveals two important observations. Firstly, the binding conformation of the resorcinol and adenine rings allows both to bind deep into the pocket and establish many of the same interactions. Next, the macrocycle of RDC does not make many specific interactions with Hsp90, supporting that further interactions in this region of the molecule should increase the affinity of RDC-based analogues for Hsp90.

III. Development of radamide a Chimera of Radicicol and Geldanamycin
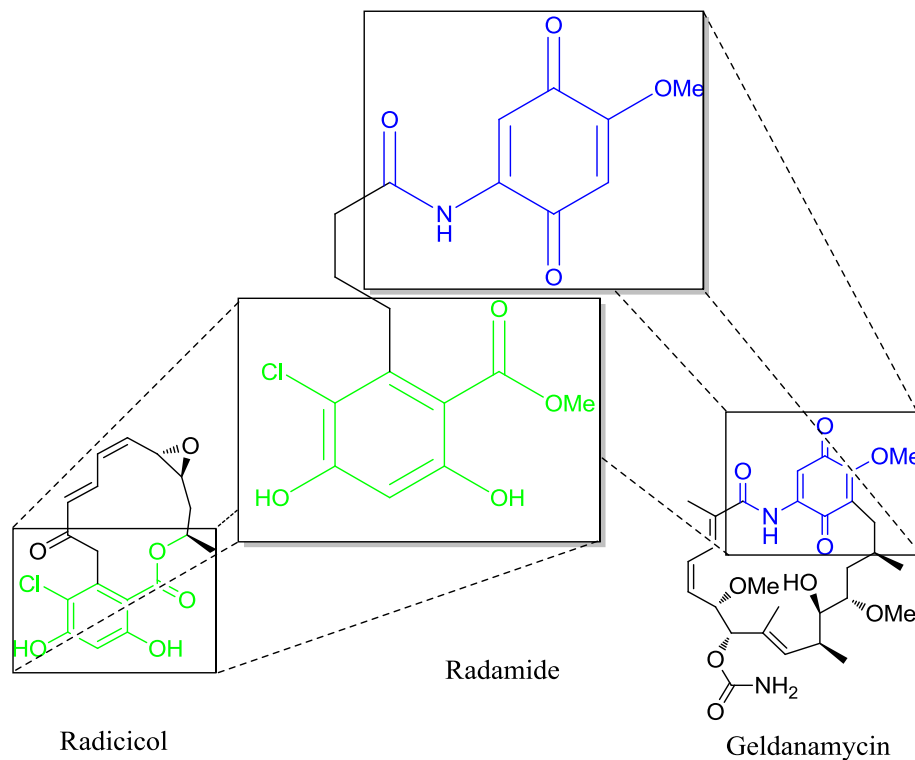
Figure 14 - Radicicol and geldanamycin combined into a chimeric molecule radamide

Through analysis of the co-crystal structures of GDA and RDC, it becomes clear that each molecule affords different interactions with Hsp90. The carbamate of GDA does not bind as deeply into the purine binding pocket as the purine base, which does not enable it to adopt the same orientation and make the same interactions. The aromatic quinone projects into the phosphate binding region, creating a significant hydrogen bonding network with Hsp90. In contrast, the resorcinol of RDC binds deeper into the ATP binding pocket and, through interactions, orients itself in the same fashion as ADP.[65] Unfortunately, the RDC macrocycle maintains only one interaction with Hsp90. In 2004, Clevenger and co-workers designed and synthesized radamide, a chimeric molecule combining the GDA and RDC through a flexible

carbon tether as shown in figure 14.[101] This flexible linker allows the resorcinol to maintain its binding orientation in the purine pocket that it observed for RDC and allows the quinone to bend over the α-helix and capitalize on the intricate hydrogen bonding network as shown as part of GDA. Radamide manifests IC_{50} values of 18.6 μM and 23.7 μM in MCF-7 and SKBr3 breast cancer cells, respectively. Further investigation into the radamide scaffold, probed the optimal linker length and investigated bioisosteric replacements for the quinone.[99]
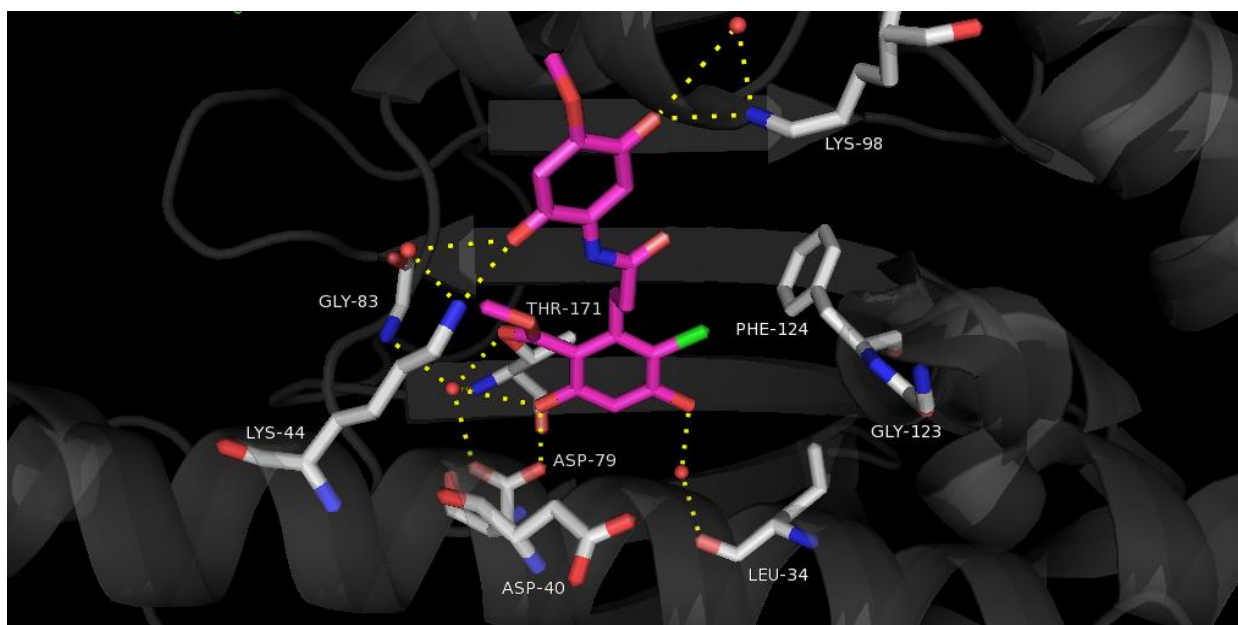
Figure 15 - Hydrogen bonds made between radamide and Hsp90

In 2009 Immormino and co-workers reported the co-crystal structure of radamide bound to the Hsp90 N-terminus. The binding orientation of radamide provides insight into the weaker binding affinity of radamide when compared to the natural products, GDA and RDC. As seen in Figure 15, the quinone of radamide does not project over in the phosphate binding pocket, partially due to the linear conformation maintained by the flexible linker. Thus, it was proposed that incorporation of conformational constraint within the flexible linker would force the quinone

to project into the phosphate binding pocket. Subsequently, compounds have been developed to contain a *cis*-cyclopropane ring to bias analogues into the desired bent conformation and capitalize on the interactions made between the quinone of GDA and Hsp90.

IV.   Hsp90 Isoforms

The Hsp90 family of proteins is comprised of four distinct isoforms that are localized to cellular compartments. There are two forms of Hsp90 found in the cytoplasm. Hsp90α, the inducible cytosolic form, comprises the majority of Hsp90 that is found in the cell. In contrast, Hsp90β is the constitutively active form and is the minor isoform found in the cytoplasm.[9,102] Glucose Regulating Protein 94 (Grp94) is the Hsp90 isoform found in the endoplasmic reticulum, while Tumor Necrosis Factor(TNF) Receptor-Associated Protein-1 (TRAP-1) is located in the mitochondrial matrix.[102] The majority of research to date has focused on the cytosolic forms, often involving a mixture of α and β since the two isoforms are difficult to separate. Since a mixture of Hsp90 isoforms is often employed in studies, little is known about the specific interactions of client proteins. Hsp90 has been shown to play a role in cell survival and the progression of cell death, through apoptosis or necrosis.[103] High expression of Hsp90α appears to be associated with tumor progression and cell cycle regulation.[102] Many of the known inhibitors of Hsp90α and β target the N-terminus, which express highly conserved ATP binding sites.[104-105] Although there is basic understanding of Hsp90 chaperone function, little is known about how each specific isoform function in this process.[102]

In 2009 Immormino and co-workers sought to identify differences in the ATP binding pockets of Grp94 and Hsp90 using the inhibitors GDA and radamide. This study showed that in order for GDA to bind Grp94, the protein must undergo conformational changes to accommodate

the ligand. The quinone of GDA exhibits a steric clash with a glycine residue, which forms the lid of the ATP pocket, which undergoes rotation to allow binding. In contrast, radamide binds to Grp94 without the need for glycine to rotate, indicating that radamide binds differently than GDA (Figure 16).[106-107]
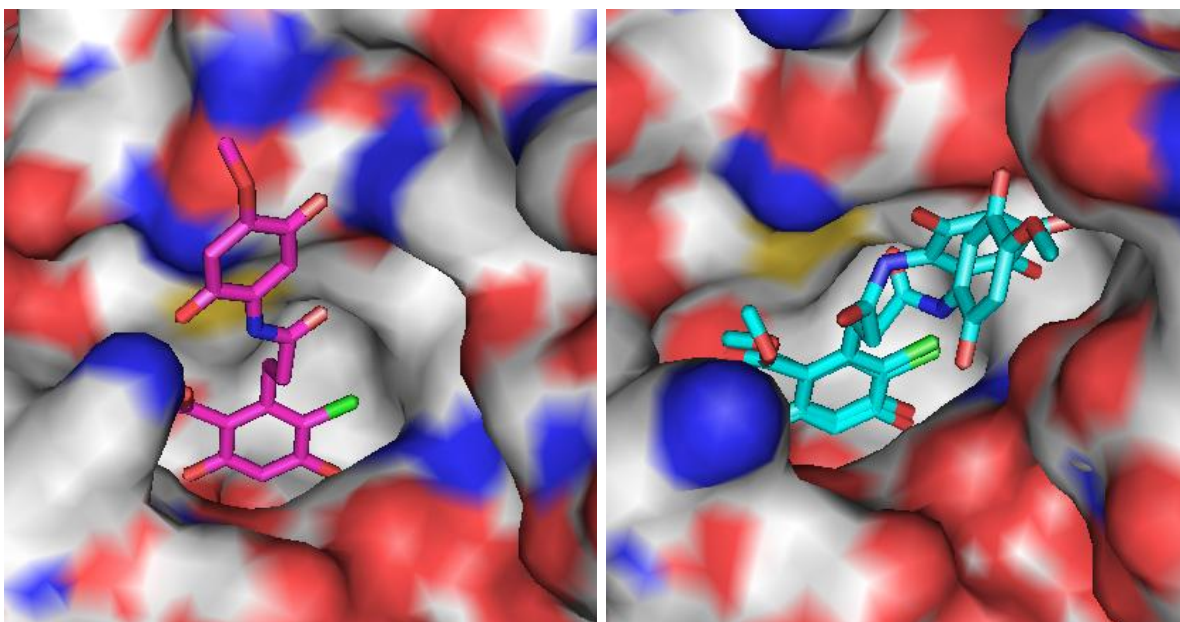
Figure 16 - Binding orientation of radamide to Hsp90 (left) and Grp94 (right)

Examination of the two structures shows that the lid of the pocket is the structural feature that differentiates the two isoforms. This attribute enables each to accommodate small molecules and offers the potential of each isoform to be selectively inhibited. The flexible linker of radamide allows for the quinone to adopt different orientations when binding the two proteins. The co-crystal structure of radamide bound to Hsp90 shows the quinone to extend toward the solvent-exposed portion of the ATP binding pocket. In contrast, the co-crystal structure of radamide bound to Grp94 shows that the small molecule adopts a different conformation, allowing the quinone to project into a Grp94 hydrophobic pocket that is not found in Hsp90.[106]

Small molecule 5'-*N*-ethylcarboxamideadenosine (NECA) was the first reported molecule to take advantage of key interactions with the Grp94-specific hydrophobic pocket, producing a K_d of 200 nM for binding to Grp94. In contrast, NECA did not demonstrate a detectable binding affinity for Hsp90.[108] Radamide is the second molecule reported to interact with this hydrophobic binding pocket, manifesting a K_d value of 520 nM for Grp94 and 870 nM for Hsp90, reflecting ~2-fold selectivity for Grp94.[106] These compounds validate the opportunity to synthesize isoform-selective inhibitors, which would enable the design of new compounds built upon the radamide scaffold that target either Hsp90 or Grp94.

The design of isoform-selective inhibitors is a promising area of study. The co-crystal structures in Figure 16 show that the Hsp90 phosphate binding pocket is wider when compared to that of Grp94, potentially due to conformational changes in the protein to accommodate the hydrophobic pocket. Using the radamide scaffold, it is possible to incorporate additional conformational constraint to project the quinone on top of the α-helix and maintain interactions with the protein. This modification would allow analogues to bind Hsp90 isoforms with better affinity than Grp94, due to unfavorable interactions between the quinone moiety and the narrower phosphate binding region found in Grp94.

V.   *cis*-Cyclopropyl radamide

Conformational constraint has been used by medicinal chemists as a tool to reduce entropy of a molecule and thus the energy required to achieve the conformation required for binding.[100,109] This structural design imparts an advantageous reduction of overall free energy upon binding its biological target.[110] When GDA binds Hsp90, it gives rise to an entropic penalty, resulting from isomerization of the amide bond. While GDA exhibits a linear orientation

in solution, it binds Hsp90 in a bent conformation. The previously described entropic penalty created by isomerization of its natural *trans*-amide bond into the *cis*-amide conformation found in the co-crystal structure is part of this conformational change.[62] Molecular modeling studies indicate that this isomerization process requires between 2.2-6.6 kcal/mol of energy.[99] It is proposed that locking GDA in its *cis* conformation would eliminate the entropic penalty and allow GDA to bind with favorable entropy. As previously discussed, the co-crystal structure of radamide revealed that it binds Hsp90 in a linear fashion, corresponding directly with the *trans*-amide orientation of GDA. Through modification of its flexible linker to predispose radamide into a bent conformation, it would be conformationally locked into a *cis*-amide orientation, mimicking that observed in the co-crystal structure of GDA. In 2009, Duerfeldt and co-workers synthesized radamide analogues that locked the amide of radamide into a *cis* orientation. These compounds manifested a 5-fold increase in affinity for Hsp90.[111] Additionally, in 2009 Hadden and co-workers investigated modifications to the flexible linker that involved introduction of *cis* and *trans* olefins. Unfortunately, integration of the olefins did not result in increased Hsp90 affinity.[99]
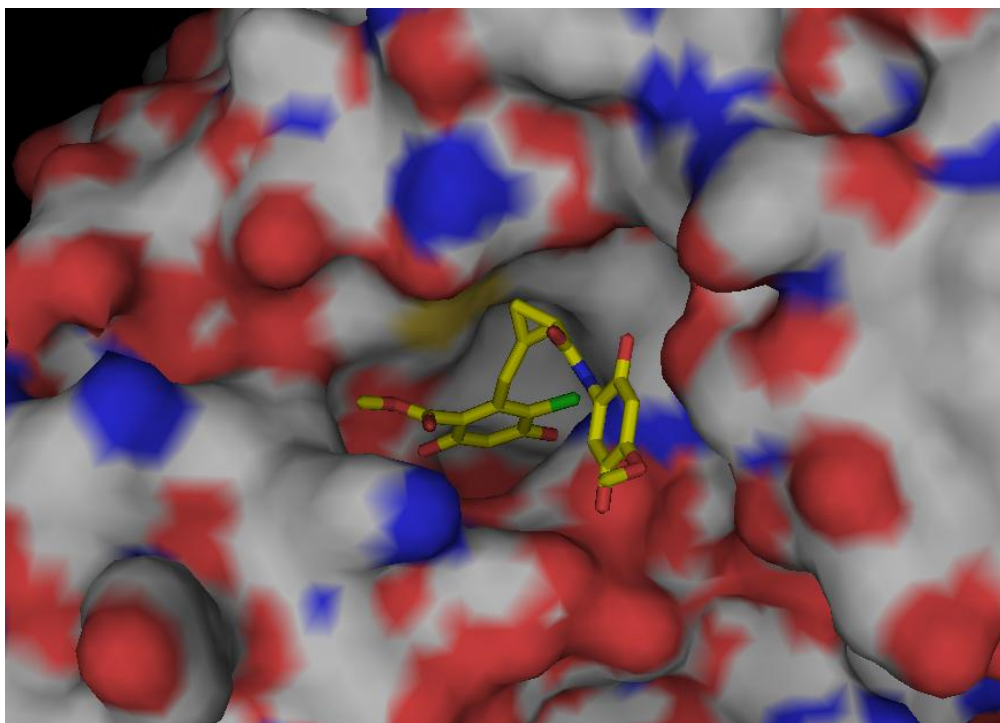
Figure 17 - Molecular modeling of cyclopropyl radamide bound to Hsp90

As shown in Figure 17, molecular modeling studies involving the radamide scaffold demonstrated that modification to the flexible linker, specifically through incorporation of a *cis*-cyclopropyl tether, would bias the quinone into the phosphate binding pocket. These molecular modeling results are in accordance with the work published by Hadden and co-workers, in which they demonstrated that a 3-carbon tether connecting the resorcinol to the amide carbonyl was optimal.[99] Moreover, it was proposed that the *cis*-cyclopropyl tether would bias the radamide scaffold into a bent conformation, which would remove the entropic penalty associated with binding and thus, increase affinity of such analogues for Hsp90. As demonstrated in molecular models, the *cis*-cyclopropyl linker extends the quinone portion of radamide toward the phosphate binding pocket, and exposes it to the solvent-exposed area of the binding pocket. This modeling

study is in agreement with the co-crystal structure of radamide bound to Hsp90, in which the quinone projects into the solvent-exposed phosphate binding pocket.[106]

VI. Synthesis of *cis*-cyclopropyl radamide analogues

As discussed above, molecular modeling studies published by Hadden and co-workers confirm that inhibition of Hsp90 is a function of both linker length and quinone conformation.[99,106] In an effort to further improve affinity, conformationally constrained radamide analogues containing different linker lengths and a *cis*-cyclopropane ring as part of these linkers were developed. The length of the cyclopropyl linkage is defined by the number of carbons between the resorcinol and amide carbonyl, which is connected to the quinone moiety. The two different linker lengths investigated contained 3- and 4-carbons. The syntheses of these analogues were accomplished through development of each individual resorcinolic and quinone portion, followed by subsequent coupling of the two fragments.

A. Three-Carbon Cyclopropyl Linker
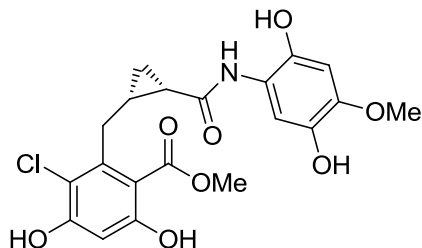
Figure 18 – Structure of the 3-carbon cyclopropyl radamide analogue

Due to incorporation of the cyclopropyl ring, the route used to access radamide and various analogues could not be employed. Thus, synthesis of the 3-carbon tethered analogue

(Figure 18) involved development of a new route for the preparation of the resorcinol, which was ultimately coupled to the previously described, protected hydroquinone.
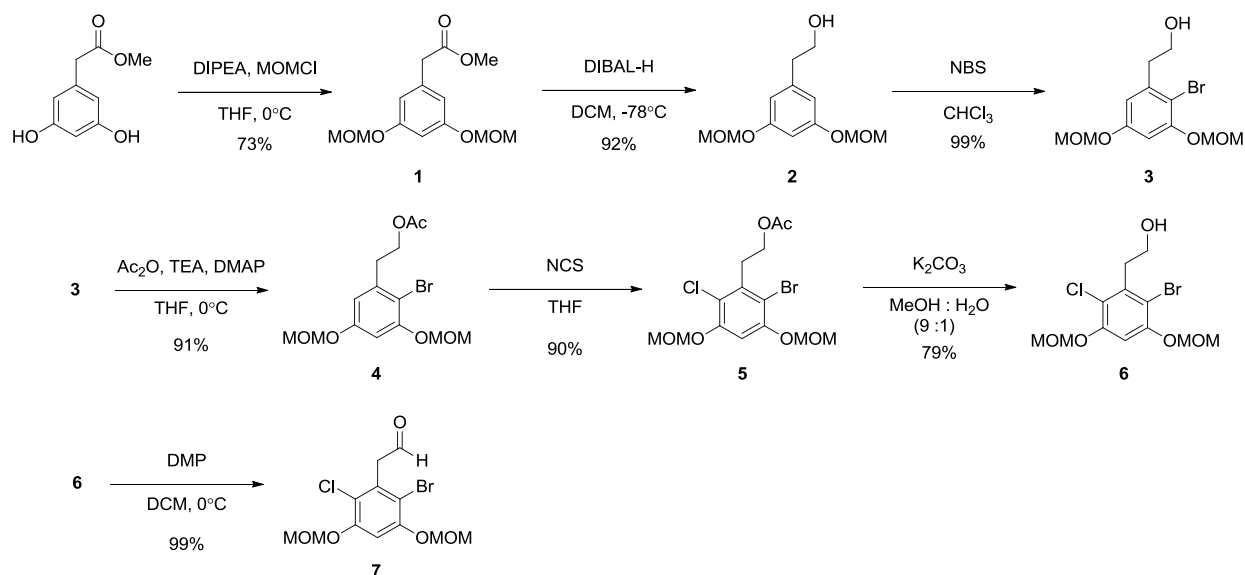
Scheme 1 - Synthetic steps toward the fully functionalized resorcinol ring

As shown in Scheme 1, synthesis of the 3-carbon linked analogue began by protection of methyl 3,5-dihydroxyphenylacetate as the corresponding alkoxy ethers. Next, the ester in protected resorcinol 1 was reduced to the corresponding aliphatic alcohol, 2 allowing for selective and nearly quantitative *ortho*-bromination of the resorcinol ring.[112] Bromination at this stage of the synthesis serves as a functionality that can be readily converted to the desired methyl ester at a later stage and one that blocks this position from reacting during subsequent steps. Acetylation of alcohol 3 furnished protected intermediate 4, which may be chlorinated in good yield to give 5.[113] Solvolysis was employed to excise the acetate ester group and furnish resorcinol 6, which was subsequently oxidized to corresponding aldehyde, 7, using Dess-Martin Periodinane (DMP). With all of the desired functionalities installed on the resorcinol ring, the *cis*-cyclopropyl linker was installed.
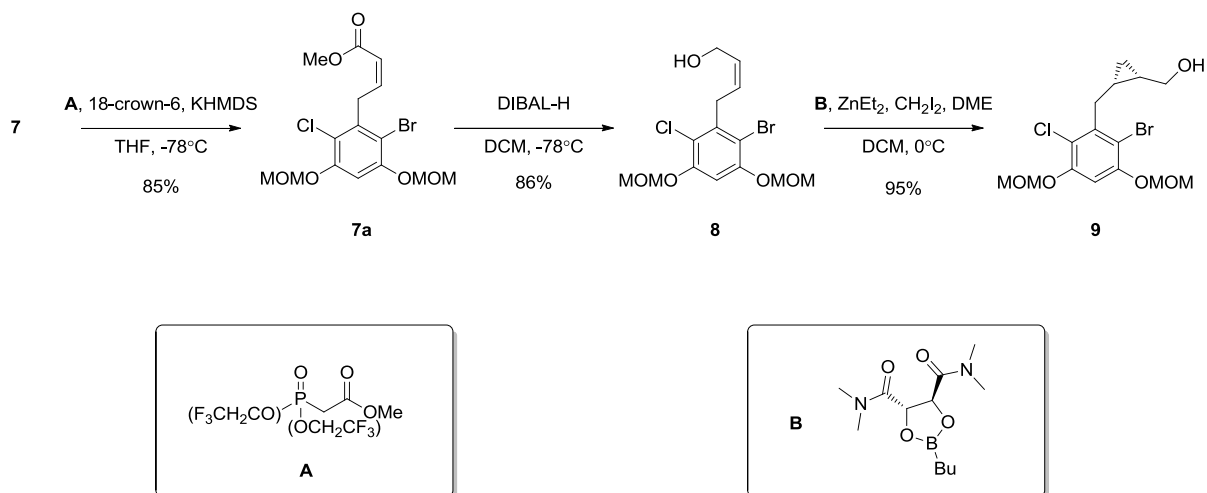
Scheme 2 - Installation of the cis-cyclopropyl tether

The *cis*-cyclopropyl linker was next synthesized. Using the Still-Gennari modification of the Horner-Wadsworth-Emmons olefination, aldehyde 7 was converted to the corresponding *cis*-α,β-unsaturated methyl ester, 7a.[114] ^{1}HNMR analyses of the olefinic protons of ester 7a revealed coupling constants of 11.4 Hz, confirming formation of the desired *cis* olefin. Next, reduction of the α,β-unsaturated ester yielded the corresponding alcohol, 8, in excellent yield over two steps. The olefinic alcohol was designed to adopt the proper configuration required for application of the Charette modification of the Simmons-Smith cyclopropanation reaction.[115-116] As shown in Scheme 2, these conditions involve use a butyl boronic ester and formation of a carbenoid to selectively produce the desired *cis*-cyclopropyl alcohol 9.
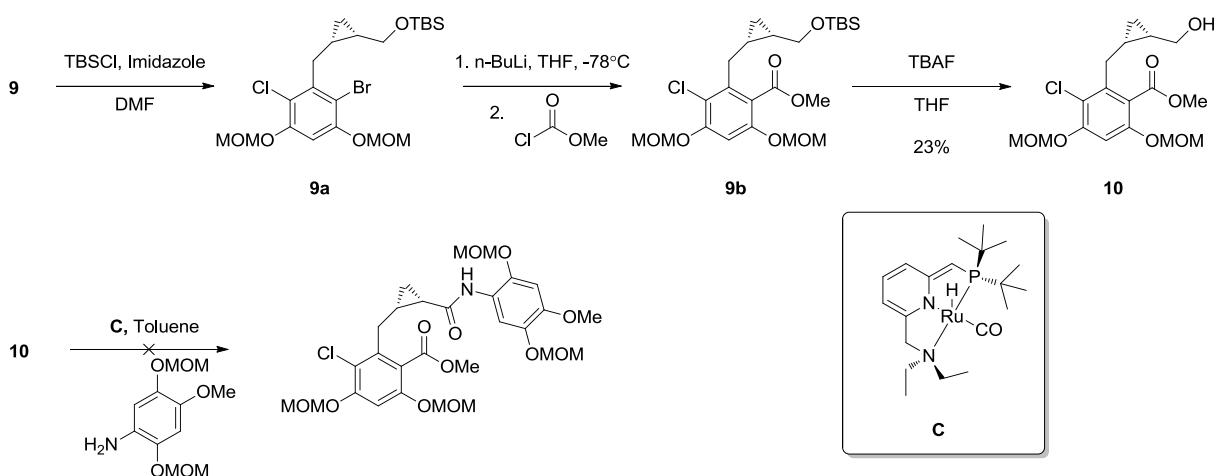
Scheme 3 - Final synthetic efforts toward 3-carbon linked cis-cyclopropyl radamide

Final steps toward the desired analogue involved exchange of the aryl bromide on 9 for a methyl ester. Toward this end, the aliphatic alcohol was protected as the corresponding silyl ether, 9a, in excellent yield. Next, lithium–halogen exchange and quenching with methyl chloroformate, converted the aryl bromide into methyl ester 9b. Cleavage of the silyl ether furnished the intact *cis*-cyclopropyl-containing resorcinol fragment of radamide. Synthesis of the quinone fragment was carried out as previously reported by Clevenger and co-workers.[101] Coupling of the two fragments was attempted between the cyclopropyl alcohol and protected quinone using a Ruthenium catalyst.[117-118] Unfortunately, these conditions did not produce coupled product and an alternate coupling procedure was pursued.
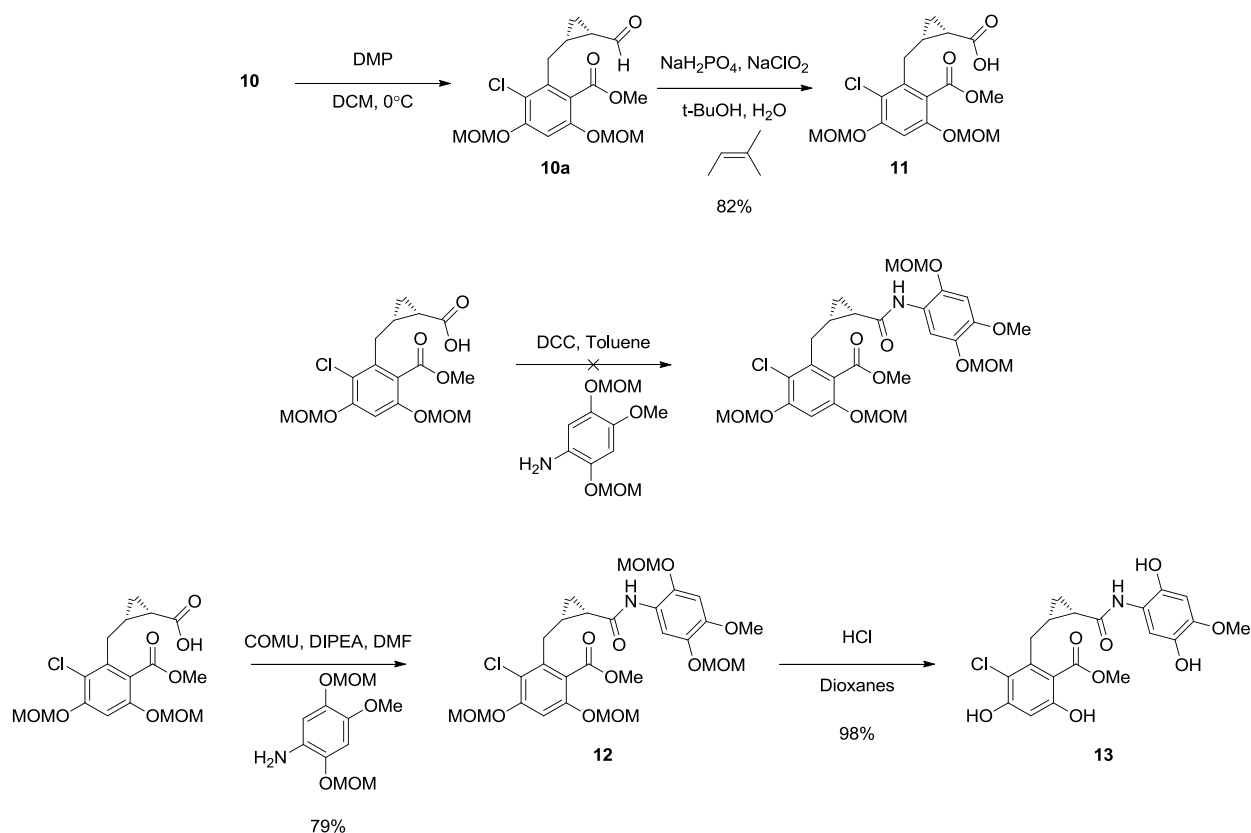
Scheme 4 - Synthesis of 3-carbon cis-cyclopropyl radamide

Oxidation of alcohol 10 to the corresponding aldehyde using DMP, followed by further oxidization using Pinnick conditions afforded the *cis*-cyclopropyl acid fragment, 11. Coupling of the cyclopropyl acid using DCC in toluene, as previously described for a similar system, did not yield the desired product.[119] However, (1-Cyano-2-ethoxy-2-oxoethylidenaminooxy)dimethylamino-morpholino-carbenium hexafluorophosphate (COMU) in the presence of Hunig's base afforded the desired *cis*-cyclopropyl amide 12 in good yield.[120] Subsequent cleavage of the alkoxy ethers using dilute acid in dioxanes produced the desired product, 13, without epimerization of the *cis*-cyclopropane in near quantative yield.

B. Four Carbon Cyclopropyl Linker
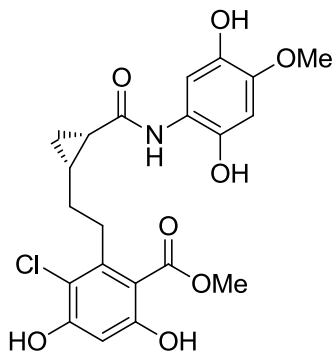
Figure 19 - Desired 4-carbon cyclopropyl radamide analogue
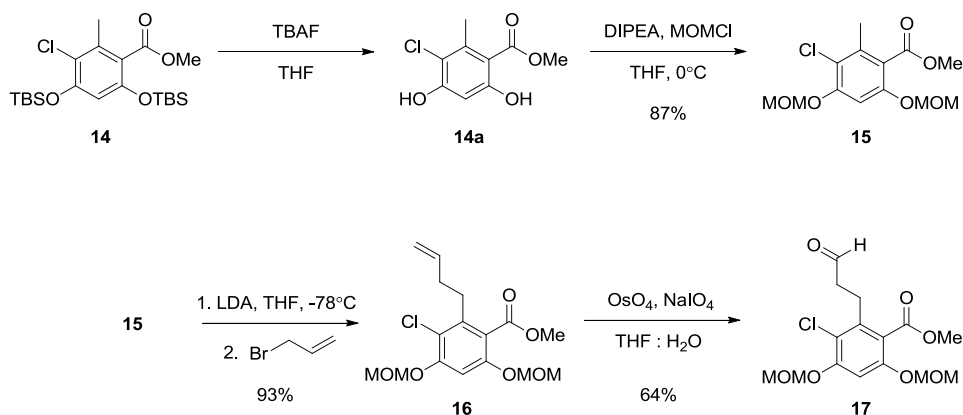
Scheme 5 - Synthesis of the 4-carbon cyclopropyl resorcinolic portion

Synthesis of the 4-carbon cyclopropyl linker (figure 19), followed a similar series of reactions as the radamide synthesis.[99,101] In contrast to the 3-carbon analogue, the resorcinol ring of the 4-carbon linked analogue is fully functionalized prior to installation of the cyclopropyl linker. Cleavage of the silyl groups on methyl 4,6-bis((tert-butyldimethylsilyl)oxy)-3-chloro-2-methylbenzoate **14** and protection of the resultant resorcinol as alkoxy ethers yielded functionalized resorcinol **15** in good yield. Next, modification of the linker started with alkylation of the benzylic position using LDA and allyl bromide to furnish compound **16** in

nearly quantitative yield. Oxidation of the terminal olefin to the corresponding aldehyde, **17**, was accomplished using osmium tetraoxide and *N*-morpholine oxide (NMO).
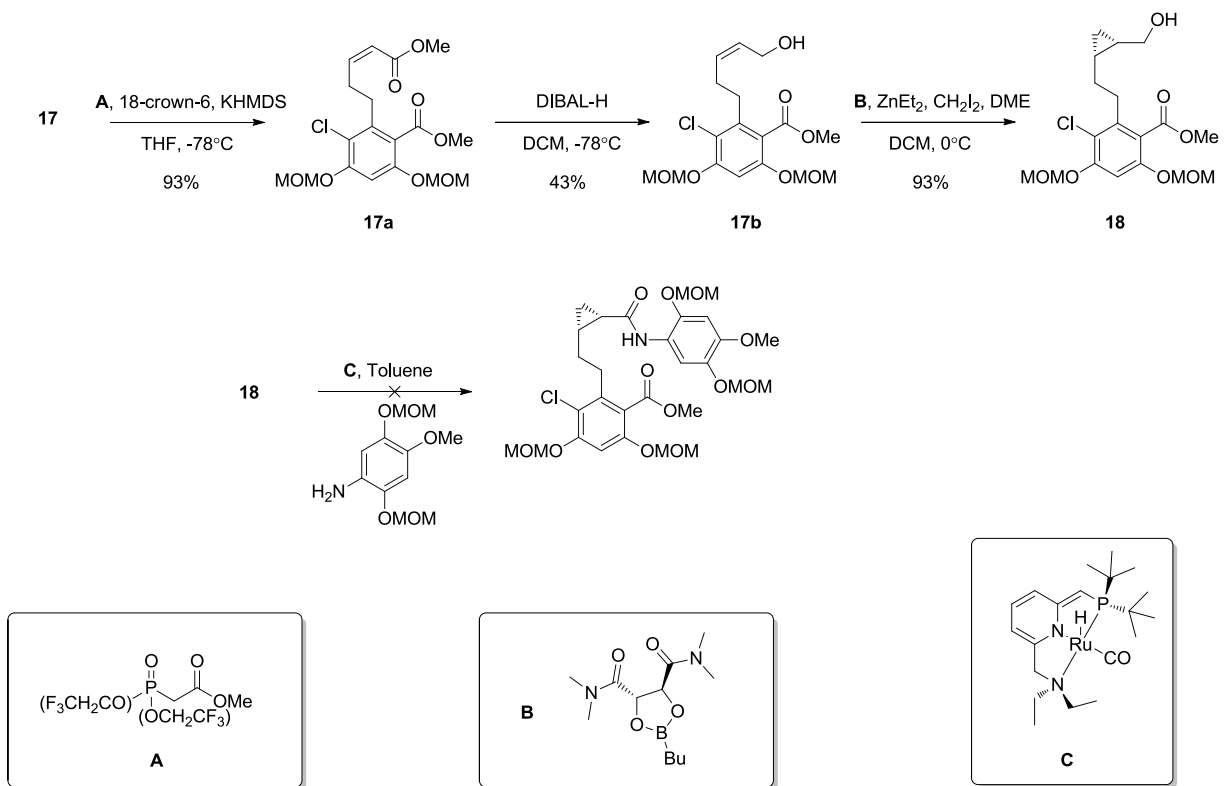
Scheme 6 - Synthetic efforts toward the 4-carbon radamide analogue

The Still-Gennari modification of the Horner-Wadsworth-Emmons olefination was carried out using aldehyde, **17,** to furnish *cis* olefin **17a**.[114] NMR analyses revealed that the coupling constants for the olefinic protons were 11.5 Hz, confirming formation of the desired *cis* olefin. Selective reduction of the aliphatic ester was accomplished using DIBAL-H at -78°C to give the corresponding alcohol, **17b,** in modest yield.[121] Using similar methodology as employed for the 3-carbon linker, properly configured alcohol **17b** was exposed to the Charette modification of the Simmons-Smith cyclopropanation reaction to selectively yield *cis*-cyclopropyl alcohol, **18,** in near quantitative yield.[115-116] As described previously, a ruthenium-

catalyzed coupling reaction was attempted.[117-118] These coupling conditions did not yield desired product and recovery of the alcohol was accomplished by washing the crude reaction mixture with dilute acid. As described with the 3-carbon constrained analogue, an alternative strategy was employed to accomplish this coupling reaction.
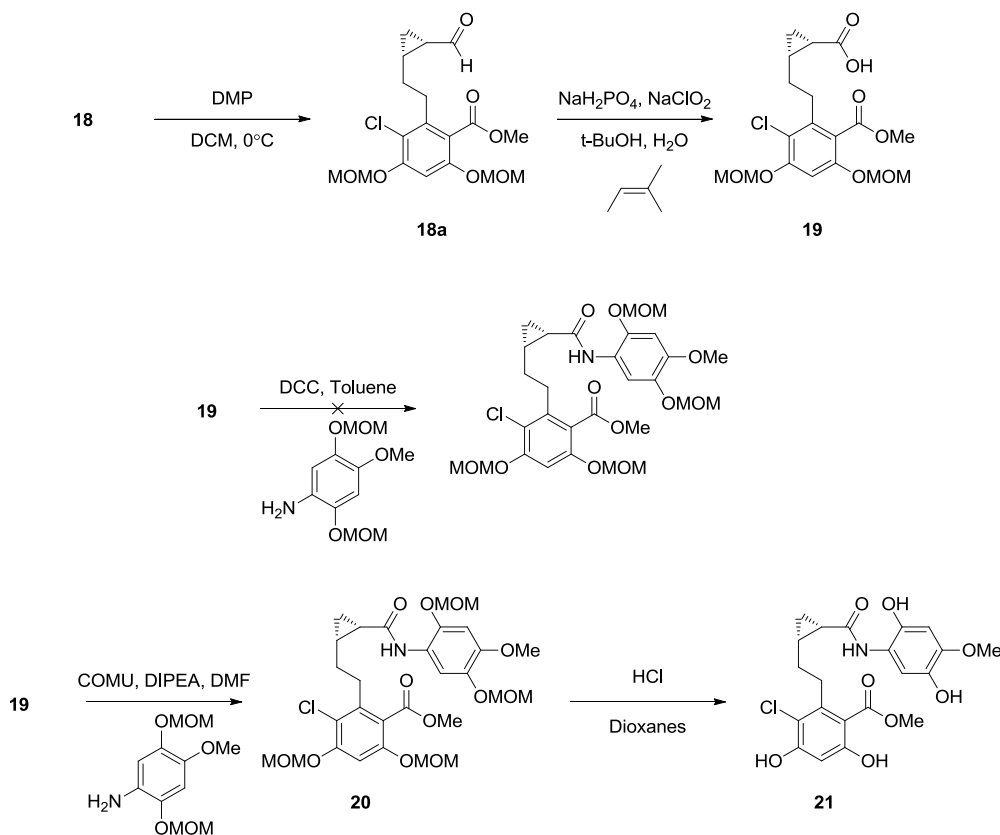
Scheme 7 - Synthesis of 4-carbon cyclopropyl radamide analogue
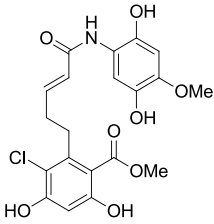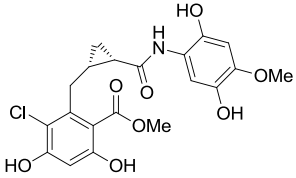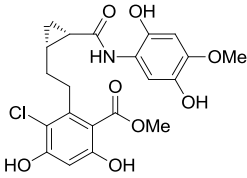
Oxidation of cyclopropyl alcohol **18** to aliphatic aldehyde **18a** was accomplished using DMP. The aldehyde was immediately oxidized to the corresponding acid, **19** using Pinnick conditions. As observed with the 3-carbon analogue, coupling attempts between cyclopropyl acid and the protected quinone using DCC in toluene were unsuccessful.[119] In contrast, reaction of cyclopropyl acid **19** and the protected quinone portion in the presence of Hunig's base and

40

COMU yielded the desired 4-carbon tethered cyclopropyl radamide analogue, **20**, in excellent yield.[120] Global cleavage of all alkoxy ethers was accomplished without epimerization using dilute hydrochloric acid in dioxanes to produce the desired final 4-carbon *cis*-cyclopropyl radamide analogue, **21**, in nearly quantative yield.

C. Biological Evaluation of *cis*-cyclopropyl analogues:

Table 2 - Anti-proliferative activities of select radamide analogues

Compound	Structure	MCF7 (μM)	SKBr3 (μM)
Two Carbon radamide		14.0 ± 1.4^{a}	23.0 ± 1.2
Three Carbon radamide		11.9 ± 0.4	14.5 ± 0.8
Four Carbon radamide		11.6 ± 0.8	12.4 ± 0.4
cis-olefin radamide		45.5 ± 4.0	71.1 ± 4.1

trans-olefin radamide		16.5 ± 2.7	26.7 ± 1.8
13		39.6 ± 1.5	51.2 ± 9.95
21		34.9 ± 0.51	36.1 ± 3.2

[a]Values represent mean ± standard deviation for at least two separate experiments performed in triplicate.

Upon synthesis of the cyclopropyl radamide analogues, the compounds were evaluated for their anti-proliferative activity against SKBr3 (estrogen receptor negative, Her2 over-expressing breast cancer cells) and MCF-7 (estrogen receptor positive breast cancer cells). As shown in Table 1, values obtained upon testing the cyclopropyl radamide analogues were directly compared with the previously described radamide analogues with variable linker lengths as well as the olefins prepared by Hadden and co-workers.[99]

Examination of the data confirmed that conformational constraint of the linker with a *cis*-cyclopropyl linker led to decreases in activity of the radamide scaffold. It is proposed that the flexible linker allows the quinone moiety to adopt an orientation more favorable for binding to Hsp90. However, direct comparison of the 4-carbon cyclopropyl radamide analogue to the closest related analogue, the *cis*-olefin, indicates a slight improvement in activity. An interesting

trend is observed when comparing the linker lengths for these analogues. A direct relationship exists between linker length and activity, such that as the flexible linker length of radamide is increased, the inhibitory concentration decreases and activity improves. A similar trend is observed when examining the cyclopropyl-containing scaffolds, such that the 4-carbon linker is more active than the 3-carbon linker. This observation is in direct contrast to the trends predicted by molecular modeling.

VII.   Conclusions and Future work

The *cis*-cyclopropyl radamide analogues although were not as active as predicted but allowed for the development of a synthesis able to make modifications to the radamide scaffold. The results indicate that the bent conformation seen in the *cis*-cyclopropyl and *cis*-olefinic analogues appear to be negatively affecting the cellular activity of these compounds. The newly developed synthesis allows for the development of various heterocycles and carbocycles to be incorporated into the radamide scaffold, which can be applied to further analogue development. Substitution of a *trans*-olefin for a cis olefin would allow for incorporation of *trans*-cyclopropyl analogues, which would more closely mimic the conformation of the flexible linker and determine if the extended conformation seen in the crystal structure modifies the cellular activity of analogues in this series. The yeast data indicates that **13** shows two-fold selectivity for Hsp90β resulting in a first in class compound. Further development of analogues incorporating this *cis* conformation can be used to increase the affinity for Hsp90β and increase the cellular activity. The inhibitors developed through this work can be used to elucidate the specific interactions between the Hsp90β and various client proteins.
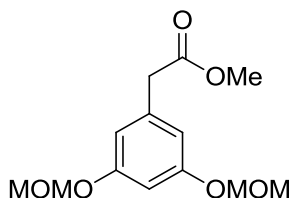
1

2-(3,5-bis(methoxymethoxy)phenyl)ethanol (1). A solution of (1.01 grams, 5.54 mmol) in THF (25 mL) was cooled to 0°C and treated with diisopropylethylamine (5.8 mL, 33.2 mmol), followed by MOMCl (5.6 mL, 33.2 mmol), which was allowed to warm to room temperature overnight. The reaction was quenched by the addition of H_2O and extracted with EtOAc (3 x 150 mL). The combined organic fractions were washed with saturated aqueous NaCl, dried (Na_2SO_4), filtered, and concentrated. The residue was purified via column chromatography (SiO_2 20% EtOAc:Hexanes) to afford 1 as a colorless oil (1.088g, 73%): ^{1}H NMR (400 MHz, $CDCl_3$) δ 6.67 (d, $J = 2.1$ Hz, 1H), 6.64 (d, $J = 2.2$ Hz, 2H), 5.16 (s, 4H), 3.71 (s, 3H), 3.58 (s, 2H), 3.49 (s, 6H); ^{13}C NMR (126 MHz, $CDCl_3$) δ 171.7, 158.3, 136.1, 110.7, 103.6, 94.5, 77.3, 77.0, 76.8, 56.1, 52.1, 41.3; IR (film) vmax 2952, 1740, 1597 1460, 1438, 1400, 1325, 1288, 1251, 1215, 1145, 1083, 1021, 993, 937, 921 844cm^{-1}; HRMS (ESI+) *m/z*: [M + Na]+ calcd for C13H18O6Na, 293.1001; found, 293.0993.

2
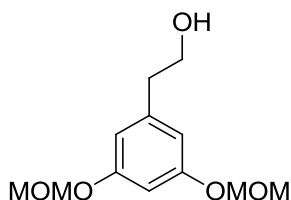
(3,5-bis(methoxymethoxy)phenyl)methanol (2). A solution of **1** (1.06 grams, 3.93 mmol) in DCM (20 mL) was cooled to -78°C and treated with fresh 1.0 M DIBAL-H solution (8.7 mL, 8.65 mmol), this solution was stirred at -78°C for 30 min, then allowed to warm to 0°C. Once the reaction was shown to be complete by TLC the reaction was quenched by the addition of saturated Sodium Potassium Tartrate solution, extracted with EtOAc (3 x 150 mL). The combined organic fractions were washed with saturated aqueous NaCl, dried (Na_2SO_4), filtered, and concentrated. The residue was purified via column chromatography (SiO_2 50% EtOAc:Hexanes) to afford **2** as a pale yellow oil (0.876 g, 92%): ^{1}H NMR (400 MHz, $CDCl_3$) δ 6.64 (t, *J* = 2.2 Hz, 1H), 6.59 (d, *J* = 2.2 Hz, 2H), 5.16 (s, 4H), 3.87 (q, *J* = 6.3 Hz, 2H), 3.49 (s, 6H), 2.83 (t, *J* = 6.5 Hz, 2H), 1.46 (t, *J* = 6.0 Hz, 1H); ^{13}C NMR (126 MHz, $CDCl_3$) δ 158.4, 141.0, 110.3, 102.9, 94.4, 63.4, 56.1, 39.4; IR (film) vmax 3423(br), 2950, 2825, 1595, 1458, 1440, 1400, 1321, 1288, 1215, 1143, 1081, 1043, 975, 924, 844 cm^{-1}; HRMS (ESI+) *m/z*: [M + Na]+ calcd for C12H18O5Na, 265.1052; found, 265.1040.
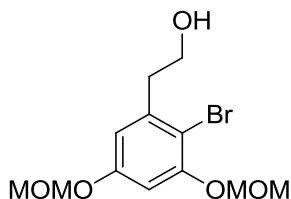
3

(2-(2-bromo-3,5-bis(methoxymethoxy)phenyl)ethanol (3). A solution of **2** (0.853 grams, 3.52 mmol) in $CHCl_3$ (15 mL) at room temperature was treated with N-Bromosuccinimide (0.634 g, 3.56 mmol) in 3 portions over 5 min. Upon completion of reaction by TLC the reaction was quenched by the addition of saturated $Na_2S_2O_3$ and Na_2HCO_3 (1:1), extracted with $CHCl_3$ (3 x

100 mL). The combined organic fractions were washed with aqueous NaCl, dried (Na$_2$SO$_4$), filtered, and concentrated. The residue was purified via column chromatography (SiO$_2$, 30% EtOAc:Hexanes) to afford **3** as a yellow oil (1.125g, 99%): ^{1}H NMR (400 MHz, CDCl$_3$) δ 6.79 (d, J = 2.7 Hz, 1H), 6.70 (d, J = 2.7 Hz, 1H), 5.24 (s, 2H), 5.16 (s, 2H), 3.90 (q, J = 6.5 Hz, 2H), 3.54 (s, 3H), 3.49 (s, 3H), 3.05 (t, J = 6.7 Hz, 2H); ^{13}C NMR (126 MHz, CDCl$_3$) δ 157.0, 154.7, 139.8, 111.9, 107.4, 103.3, 95.2, 94.6, 77.3, 77.0, 76.8, 62.0, 56.5, 56.2, 39.8; IR (film) νmax 3419(br), 2931, 1585, 1452, 1396, 1317, 1213, 1134, 1085, 1041, 1016, 972, 923, 845 cm^{-1}; HRMS (ESI+) m/z: [M + Na]+ calcd for C12H17BrO5Na, 343.0157; found, 343.0160.
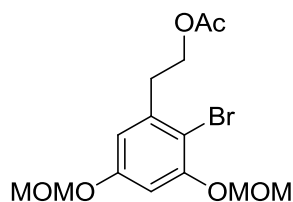
4

2-bromo-3,5-bis(methoxymethoxy)phenethyl acetate (4). A solution of **3** (1.03 grams, 3.22 mmol) in DCM (15 mL) was cooled to 0°C and treated with acetic anhydride (1.0 mL, 9.66 mmol), 4-dimethylaminopyridine (0.040 g, 0.32 mmol) and triethylamine (1.4 mL, 9.66 mmol) which was monitored by TLC. Upon consumption of starting material the reaction was quenched by the addition of saturated NH$_4$Cl and extracted with EtOAc (3 x 150 mL). The combined organic fractions were washed with saturated aqueous NaCl, dried (Na$_2$SO$_4$), filtered, and concentrated. The residue was purified via column chromatography (SiO$_2$ 30% EtOAc:Hexanes) to afford **4** as a colorless oil (1.06 g, 91%): ^{1}H NMR (400 MHz, CDCl$_3$) δ 6.79 (d, J = 2.7 Hz, 1H), 6.68 (d, J = 2.7 Hz, 1H), 5.24 (s, 2H), 5.15 (s, 2H), 4.31 (t, J = 7.0 Hz, 2H), 3.53 (s, 3H),

3.48 (s, 3H), 3.10 (t, J = 7.0 Hz, 2H), 2.06 (s, 3H); ^{13}C NMR (126 MHz, CDCl$_3$) δ 171.0, 157.0, 154.6, 139.2, 111.7, 107.4, 103.5, 95.2, 94.6, 77.3, 77.0, 76.8, 63.3, 56.5, 56.1, 35.7, 21.0; IR (film) vmax 2956, 1739, 1587, 1454, 1319, 1238, 1154, 1085, 1041, 1018, 923 cm^{-1}; HRMS (ESI+) m/z: [M + Na]+ calcd for C$_{14}$H$_{19}$BrO$_6$, 385.0263; found, 385.0255.

5

2-bromo-6-chloro-3,5-bis(methoxymethoxy)phenethyl acetate (5). A solution of **4** (0.916 grams, 2.53 mmol) in THF (15 mL) cooled to 0°C and was treated with N-Chlorosuccinimide (0.610 g, 4.55 mmol) over 5 min. The reaction was stirred at 0°C for 2 h then warmed to room temperature and monitored by TLC. Upon consumption of X by TLC the reaction was quenched by the addition of saturated Na$_2$S$_2$O$_3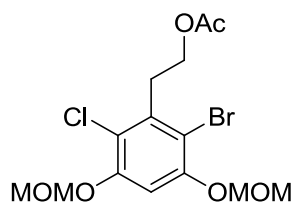$, extracted with EtOAc (3 x 150 mL). The combined organic fractions were washed with aqueous NaCl, dried (Na$_2$SO$_4$), filtered, and concentrated. The residue was purified via column chromatography (SiO$_2$, 30% EtOAc:Hexanes) to afford **5** as a yellow oil (0.903 g, 90%): ^{1}H NMR (400 MHz, CDCl$_3$) δ 7.02 (s, 1H), 5.24 (d, J = 2.8 Hz, 4H), 4.31 (t, J = 7.2 Hz, 2H), 3.54 (s, 6H), 3.42 (t, J = 7.2 Hz, 2H), 2.07 (s, 3H). ^{13}C NMR (126 MHz, CDCl$_3$) δ 171.0, 153.0, 152.7, 136.9, 118.2, 108.9, 103.4, 95.5, 77.3, 77.0, 76.8, 61.9, 56.6, 33.7, 21.1; IR (film) vmax 3384, 2958, 2829, 2358, 2341, 1739, 1574, 1442, 1323, 1232, 1165, 1109, 1091, 1064, 1046, 972, 937, 923, 831 cm^{-1}; HRMS (ESI+) m/z: [M + Na]+ calcd for C$_{14}$H$_{18}$BrClO$_6$Na, 418.9873; found, 418.9872.
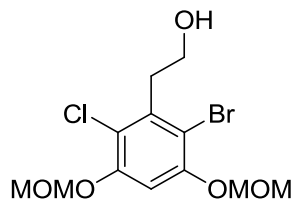
6

2-(2-bromo-6-chloro-3,5-bis(methoxymethoxy)phenyl)ethanol (6). A solution of **5** (1.03 grams, 2.6 mmol) in a mixture of MeOH and H_2O (9:1, 15 mL) was treated with Potassium Carbonate (1.10 g, 7.8 mmol). Upon consumption of starting material by TLC the reaction was quenched by the addition of H_2O, extracted with EtOAc (3 x 150 mL). The combined organic fractions were washed with aqueous NaCl, dried (Na_2SO_4), filtered, and concentrated. The residue was purified via column chromatography (SiO_2, 30% EtOAc:Hexanes) to afford **6** as an amorphous colorless solid (0.731g, 79%): ^{1}H NMR (400 MHz, $CDCl_3$) δ 7.01 (s, 1H), 5.24 (d, *J* = 2.8 Hz, 4H), 3.89 (dd, *J* = 13.4, 7.2 Hz, 2H), 3.53 (s, 6H), 3.38 (t, *J* = 7.3 Hz, 2H); ^{13}C NMR (126 MHz, $CDCl_3$) δ 153.0, 152.8, 137.4, 118.0, 108.8, 103.1, 95.4, 77.3, 77.0, 76.8, 61.0, 56.6, 37.7; IR (film) vmax 3222(br), 2958, 2349, 2333, 1577, 1444, 1308, 1242, 1167, 1089, 1045, 1022, 939, 844 cm^{-1}; HRMS (ESI+) *m/z*: [M + Na]+ calcd for C12H16BrClO5Na, 376.9767; found, 376.9763.
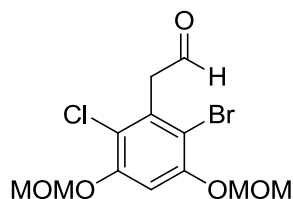
7

2-(2-bromo-6-chloro-3,5-bis(methoxymethoxy)phenyl)acetaldehyde (7). A solution of **6** (0.699 grams, 1.97 mmol) in DCM (10 mL) was treated with Dess-Martin Periodinane (0.996g, 2.36 mmol) and allowed to react overnight. The reaction was quenched by the addition of a (1:1) mixture of saturated aqueous sodium bicarbonate and sodium thiosulfate, extracted with EtOAc (3 x 100 mL). The combined organic fractions were dried (Na$_2$SO$_4$), filtered, and concentrated. The residue was run through a silica plug (SiO$_2$, 30% EtOAc:Hexanes) to afford **7** as an amorphous pale yellow solid (0.688g, 99%): ^{1}H NMR (400 MHz, CDCl$_3$) δ 9.74 (s, 1H), 9.74 (s, 1H), 7.28 (s, 2H), 7.10 (s, 1H), 7.10 (s, 1H), 5.26 (d, J = 2.4 Hz, 5H), 5.26 (d, J = 2.4 Hz, 5H), 4.24 (d, J = 1.1 Hz, 2H), 4.24 (d, J = 1.1 Hz, 2H), 3.54 (s, 7H), 3.54 (s, 7H); ^{13}C NMR (126 MHz, CDCl$_3$) δ 197.0, 153.2, 152.9, 133.0, 118.2, 108.8, 103.8, 95.5, 77.3, 77.0, 76.8, 56.6, 48.9; IR (film) vmax 2956, 2830, 2725, 1724, 1593, 1471, 1433, 1400, 1315, 1296, 1263, 1222, 1153, 1108, 1043, 968, 937, 827 756, 715 cm^{-1}; HRMS (ESI+) *m/z*: [M + Na]+ calcd for C12H14BrClO5Na, 374.9611; found, 374.9603.
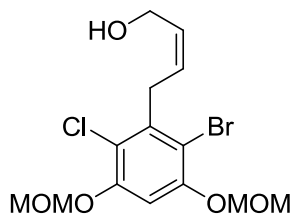
8

(Z)-4-(2-bromo-6-chloro-3,5-bis(methoxymethoxy)phenyl)but-2-en-1-ol (8). A solution of 18-crown-6 (2.61 grams, 9.9 mmol) in THF (50 mL) was added methyl 2-(bis(2,2,2-trifluoroethoxy)phosphoryl)acetate (0.47 mL, 2.2 mmol) and cooled to -78°C followed by treatment of a 0.5 M solution of KHMDS in toluene (5.0 mL, 2.5 mmol) and stirred for 45 min.

A separate solution of the crude aldehyde (0.699 grams, 1.98 mmol) was dissolved in THF (10 mL) and cooled to -78°C and added dropwise to first solution and stirred for 30 min at -78°C. The reaction was quenched by the addition of saturated aqueous ammonium chloride and extracted with EtOAc (3x150mL). The combined organic fractions were washed with aqueous NaCl, dried (Na$_2$SO$_4$), filtered, and concentrated. The residue was purified via column chromatography (SiO$_2$, 30% EtOAc:Hexanes) to afford crude α,β ester as a yellow oil (0.683g, 85%): ^{1}H NMR (400 MHz, CDCl$_3$) δ 7.02 (s, 1H), 6.07 (dt, J = 11.4, 6.3 Hz, 1H), 5.93 (dt, J = 11.4, 2.2 Hz, 1H), 5.24 (s, 4H), 4.47 (dd, J = 6.3, 2.2 Hz, 2H), 3.80 (s, 3H), 3.53 (s, 6H);

A solution of the α,β ester **7a** (0.624 grams, 1.53 mmol) in THF (10 mL) was cooled to -78°C and treated dropwise with fresh 1.0M solution of DIBAL-H in THF (3.4 mL, 3.4 mmol), this solution was stirred at -78°C for 30 min, then allowed to warm to 0°C. Once the reaction was shown to be complete by TLC the reaction was quenched by the addition of saturated aqueous sodium potassium tartrate solution, extracted with EtOAc (3 x 100 mL). The combined organic fractions were washed with saturated aqueous NaCl, dried (Na$_2$SO$_4$), filtered, and concentrated. The residue was purified via column chromatography (SiO$_2$ 40% EtOAc:Hexanes) to afford **8** as a pale yellow oil (0.498 g, 86%): ^{1}H NMR (400 MHz, CDCl$_3$) δ 7.00 (s, 1H), 5.73 (ddd, J = 11.0, 5.5, 3.5 Hz, 1H), 5.53 (dd, J = 6.7, 5.4 Hz, 1H), 5.24 (d, J = 2.5 Hz, 4H), 4.44 (t, J = 6.0 Hz, 2H), 3.86 (dd, J = 7.1, 1.5 Hz, 2H), 3.53 (s, 7H), 1.38 (t, J = 5.9 Hz, 1H); ^{13}C NMR (126 MHz, CDCl$_3$) δ 152.8, 139.0, 129.9, 127.3, 117.5, 108.3, 102.9, 95.5, 63.5, 61.0, 59.0, 56.6, 33.3; IR (film) νmax 3404, 2931, 2829, 2347, 1573, 1442, 1400, 1321, 1222, 1153, 1089, 1037, 929, 723 cm^{-1}; HRMS (ESI+) m/z: [M + Na]+ calcd for C14H18BrClO5Na, 402.9924; found, 402.9915.
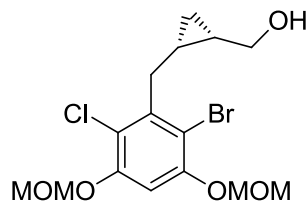
9

((1S,2S)-2-(2-bromo-6-chloro-3,5-bis(methoxymethoxy)benzyl)cyclopropyl)methanol (9). A solution of 8 (0.442 grams, 1.16 mmol) in DCM (5 mL) was added (4R,5R)-2-Butyl-N,N,N',N'-tetramethyl-1,3,2-dioxaborolane-4,5-dicarboxamide (0.32 mL, 1.22 mmol) and stirred for 30 min. A second solution of 1.1M ZnEt$_2$ (4.75 mL, 5.22 mmol) in Toluene was added to DCM (10 mL) at 0°C was added DME (0.75 mL, 5.22 mmol) followed by dropwise addition of Diiodomethane (0.85 mL, 10.44 mmol) and stirred for 15 minutes. Solution containing **8** was added dropwise to the second solution, warmed to room temperature and react overnight. The reaction was quenched by addition of saturated ammonium chloride solution and extracted with EtOAc (3 x 100 mL). The combined organic fractions were washed with saturated aqueous NaCl, dried (Na$_2$SO$_4$), filtered, and concentrated. The residue was purified via column chromatography (SiO$_2$ 40% EtOAc:Hexanes) to afford **9** as a colorless oil (0.436 g, 95%): $[\alpha]_D^{25}$ = -25.33 (c = 0.198 CHCl$_3$); ^{1}H NMR (400 MHz, CDCl$_3$) δ 7.00 (s, 1H), 5.25 (d, *J* = 2.9 Hz, 4H), 3.67 (dd, *J* = 5.8, 3.6 Hz, 1H), 3.58 (dd, *J* = 5.7, 3.6 Hz, 1H), 3.54 (d, *J* = 3.5 Hz, 6H), 3.38 (s, 1H), 2.94 (dd, *J* = 13.6, 10.0 Hz, 1H), 1.41 (s, 1H), 1.35 (d, *J* = 4.2 Hz, 1H), 1.29 – 1.18 (m, 1H), 0.69 (dt, *J* = 8.4, 4.2 Hz, 1H), 0.56 – 0.49 (m, 1H); ^{13}C NMR (126 MHz, CDCl$_3$) δ 153.0, 141.4, 117.5, 108.4, 102.8, 95.5, 71.9, 70.6, 63.5, 59.1, 56.6, 32.5, 18.5, 15.1, 9.2; IR (film) vmax 3379(br), 2931, 2391, 1573, 1440, 1400, 1321, 1222, 1153, 1091, 1035, 929 cm^{-1}; HRMS (ESI+) *m/z*: [M + Na]+ calcd for C15H20BrClO5Na, 417.0080; found, 417.0077.
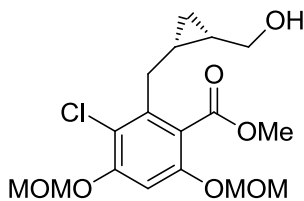
10

Methyl-3-chloro-2-(((1S,2S)-2-(hydroxymethyl)cyclopropyl)methyl)-4,6-bis(methoxymethoxy)benzoate (10). A solution of **9** (0.453 grams, 1.15 mmol) in DMF (6 mL) was added Imidazole (0.248 grams, 3.45 mmol) followed by addition of tert-butylchlorodimethylsilane (0.530 grams, 3.45 mmol) at room temperature and stirred overnight. The reaction was quenched with H_2O and extracted with EtOAc (3 x 50 mL). The combined organic fractions were washed with saturated aqueous NaCl, dried (Na_2SO_4), filtered, and concentrated to produce silyl protected alcohol (~99% yield). This residue carried on without further purification.

A solution of the residue (0.562 grams, 1.1 mmol) in THF (6 mL) was cooled to -78°C and treated by dropwise addition of n-BuLi (0.5 mL, 1.22 mmol) and stirred for 20 min at -78°C and added methyl chloroformate (0.15 mL, 1.7 mmol) dropwise at -78°C for 30 min. It was then warmed to room temperature and stirred for 30 min. The reaction was then quenched by addition of H_2O and extracted with EtOAc (3 x 50 mL). The combined organic fractions were washed with saturated aqueous NaCl, dried (Na_2SO_4), filtered, and concentrated to produce desired benzoic ester (0.19 grams, 35%). This residue carried on without further purification.

A solution of this residue (0.19 grams, 0.39 mmol) in THF (3 mL) was added tetrabutylammonium fluoride (1.2 mL, 1.17 mmol) at room temperature and stirred until reaction was shown to be complete by TLC. The reaction was quenched by addition of saturated

ammonium chloride and extracted with EtOAc (3 x 50 mL). The combined organic fractions were washed with saturated aqueous NaCl, dried (Na$_2$SO$_4$), filtered, and concentrated. The residue was purified via column chromatography (SiO$_2$ 40% EtOAc:Hexanes) to afford **10** over three steps as a colorless oil (0.105 g, 23%): $[\alpha]_D^{25}$ = -25.38 (c=0.0524 CHCl$_3$); ^{1}H NMR (400 MHz, CDCl$_3$) δ 6.95 (s, 1H), 5.27 (s, 2H), 5.17 (s, 2H), 3.91 (s, 3H), 3.83 (d, *J* = 5.1 Hz, 1H), 3.65 − 3.56 (m, 1H), 3.53 (s, 3H), 3.49 (s, 3H), 3.12 (dd, *J* = 14.0, 4.2 Hz, 1H), 2.57 (dd, *J* = 14.0, 9.1 Hz, 1H), 1.50 (s, 1H), 1.31 − 1.15 (m, 2H), 0.71 (td, *J* = 8.5, 5.0 Hz, 1H), 0.31 (q, *J* = 5.4 Hz, 1H); ^{13}C NMR (126 MHz, CDCl$_3$) δ 168.1, 154.5, 153.3, 139.3, 119.7, 117.0, 101.7, 95.2, 95.1, 63.2, 56.5, 56.4, 52.5, 29.6, 18.7, 15.8, 9.5; IR (film) vmax 2952, 2829, 2358, 2341, 1728, 1593, 1579, 1467, 1433, 1398, 1321, 1261, 1220, 1153, 1107, 1093, 1037, 968, 931, 827, 784, 713 cm^{-1}; HRMS (ESI+) *m/z*: [M + Na]+ calcd for C17H23ClO7Na, 397.1030; found, 387.1037.
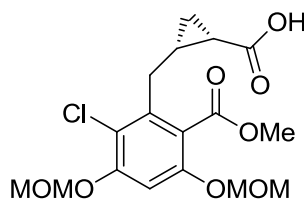
11

(1S,2S)-2-(2-chloro-6-(methoxycarbonyl)-3,5-bis(methoxymethoxy)benzyl)cyclopropanecarboxylic acid (11). A solution of **10** (0.08 grams, 0.214 mmol) in DCM (2 mL) was cooled to 0°C and treated with Dess-Martin Periodinane (0.111 grams, 0.26 mmol), which was stirred at 0°C for 1 hr then allowed to warm to room temperature and stirred for 3 hrs. The reaction was quenched by the addition of a (1:1) mixture of saturated aqueous sodium bicarbonate and sodium thiosulfate, allowed to stir for 30 min, and

extracted with EtOAc (3 x 30 mL). The combined organic fractions were washed with saturated aqueous NaCl, dried (Na$_2$SO$_4$), filtered, and concentrated. The residue was used without further purification.

The residue was dissolved in t-BuOH (1.0 mL) and 2-methyl-2-butene (0.70 mL, 6.12 mmol), while a separate solution of 80% sodium chlorite (0.133 grams, 1.16 mmol) in a buffered aqueous solution of sodium phosphate monobasic (0.189 grams, 1.53 mmol) in H$_2$O (3 mL). The oxidizing solution was added dropwise to the solution containing the aldehyde and allowed to react for 12 hrs. This reaction was diluted with saturated aqueous NaH$_2$PO$_4$ and extracted with DCM (3 x 50 mL), dried (Na$_2$SO$_4$), filtered, and concentrated to afford **11** as a pale yellow oil (0.68 g, 82%): $[\alpha]_D^{25}$ = -30.23 (c= 0.030 CHCl$_3$); ^{1}H NMR (400 MHz, CDCl$_3$) δ 6.97 (s, 1H), 5.27 (s, 2H), 5.17 (s, 2H), 3.93 (s, 3H), 3.53 (s, 3H), 3.49 (s, 3H), 3.11 (dd, J = 14.1, 3.8 Hz, 1H), 2.92 (dd, J = 14.0, 9.6 Hz, 1H), 1.80 (td, J = 8.2, 5.5 Hz, 1H), 1.76 − 1.66 (m, 1H), 1.26 (m, 1H), 1.09 (td, J = 8.3, 4.8 Hz, 1H); ^{13}C NMR (126 MHz, CDCl$_3$) δ 178.9, 167.7, 154.4, 153.2, 138.3, 120.4, 117.2, 101.9, 95.1, 56.5, 52.5, 28.6, 21.6, 18.5, 14.7; IR (film) νmax 2952, 2850, 2358, 2341, 1731, 1693, 1593, 1467, 1433, 1400, 1321, 1296, 1263, 1220, 1191, 1155, 1107, 1091, 1041, 968, 927, 713 cm^{-1}; HRMS (ESI+) *m/z*: [M + Na]+ calcd for C17H21ClO8Na, 411.0823; found, 411.0830.
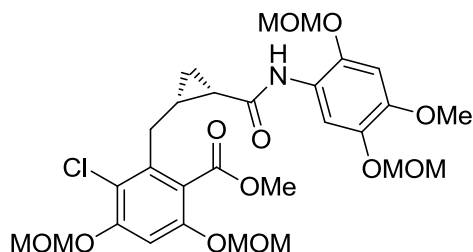
12

Methyl-3-chloro-2-((((1S,2S)-2-((4-methoxy-2,5-bis(methoxymethoxy)phenyl)carbamoyl)cyclopropyl)methyl)-4,6-bis(methoxymethoxy)benzoate (12). A solution of **11** (18 mg, 0.046 mmol) in (0.5 mL) DMF was added to a premade solution of (12 mg, 0.046 mmol) of 4-methoxy-2,5-bis(methoxymethoxy)aniline[101] in (0.5 mL) of DMF and cooled to 0°C followed by the dropwise addition of diisopropylethyl amine (16 μL, 0.092 mmol) and COMU (20 mg, 0.046 mmol). This was stirred for 1 hr at 0°C, then allowed to warm to room temperature and stirred for an additional 2 hrs. The solution was diluted with EtOAc (50 mL) and washed with 1 N HCl (10 mL), saturated aqueous $NaHCO_3$ (10 mL), and saturated aqueous NaCl (3 x 30 mL). The organic fraction was dried (Na_2SO_4), filtered, and concentrated. The residue was purified via column chromatography (SiO_2 45% EtOAc:Hexanes) to afford **11** as a yellow oil (22.4 mg, 79%): $[\alpha]_D^{25}$ = -18.39 (c=0.0112 $CHCl_3$); ^{1}H NMR (400 MHz, $CDCl_3$) δ 8.27 (s, 1H), 7.84 (s, 1H), 6.95 (s, 1H), 6.83 (s, 1H), 5.26 (s, 2H), 5.20 (d, J = 5.7 Hz, 5H), 5.16 (d, J = 0.8 Hz, 2H), 3.95 (s, 3H), 3.86 (s, 3H), 3.58 – 3.51 (m, 9H), 3.48 (s, 3H), 3.02 (ddd, J = 23.0, 14.1, 5.9 Hz, 2H), 1.69 (t, J = 6.8 Hz, 1H), 1.62 – 1.54 (m, 1H), 1.41 – 1.32 (m, 1H), 1.00 (td, J = 8.1, 4.7 Hz, 1H); ^{13}C NMR (126 MHz, $CDCl_3$) δ 169.0, 167.7, 154.3, 153.1, 146.1, 141.4, 140.8, 139.0, 122.1, 120.4, 117.2, 110.8, 101.8, 101.0, 96.3, 95.2, 56.4, 52.6, 28.7, 21.9, 20.6, 12.6; IR (film) νmax 3350, 2952, 2925, 2829, 1730, 1674, 1593, 1523, 1450, 1392, 1321, 1263, 1218, 1141, 995, 970, 929, 831, 754 cm^{-1}; HRMS (ESI+) *m/z*: [M + Na]+ calcd for C28H36ClNO12Na, 636.1824; found, 636.1804.

13

Methyl-3-chloro-2-(((1S,2S)-2-((2,5-dihydroxy-4-methoxyphenyl)carbamoyl)cyclopropyl)methyl)-4,6-dihydroxybenzoate (13). **12** (19 mg, 0.031 mmol) was dissolved in a 4 N solution of HCl in Dioxanes (1.5 mL) and stirred for 10 min. The reaction was quenched by addition of H_2O, extracted with EtOAc (3 x 25 mL) The combined organic fractions were washed with saturated aqueous NaCl, dried ($Na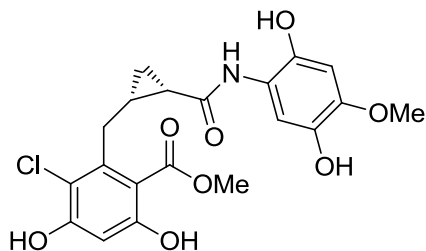_2SO_4$), filtered, and concentrated. The residue was purified via column chromatography (SiO_2 4% MeOH:$CHCl_3$) to afford **13** as a pale yellow oil (13.4 mg, 98%): $[\alpha]_D^{25}$ = -6.17 (c = 0.007 $CHCl_3$); ^{1}H NMR (400 MHz, $CDCl_3$) δ 11.33 (s, 1H), 8.66 (s, 1H), 7.54 (s, 1H), 6.61 (s, 1H), 6.60 (s, 1H), 6.53 (s, 1H), 6.15 (s, 1H), 5.28 (s, 1H), 3.99 (s, 3H), 3.88 (s, 3H), 1.80 (td, J = 8.2, 5.3 Hz, 1H), 1.57 − 1.50 (m, 1H), 1.40 (dt, J = 6.9, 5.1 Hz, 1H), 1.09 (td, J = 8.3, 4.6 Hz, 1H); ^{13}C NMR (101 MHz, $CDCl_3$) δ 171.7, 171.0, 170.8, 163.0, 156.2, 145.7, 142.7, 142.4, 139.1, 118.0, 107.8, 107.0, 103.3, 102.8, 56.1, 52.5, 29.1, 22.2, 21.1, 13.2; IR (film) vmax 3018, 2399, 1658, 1604, 1496, 1434, 1319, 1238, 1207, 1172, 1122, 754, 669 cm^{-1}; HRMS (ESI+) *m/z*: [M + Na]+ calcd for C20H20ClNO8Na, 460.0775; found, 460.0757.
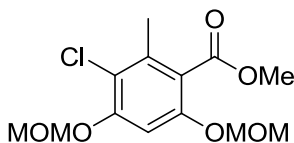
15

Methyl 2,4-bis(methoxymethoxy)-6-methylbenzoate (15). A solution of methyl **14**[101] (4.54 grams, 10.2 mmol) in THF (50 mL) was treated with a 1.0 M solution of tetrabutylammonium fluoride (30 mL, 30 mmol) and allowed to stir for 12 hours. The reaction was quenched by the addition of saturated aqueous ammonium chloride and extracted with EtOAc (3 x 150 mL). The combined organic fractions were washed with saturated aqueous NaCl, dried (Na_2SO_4), filtered, and concentrated. The residue was purified via column chromatography (SiO_2 30% EtOAc:Hexanes) to afford crude product as a colorless oil (2.15g, 97%)

The crude product (2.15 grams, 9.95 mmol) in THF (50 mL) was cooled to 0°C and treated dropwise with diisopropylethyl amine (7.0 mL, 39.8 mmol) followed by the addition of MOMCl (6.75 mL, 39.8 mmol) and allowed to warm to room temperature overnight. The reaction was quenched by the addition of H_2O and extracted with EtOAc (3 x 150mL). The combined organic fractions were washed with saturated aqueous NaCl, dried (Na_2SO_4), filtered, and concentrated. The residue was purified via column chromatography (SiO_2 20% EtOAc:Hexanes) to afford **14** over two steps as a colorless oil (2.679g, 87%): ^{1}H NMR (400 MHz, $CDCl_3$) δ 6.91 (s, 1H), 5.26 (s, 2H), 5.16 (s, 2H), 3.92 (s, 3H), 3.52 (s, 3H), 3.48 (s, 3H), 2.33 (s, 3H); ^{13}C NMR (126 MHz, $CDCl_3$) δ 167.9, 154.1, 152.9, 135.3, 120.0, 117.4, 101.4, 95.1, 56.5, 56.3, 52.4, 17.6; IR (film) vmax 3419, 2952, 2347, 1731, 1595, 1477, 1433, 1400, 1321, 1261, 1220, 1135, 1108, 1041, 962, 931, 827, 713 cm^{-1}; HRMS (ESI+) *m/z*: [M + Na]+ calcd for C13H17ClO6Na, 327.0611; found, 327.0599.
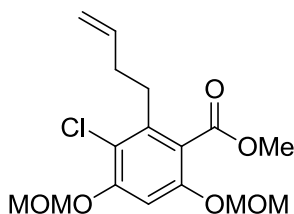
methyl 2-(but-3-en-1-yl)-3-chloro-4,6-bis(methoxymethoxy)benzoate (16). A solution of **14** (1.27 grams, 4.19 mmol) in THF (25 mL) was treated with a fresh 1.0M solution of Lithium Diisopropylamine (4.6 mL, 4.6 mmol) at -78°C and stirred for 5 min. followed by the addition of Allyl Bromide (0.55 mL, 6.3 mmol) at -78°C and warmed to room temperature. The reaction was quenched by the addition of H_2O and extracted with EtOAc (3 x 100 mL). The combined organic fractions were washed with saturated aqueous NaCl, dried (Na_2SO_4), filtered, and concentrated. The residue was purified via column chromatography (SiO_2 30% EtOAc:Hexanes) to afford **15** as a colorless oil (1.346 g, 93%): ^{1}H NMR (500 MHz, $CDCl_3$) δ 6.93 (s, 1H), 5.98 − 5.82 (m, 1H), 5.27 (s, 2H), 5.17 (s, 2H), 5.15 − 4.95 (m, 2H), 3.91 (s, 3H), 3.53 (s, 3H), 3.49 (s, 3H), 2.86 − 2.70 (m, 2H), 2.35 (ddd, J = 11.0, 7.9, 6.7 Hz, 2H); ^{13}C NMR (126 MHz, $CDCl_3$) δ 167.8, 154.4, 153.1, 138.9, 137.7, 119.8, 116.9, 115.0, 101.6, 95.1, 77.3, 77.0, 76.8, 56.5, 56.4, 52.3, 33.4, 31.5; IR (film) vmax 2952, 2829, 2359, 1731, 1593, 1471, 1433, 1398, 1319, 1261, 1220, 1155, 1108, 1093, 1045, 962, 937, 921, 831, 713 cm^{-1}; HRMS (ESI+) *m/z*: [M + Na]+ calcd for C16H21ClO6Na, 367.0924; found, 367.0910.
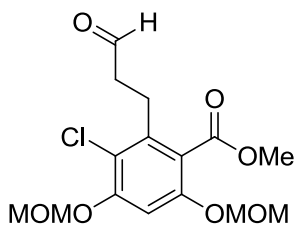
17

methyl 3-chloro-4,6-bis(methoxymethoxy)-2-(3-oxopropyl)benzoate (17). A solution of **15** (1.57 grams, 4.56 mmol) in a mixture of THF:H_2O (1.5 : 1.0, 30 : 10 mL) was treated with Osmium tetraoxide (0.48 mL, 0.3%/wt) and Sodium metaperiodide (2.94 grams, 13.7 mmol) and

allowed to react overnight. The reaction was diluted with H_2O and extracted EtOAc (3 x 150 mL). The combined organic fractions were washed with aqueous NaCl, dried (Na_2SO_4), filtered, and concentrated. The residue was purified via column chromatography (SiO_2, 20% EtOAc:Hexanes) to afford **16** as a yellow oil (1.018 g, 64%): ^{1}H NMR (500 MHz, $CDCl_3$) δ 9.84 (s, 1H), 6.96 (s, 1H), 5.27 (s, 2H), 5.17 (s, 2H), 3.90 (s, 3H), 3.53 (s, 3H), 3.49 (s, 3H), 2.99 (dd, $J = 9.3$, 6.6 Hz, 2H), 2.82 (dd, $J = 9.3$, 6.5 Hz, 2H); ^{13}C NMR (126 MHz, $CDCl_3$) δ 200.8, 167.5, 154.5, 153.4, 137.6, 119.7, 116.7, 101.9, 95.1, 56.6, 56.4, 52.5, 43.3, 24.4; IR (film) vmax 2952, 2906, 2829, 1724, 1593, 1473, 1433, 1400, 1321, 1298, 1263, 1223, 1155, 1107, 1094, 1043, 968, 939, 827, 756, 713 cm^{-1}; HRMS (ESI+) *m/z*: [M + Na]+ calcd for C15H19ClO7Na, 369.0717; found, 369.0724.
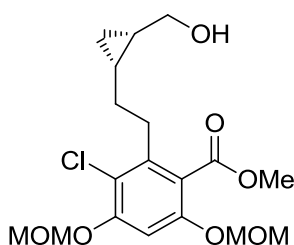
18

(Z)-methyl 3-chloro-2-(5-methoxy-5-oxopent-3-en-1-yl)-4,6-bis(methoxymethoxy)benzoate (18). A solution of 18-crown-6 (3.80 grams, 14.3 mmol) in THF (50 mL) was added methyl 2-(bis(2,2,2-trifluoroethoxy)phosphoryl)acetate (0.64 mL, 3.0 mmol) and cooled to -78°C followed by treatment with a 0.5M solution of KHMDS in toluene (6.3 mL, 3.15 mmol) and stirred for 45 min. A separate solution of **16** (0.988 grams, 2.86 mmol) was dissolved in THF (10 mL) and cooled to -78°C and added dropwise to the first solution and stirred for 30 min at -78°C. The

reaction was quenched by the addition of saturated aqueous ammonium chloride and extracted with EtOAc (3x150mL). The combined organic fractions were washed with aqueous NaCl, dried (Na$_2$SO$_4$), filtered, and concentrated. The residue was run through a plug (SiO$_2$, 20% EtOAc:Hexanes) to afford crude *cis*-ester as a pale yellow oil as a yellow oil (1.073g, 93%): ^{1}H NMR (400 MHz, CDCl$_3$) δ 6.94 (s, 1H), 6.26 (dt, *J* = 11.5, 7.3 Hz, 1H), 5.81 (dt, *J* = 11.5, 1.5 Hz, 1H), 5.26 (s, 2H), 5.16 (s, 2H), 3.91 (s, 3H), 3.72 (s, 3H), 3.53 (s, 3H), 3.48 (s, 3H), 2.96 (dd, *J* = 9.7, 5.7 Hz, 2H), 2.89 – 2.76 (m, 2H).

A solution of crude *cis-ester* (0.061 grams, 0.15 mmol) in DCM (1.5 mL) was cooled to -78°C and treated with fresh 1.0M solution of DIBAL-H (0.25 mL, 0.23 mmol), this solution was stirred at -78°C and monitored by TLC. Once the reaction was shown to be complete by TLC the reaction was quenched by the addition of MeOH at -78°C and allowed to warm to room temperature. Once the reaction was warmed to room temperature saturated sodium potassium tartrate was added to the stirring solution and extracted with EtOAc (3 x 30 mL). The combined organic fractions were washed with saturated aqueous NaCl, dried (Na$_2$SO$_4$), filtered, and concentrated. The residue was purified via column chromatography (SiO$_2$ 2% MeOH:DCM) to afford crude alcohol as a pale yellow oil (0.024g, 43%): ^{1}H NMR (400 MHz, CDCl$_3$) δ 6.93 (s, 1H), 5.75 – 5.53 (m, 2H), 5.26 (s, 2H), 5.16 (s, 2H), 4.18 (d, *J* = 5.9 Hz, 2H), 3.91 (d, *J* = 3.2 Hz, 3H), 3.53 (s, 3H), 3.48 (s, 3H), 2.82 – 2.66 (m, 2H), 2.50 – 2.28 (m, 2H), 1.47 (s, 1H).

A solution of crude alcohol (0.104 grams, 0.28 mmol) in DCM (1.5 mL) was added (4R,5R)-2-Butyl-N,N,N',N'-tetramethyl-1,3,2-dioxaborolane-4,5-dicarboxamide (0.09 mL, 0.30 mmol) and stirred for 30 min. A second solution of ZnEt$_2$ (1.2 mL, 1.26 mmol) in DCM (2 mL) at 0°C was added DME (0.19 mL, 1.26 mmol) followed by dropwise addition of Diiodomethane (0.21 mL, 2.52 mmol) and stirred for 15 minutes. The solution containing the alcohol was added

dropwise to the solution containing the carbenoid, warmed to room temperature and allowed to react overnight. The reaction was quenched by addition of saturated ammonium chloride solution and extracted with EtOAc (3 x 150 mL). The combined organic fractions were washed with saturated aqueous NaCl, dried (Na$_2$SO$_4$), filtered, and concentrated. The residue was purified via column chromatography (SiO$_2$ 2% MeOH:DCM) to afford **18** (0.083g, 76%) as a colorless oil: [α]$_D^{25}$ = -15.89 (c = 0.041 CHCl$_3$); ^{1}H NMR (500 MHz, CDCl$_3$) δ 6.92 (s, 1H), 5.26 (s, 2H), 5.16 (s, 2H), 3.92 (s, 3H), 3.72 (dd, J = 11.4, 6.7 Hz, 1H), 3.59 – 3.54 (m, 1H), 3.52 (s, 3H), 3.48 (s, 3H), 2.81 (ddd, J = 9.6, 6.4, 2.9 Hz, 2H), 1.81 – 1.54 (m, 3H), 1.18 (ddd, J = 8.4, 6.6, 5.7 Hz, 1H), 1.01 – 0.92 (m, 1H), 0.75 (td, J = 8.4, 4.7 Hz, 1H), 0.01 (dd, J = 10.4, 5.4 Hz, 1H); ^{13}C NMR (126 MHz, CDCl$_3$) δ 168.1, 154.4, 153.1, 139.2, 119.6, 116.8, 101.5, 95.1, 63.0, 56.5, 56.3, 52.5, 32.4, 28.5, 18.6, 16.2, 9.0; IR (film) vmax 2950, 2829, 2362, 1730, 1591, 1467, 1433, 1400, 1319, 1263, 1220, 1184, 1153, 1108, 1093, 1045, 962, 933, 831, 713 cm^{-1}; HRMS (ESI+) *m/z*: [M + Na]+ calcd for C18H25ClO7Na, 411.1187; found, 411.1182.
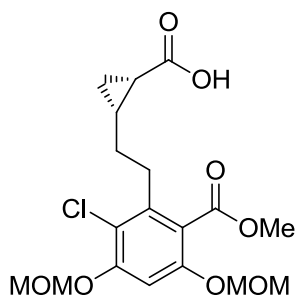

19

(1S,2R)-2-(2-chloro-6-(methoxycarbonyl)-3,5-bis(methoxymethoxy)phenethyl)cyclopropanecarboxylic acid (19). A solution of **18** (0.088 grams, 0.226 mmol) in DCM (2 mL) was cooled to 0°C and treated with (0.114 grams, 0.27

mmol) Dess-Martin Periodinane, which was stirred at 0°C for 1 hr then allowed to warm to room temperature and stirred for 3 hrs. The reaction was quenched by the addition of a (1:1) solution of saturated Sodium Bicarbonate and saturated Sodium Thiosulfate and allowed to stir for 30 min and extracted with EtOAc (3 x 50 mL). The combined organic fractions were washed with saturated aqueous NaCl, dried (Na$_2$SO$_4$), filtered, and concentrated. The residue was purified via column chromatography (SiO$_2$ 40% EtOAc:Hexanes) to afford crude aldehyde as a colorless oil (0.059g, 68%).

The crude aldehyde was dissolved in t-BuOH (1 mL) and treated with of 2-methyl-2-butene (0.65 mL, 5.51 mmol), while a separate solution of sodium chlorite (0.118 grams, 1.04 mmol) in a buffered solution of made of sodium phosphate monobasic (0.169 grams, 1.38 mmol) in H$_2$O (3 mL). The oxidizing solution was added dropwise to the solution containing aldehyde and allowed to react for 12 hrs. This reaction was diluted with saturated aqueous NaH$_2$PO$_4$ and extracted with DCM (3 x 50 mL), dried (Na$_2$SO$_4$), filtered, and concentrated to afford **19** as a pale yellow oil (0.58 g, 94%): $[\alpha]_D^{25}$ = -11.53 (c = 0.0189 CHCl$_3$); ^{1}H NMR (500 MHz, CDCl$_3$) δ 6.83 (s, 1H), 5.16 (d, J = 2.4 Hz, 2H), 5.07 (s, 2H), 3.82 (s, 3H), 3.44 (s, 3H), 3.39 (s, 3H), 2.80 – 2.65 (m, 2H), 1.82 (td, J = 8.6, 1.5 Hz, 2H), 1.67 – 1.59 (m, 1H), 1.32 – 1.25 (m, 1H), 1.01 (td, J = 8.1, 4.5 Hz, 1H), 0.90 (dt, J = 7.3, 5.1 Hz, 1H); ^{13}C NMR (126 MHz, CDCl$_3$) δ 178.3, 167.8, 154.3, 153.1, 138.7, 120.1, 117.2, 102.0, 95.3, 95.1, 56.5, 56.3, 52.4, 31.4, 26.6, 22.7, 18.2, 14.1; IR (film) vmax 2952, 2831, 1731, 1695, 1591, 1456, 1433, 1398, 1319, 1259, 1220, 1182, 1155, 1107, 1091, 1043, 962, 939, 923, 831, 713 cm^{-1}; HRMS (ESI+) *m/z*: [M + Na]+ calcd for C18H23ClO8Na, 425.0979; found, 425.0972.
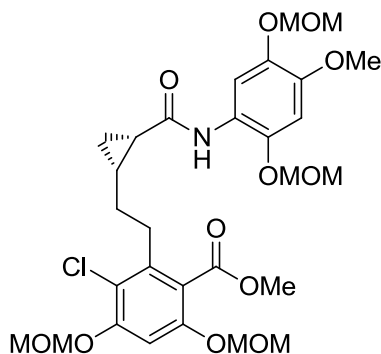
20

Methyl-3-chloro-2-(2-((1R,2S)-2-((4-methoxy-2,5-bis(methoxymethoxy)phenyl)carbamoyl)cyclopropyl)ethyl)-4,6-bis(methoxymethoxy)benzoate (20). A solution of **19** (0.015 grams, 0.037 mmol) in DMF (0.5 mL) was added to a premade solution of 4-methoxy-2,5-bis(methoxymethoxy)aniline (0.010 grams, 0.037 mmol) in DMF (0.5 mL) and cooled to 0°C followed by the dropwise addition of diisopropylethyl amine (0.013 mL, 0.075 mmol) and COMU (0.016 grams, 0.037 mmol). This was stirred for 1 hr at 0°C, then allowed to warm to room temperature and stirred for an additional 2 hrs. The solution was diluted with EtOAc (50 mL) and washed with 1 N HCl, saturated aqueous NaHCO$_3$, and saturated aqueous NaCl. The organic fraction was dried (Na$_2$SO$_4$), filtered, and concentrated. The residue was purified via column chromatography (SiO$_2$ 2% MeOH:DCM) to afford **20** (0.0195 g, 84%) as a yellow oil: $[\alpha]_D^{25}$ = -17.72 (c = 0.010 CHCl$_3$); ^{1}H NMR (500 MHz, CDCl$_3$) δ 8.14 (s, 1H), 7.69 (s, 1H), 6.78 (s, 1H), 6.72 (s, 1H), 5.23 – 4.94 (m, 8H), 3.88 – 3.73 (m, 6H), 3.44 (t, J = 4.0 Hz, 6H), 3.41 (s, 3H), 3.38 (s, 3H), 2.77 – 2.66 (m, 2H), 1.81 (ddd, J = 15.5, 12.9, 7.6 Hz, 2H), 1.63 – 1.55 (m, 2H), 1.05 – 0.98 (m, 1H), 0.96 – 0.88 (m, 1H); ^{13}C NMR (126 MHz, CDCl$_3$) δ 168.9, 167.8, 154.3, 153.0, 146.0, 141.3, 140.8, 139.0, 122.2, 120.0, 117.1, 110.7, 101.5, 101.0, 96.3, 95.1, 56.4, 52.4, 31.5, 29.8, 26.7,

21.7, 21.4, 11.8; IR (film) vmax 2952, 2852, 1728, 1677, 1591, 1523, 1469, 1392, 1319, 1265, 1213, 1186, 1151, 1108, 1081, 1043, 991, 970, 923, 869, 833, 713 cm^{-1}; HRMS (ESI+) *m/z*: [M + Na]+ calcd for C29H38ClO12Na, 650.1980; found, 650.1960.
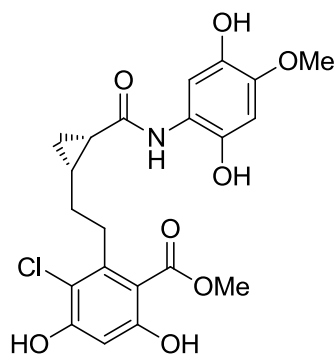
21

methyl3-chloro-2-(2-((1R,2S)-2-((2,5-dihydroxy-4-methoxyphenyl)carbamoyl)cyclopropyl)ethyl)-4,6-dihydroxybenzoate (21). **20** (0.017 grams, 0.027 mmol) was dissolved in a 4 N solution of HCl in Dioxanes (1.5 mL) and stirred for 10 min. The reaction was quenched by addition of H_2O, extracted with EtOAc (3 x 25 mL) The combined organic fractions were washed with saturated aqueous NaCl, dried (Na_2SO_4), filtered, and concentrated. The residue was purified via column chromatography (SiO_2 4% MeOH:CHCl$_3$) to afford **21** (0.0084g, 69%) as a pale yellow oil: $[\alpha]_D^{25}$ = -1.43 (c = 0.0042 CHCl$_3$); ^{1}H NMR (400 MHz, CDCl$_3$) δ 11.40 (s, 1H), 8.67 (s, 1H), 7.45 (s, 1H), 6.58 (s, 1H), 6.53 (s, 1H), 6.49 (s, 1H), 6.14 (s, 1H), 5.26 (s, 1H), 3.96 (s, 3H), 3.86 (s, 3H), 3.25 − 3.17 (m, 2H), 1.95 − 1.84 (m, 2H), 1.76 (td, *J* = 7.9, 5.3 Hz, 1H), 1.41 (dt, *J* = 15.7, 7.9 Hz, 1H), 1.20 − 1.12 (m, 2H); ^{13}C NMR (126 MHz, CDCl$_3$) δ 171.7, 171.0, 163.0, 156.1, 145.6, 142.8, 142.6, 139.0, 118.1, 118.0, 107.7, 103.3, 102.5, 56.1, 52.4, 32.5, 26.6, 22.4, 20.8, 12.8; IR (film) vmax 3352, 2952, 2358, 2341, 1654, 1602, 1496, 1436, 1319, 1240, 1205, 1172, 1120, 948, 873, 844,

804, 754, 721 cm^{-1}; HRMS (ESI+) *m/z*: [2M + Na]+ calcd for C42H44Cl2N2O16Na, 925.1966; found, 925.1924.

Anti-proliferation Assay

MCF-7 and SKBr3 cells were maintained in a 1:1 mixture of Advanved DMEM/F12 (Gibco) supplemented with non-essential amino acids, L-glutamine (2 mM), streptomycin (500 µg/mL), penicillin (100 units/mL), and 10% FBS. Cells were grown to confluence in a humidified atmosphere (37°C, 5% CO_2), seeded (2000/well, 100 µL) in 96-well plates, and allowed to attach overnight. Each compound or GDA at varying concentrations in DMSO (1% DMSO final concentration) was added, and cells were returned to the incubator for 72 hours. At 72 hours, the number of viable cells was determined using an MTS/PMS cell proliferation kit (Promega) per the manufacturer's instructions. Cells incubated in 1% DMSO were used as 100% proliferation, and values were adjusted accordingly. IC_{50} values were calculated from separate experiments performed in triplicate using GraphPad Prism.

Chapter 3

Development of (-)-Epigallocatechin 3-gallate (EGCG) as an Hsp90 Inhibitor

I.   Introduction

Green tea, the second most widely consumed beverage worldwide, contains a class of polyphenolic catechins that account for approximately 40% of the total dry weight of green tea leaves. (-)-Epigallocatechin 3-gallate (EGCG) shown in figure 20 is the main polyphenolic catechin within this class, which, because of its anti-oxidative properties, has been considered as a potential treatment for several diseases.[122-125] Moreover, anti-tumor properties have been associated with EGCG. Although the pathway through which EGCG exerts its anti-cancer activity is unknown, cyclin dependant kinases, mitogen-activated protein

Figure 20 - Structure of EGCG

kinase (MAPK), matrix metalloproteinases, proteosomes, DNA methyltransferase, BCL-2, receptor tyrosine kinase (RTK) pathways, aryl hydrocarbon receptor (AhR) and Hsp90 have been implicated as potential targets for EGCG.[90,126]
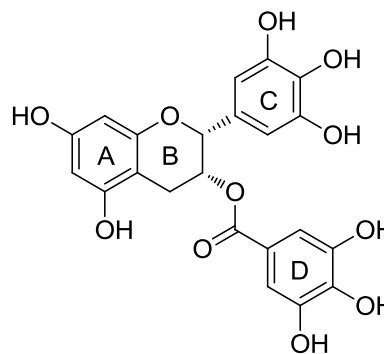
In an effort to elucidate the mechanism through which EGCG exerts its activity, its interaction with the aryl hydrocarbon receptor (AhR) was identified. EGCG was believed to bind the AhR and act as an antagonist, thereby preventing tumor progression. However, this activity was subsequently attributed to the ability of EGCG to bind Hsp90.

Knowledge that EGCG binds Hsp90 and subsequent studies identified this interaction to be specific to the C-terminus and were essential in guiding the design of Hsp90-specific inhibitors based upon the EGCG scaffold. Computer modeling of EGCG using a model of the Hsp90 C-terminal nucleotide binding site allowed the potential identification of key substitutions for explorations aimed at increasing its affinity for Hsp90.[127] Structural similarities between EGCG and the KU series of novobiocin analogues allowed for the incorporation of previously determined SAR into the development of EGCG-based inhibitors.

II.   EGCG as an AhR Antagonist

AhR is a ligand-activated transcription factor, which, upon activation by flavonoids, environmental contaminants or indoles, mediates the toxic effects of these molecules. AhR is found in a dormant state in the cellular cytoplasm and associates with two Hsp90 homodimers, XAP2, and p23.[128] Upon ligand binding, a cascade occurs, including translocation to the nucleus, release of the Hsp90 homodimers, and dimerization with aryl hyrdocarbon receptor nuclear translocator (AHRT).[88] This AhR-AHRT complex binds consensus sequences located in the promoter regions of responsive genes to modulate transcription (Figure 21). The mechanism of forming the intact complex and translocation into the cell nucleus are not well characterized, but experiments using 2,3,7,8-tetrachlorodibenzo-*p*-dioxin (TCDD) have resulted in the proposed mechanism described in Figure 2. TCDD-induced *CYP1A1* gene expression studies indicated that the TCDD-AHRT complex enhances translation through specific interactions with genomic sequences, resulting in increased *CYP1A1* expression levels.[129] Subsequent studies using Hepa 1c1c7 cells, which are deficient in AHRT, did not show increased levels of *CYP1A1* and confirmed the essential role of AHRT in mediating the observed changes in expression.
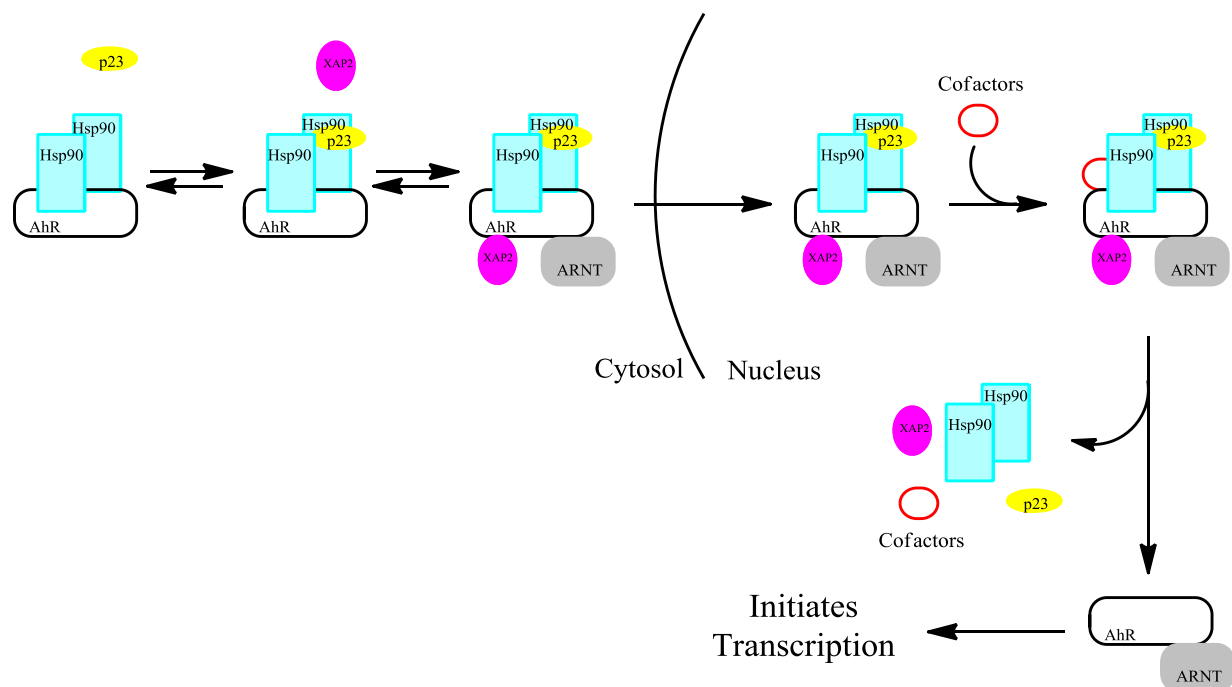
Figure 21 - Mechanism of AhR-mediated transcription
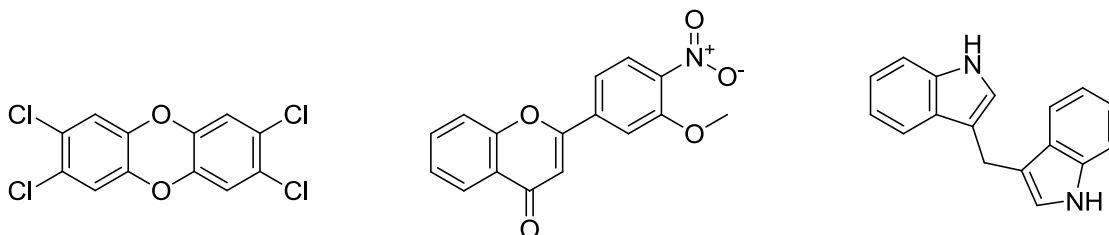
Figure 22 - Antagonists of AhR: TCDD (left), 3M4NF (center), and DIM (right)

Hsp90 has been implicated as an essential component in this pathway, specifically mediating proper folding and stabilizing the intact complex. Additional studies have shown that while in Hsp90 is complexed with AhR, it inhibits transcriptional activation either through interfering with ARNT dimerization or blocking interactions with the C-terminal transactivation domains or other cofactors.[130-131] Two of the most characterized AhR antagonists are 3'-methoxy-4'-nitroflavone (3M4NF), a synthetic flavonoid, and 3,3'-diindolylmethane (DIM), an indole derivative (Figure 22). These inhibitors function as antagonists through direct competitive

binding to the AhR ligand binding site. Although both molecules target the same binding site, they produce divergent effects on AhR.
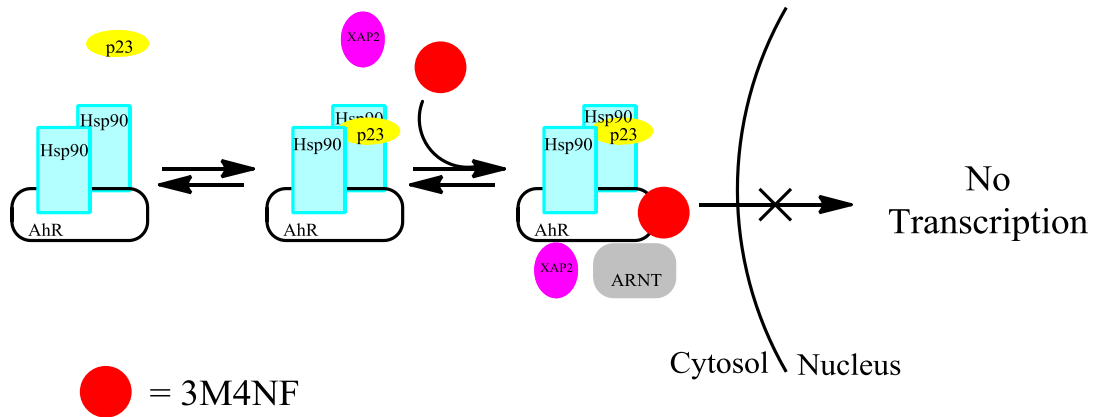
Figure 23 - 3M4NF-mediated mechanism of AhR inhibition

Binding of the inhibitor, 3M4NF, to the AhR complex results in a conformational change within the AhR complex, which prevents exposure of its nuclear localization sequence. Because this sequence is not recognizable, the AhR complex is unable to translocate to the nucleus of the cell and the intact complex is retained in the cytoplasm (Figure 23). In contrast, binding of DIM to AhR does not inhibit complex formation or translocation into the nucleus. However, once in the nucleus, the DIM-bound complex is unable to recruit the proper cofactors to initiate transcription (Figure 24). These findings indicate that structurally diverse molecules are capable of binding and inhibiting AhR through divergent mechanisms.
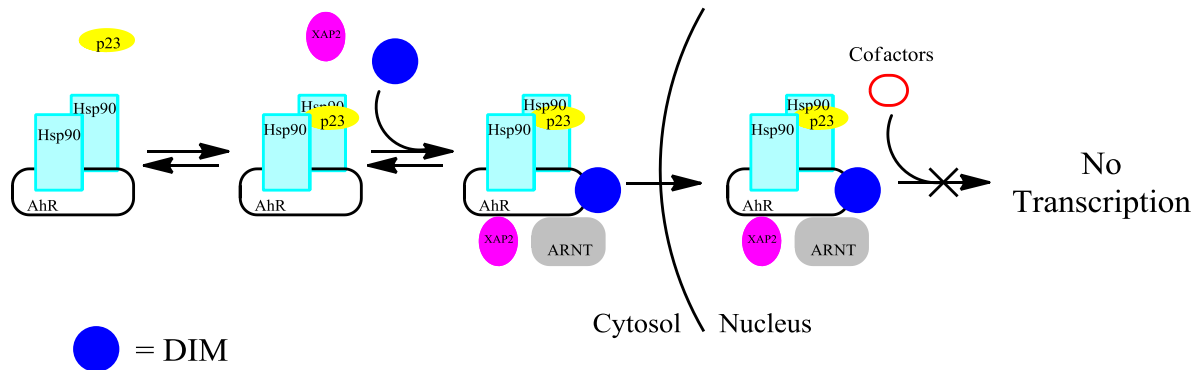
Figure 24 - DIM-mediated mechanism AhR inhibition

In 2005 Palermo and co-workers identified that EGCG antagonizes AhR. Due to structural similarities between EGCG and 3M4NF, this group proposed that EGCG was functioning as a competitive inhibitor of AhR. However, competitive binding assays using low-affinity conditions did not produce the expected results, suggesting EGCG does not bind directly to the AhR. Further investigation indicated that EGCG binds Hsp90, allowing for nuclear translocation of the AhR complex, but this complex is unable to bind DNA thus is unable to promote gene transcription. In 2009 Yin and co-workers sought to identify the binding site of EGCG on Hsp90. As previously discussed, GDA and novobiocin bind to and inhibit Hsp90 through interactions with N-terminal and C-terminal nucleotide binding sites, respectively. Proteolytic footprinting is a technique used to characterize Hsp90 inhibitors based upon the differential fragmentation patterns of Hsp90 produced upon exposure to each inhibitor. Based upon the class of inhibitors used, a unique footprint for N-terminal inhibitors and C-terminal inhibitors is observed. Thus, the EGCG footprinting experiments, in combination with Hsp90 terminus-specific antibodies, determined that EGCG binds to a 50 kDa band located within the Hsp90 C-terminus. Comparison of these proteolytic footprints of EGCG to those for novobiocin

confirmed the two to be very similar, indicating that EGCG binds the C-terminus.[132] The proposed mechanism of AhR inhibition by EGCG is summarized in Figure 25.
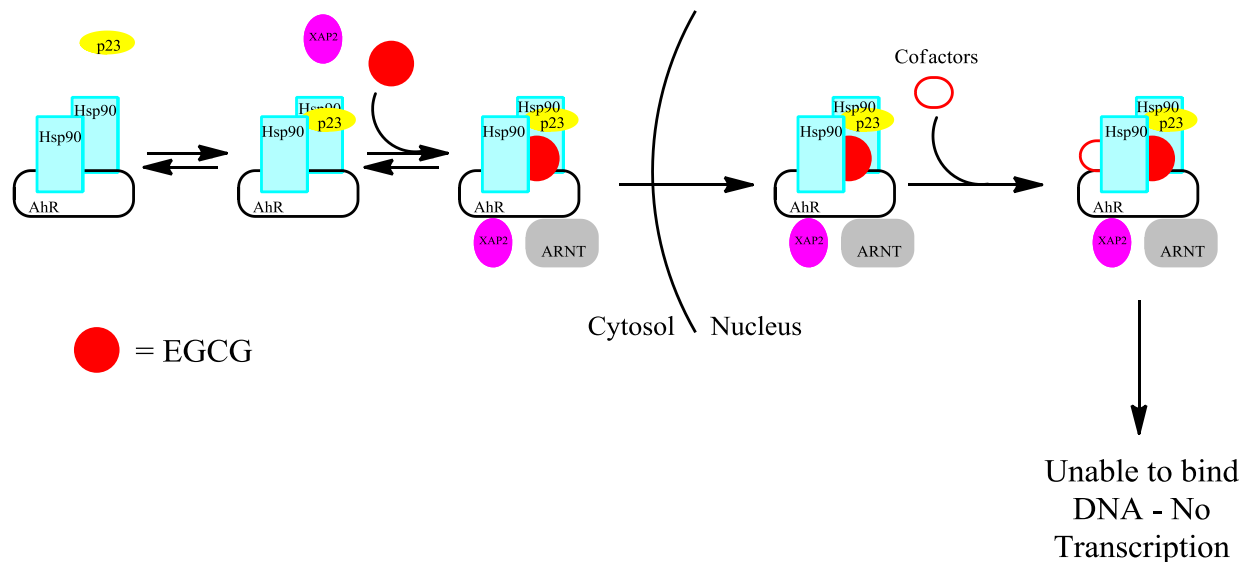
Figure 25 - EGCG-mediated mechanism of AhR inhibition

Further investigation into EGCG inhibition of Hsp90 was executed using a firefly luciferase assay. This assay employs Hsp90 to refold heat denatured firefly luciferase and examines the ability of a compound to interfere with this normal Hsp90 function. Hsp90, Hsp70, and Hsp40, isolated from rabbit reticulysate and incubated with EGCG, showed concentration-dependent inhibition of luciferase refolding. This data further confirms that EGCG manifests its activity through Hsp90 inhibition and validated this compound as a novel scaffold for use in the development of C-terminal Hsp90 inhibitors.

III.   EGCG Analogue Development
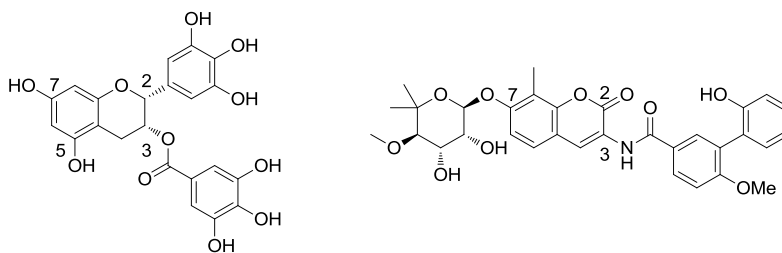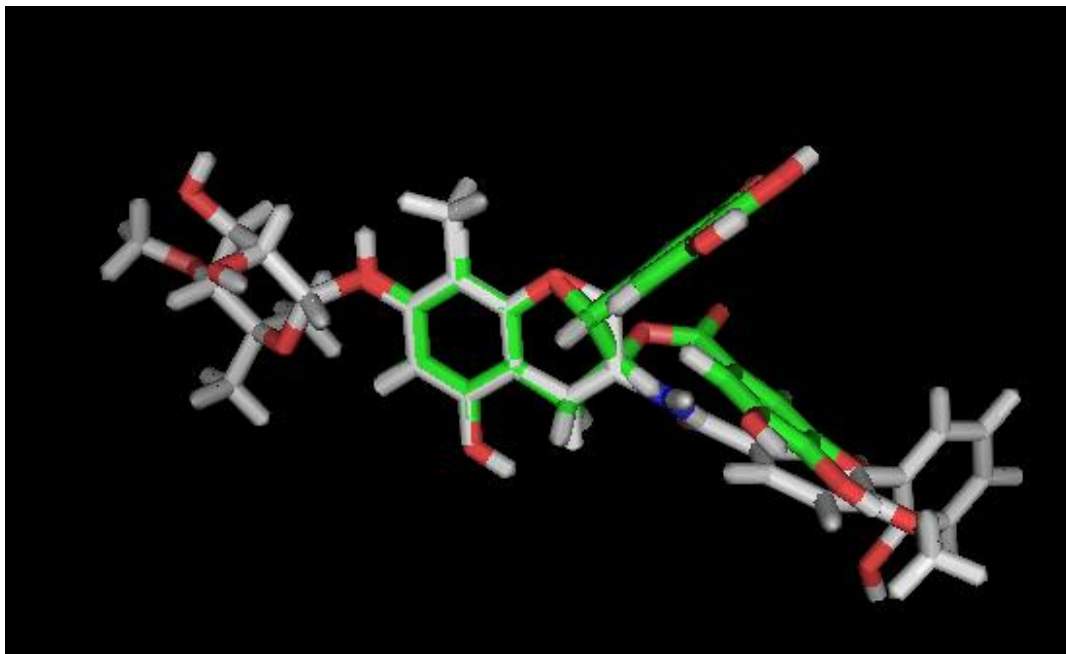
Figure 26 - Overlay of EGCG (green, left) and KU-113 (white, right)

A co-crystal structure with the Hsp90 C-terminal nucleotide binding site has not yet been solved. The known natural antibiotic novobiocin, however, has been identified as a C-terminal binding agent, manifesting an IC_{50} of ~700 μM against SKBr3 cancer cells. In 2008, Burlison and co-workers modified the novobiocin benzamide side chain to improve the anti-cancer activity of this scaffold, identifying KU-113 (Figure 26) as a potent analogue. As seen in Figure 26, structural comparison of EGCG to low micromolar C-terminal novobiocin analogue KU-113 ($IC_{50} = 1.5 \pm 0.1$ μM), revealed the two compounds to exhibit several structural similarities. By

aligning the catechin core of EGCG with the coumarin core of KU-113, a similar substitution pattern becomes evident. The important positions of the KU compounds, especially the 3- and 7-positions, align well with the same positions on EGCG. The noviose sugar, attached through at the 7-position of the coumarin core, has primarily been proposed as a structural feature that can be modified to increase solubility of inhibitors. In addition to the noviose sugar, the 3-position is appended to the biaryl amide, which was identified as a side chain capable of increasing anti-Hsp90 activity. The overlay of EGCG with KU-113 shows the D-ring at the 3-position of EGCG to align and share a common orientation with the benzamide side chain. Using this insight, it was proposed that SAR elucidated for the novobiocin scaffold, specifically with respect to the benzamide side chain, could be applied to the EGCG scaffold to improve its Hsp90 affinity. Incorporation of the prenylated and biaryl side chains, known to result in potent novobiocin analogues upon attachment to the novobiocin scaffold, were selected as structural motifs capable of increasing activity when attached to EGCG. Based upon the structural alignment, the 2-position aryl-linked phenolic ring does not appear make important interactions and was therefore removed from the EGCG analogues, without altering Hsp90 affinity.

A. Computer Modeling of EGCG with the C-terminal Model of Hsp90

Numerous analogues containing modifications to the benzamide side chain, coumarin core, and noviose sugar of novobiocin provided a substantial data that could be used to create a CoMFA model. Laura Peterson, a co-worker in the Blagg laboratory, in association with Dr. Verkhivker, was instrumental in the development of a C-terminal Hsp90 model, which was subsequently applied to the rational development of EGCG analogues. Modeling EGCG to the Hsp90 C-terminus nucleotide site, provided insight into its potential binding orientation.
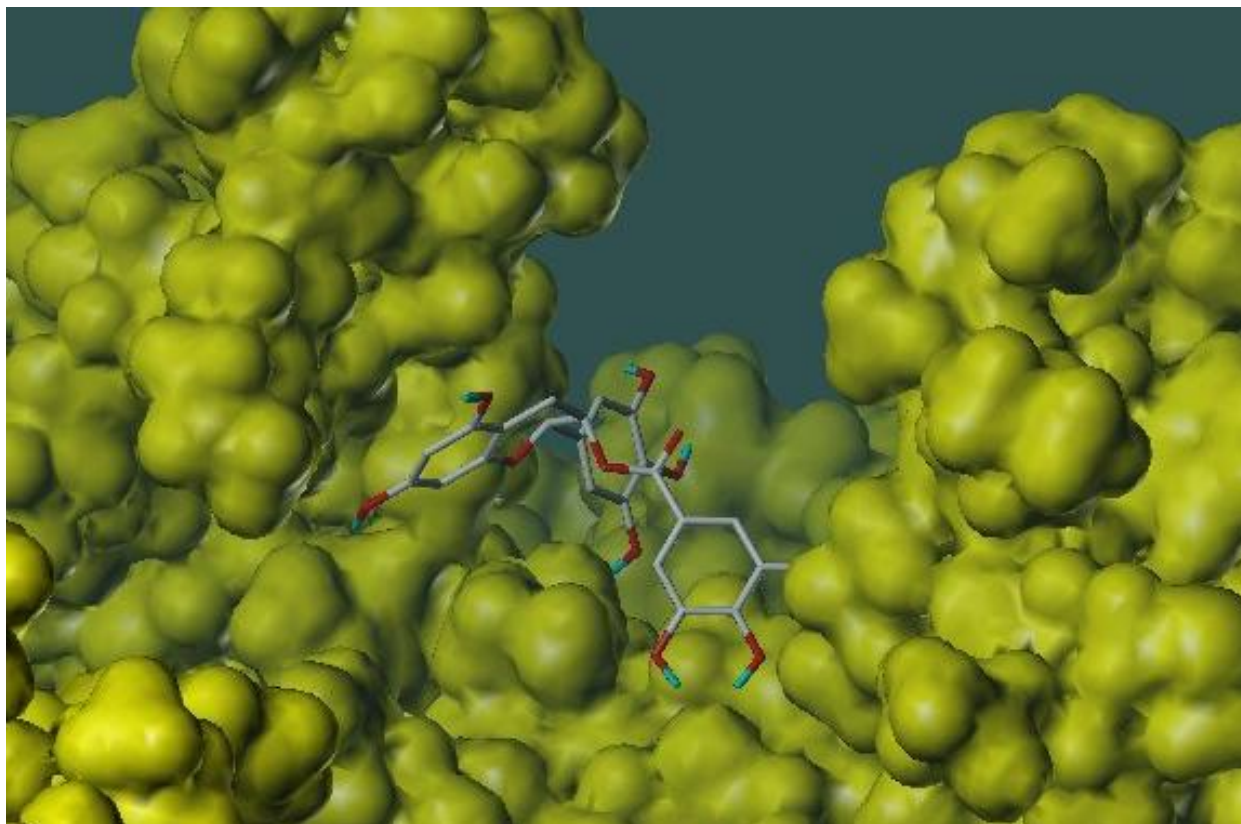
Figure 27 - Modeling of EGCG in the Hsp90α C-terminal model

The modeling study (figure 27) demonstrates that the catechin, comprised of the A- and B-rings, sits in a spacious region of the binding pocket. As such, this portion of the scaffold appears to make essential interactions with the pocket and thus, only slight modifications are likely tolerated without the loss of activity. EGCG binds in a slightly bent conformation, allowing the catechin core to interact on one side, while the ester linked D-ring interacts with the opposing side. The D-ring of EGCG appears to make key interactions with the binding pocket, contacts that can be taken advantage of to increase its Hsp90 affinity. The *meta* position of the D-ring appears to fit into a cavity that would potentially allow for the incorporation of functional groups of various bulk. Substitution at the adjacent *meta* position appears to project directly into the protein, thus substitution at the second *meta* position is thought to be detrimental to Hsp90

affinity. In addition, the *para* position appears to have adequate space for incorporation of various functional groups, although large substituents are not likely to be tolerated. Analogues proposed will probe the size that can be tolerated at the *para* position. In contrast, the C-ring projects out into solvent and, therefore, would not be essential for EGCG binding to Hsp90. Thus, it is envisioned that the C-ring can be excised altogether without compromising the affinity of EGCG for Hsp90. Incorporation of a hydrophobic group in place of the C-ring could be used to increased analogue solubility similar to the manner in which noviose assists novobiocin.

B. Design of Initial EGCG Analogues

In 2008 Jia and co-workers were investigating the effects of EGCG on human hemoglobin and determined that EGCG was capable of producing hydrogen peroxide *in vivo*.[133] EGCG reacts with dissolved oxygen in aqueous media, initiating the production of H_2O_2. Upon further investigation, EGCG was found to produce a molar equivalent of H_2O_2 in solution.[133-134] Analogues based upon EGCG still have the ability to produce H_2O_2 unless specific structural modifications are incorporated to avoid this issue. A study by Arakawa and co-workers showed that increasing the concentration of H_2O_2 with and without similar concentrations of EGCG produced similar antibacterial results. This data indicates that the bactericidal properties of EGCG are likely be attributed to the generation of H_2O_2 rather than EGCG itself.[135] With this property of EGCG in mind, SAR development needed to focus on an inhibitor of Hsp90 that does not produce H_2O_2. Masking the phenols of the catechin as methyl ethers was proposed as a structural modification that could be employed to prevent formation of H_2O_2, which results upon oxidation of the catechol to the *ortho* quinone. Since, it was understood that oxidation of the catechol on the EGCG D-ring under physiological pH has the ability to generate *ortho*-quinones, these electron deficient quinones would have the ability to covalently modify Hsp90 and further

supported masking the phenols as methyl ethers.[136] Thus, initial analogues were designed to mask the EGCG phenols as methyl ethers. Next, as stated above, it was proposed that modifications to the D-ring will allow for the most significant gains in activity and consequently, choices of benzoic acids were carefully considered.
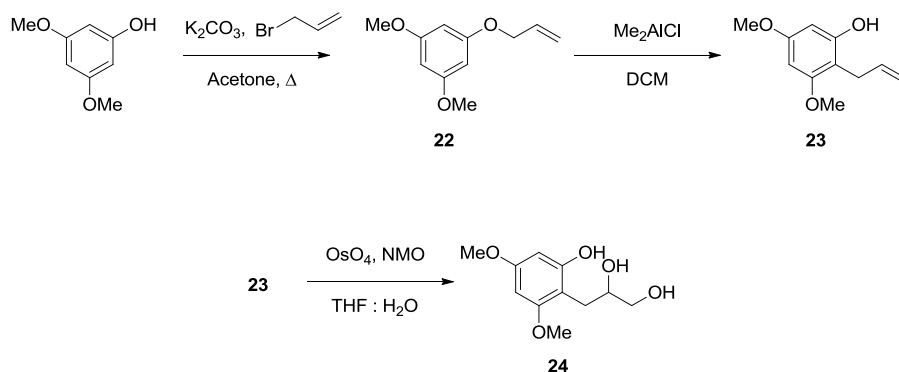
IV.   Synthesis of the Methyl Ether Catechin and Analogues
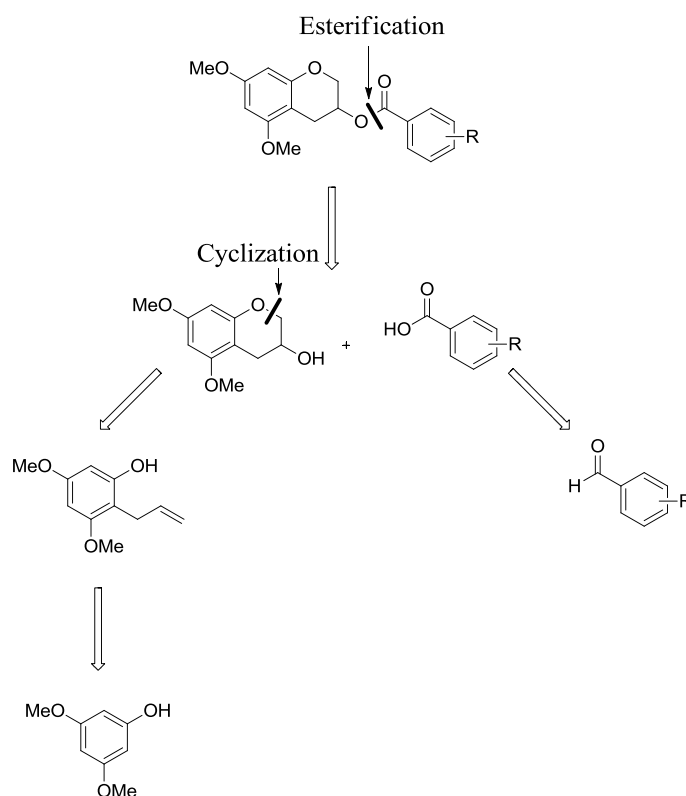
Scheme 8 - Retrosynthetic analysis of EGCG analogues

Retrosynthesis of the EGCG analogues is illustrated in Scheme 8. The intact catechin and the various benzoic acids could be coupled together using standard esterification conditions, which allow for addition of the functionalized D-ring portion of the EGCG analogues at a late

stage in the synthesis. Cyclization of the desired 6–membered catechin could then be accomplished from the allylated dimethoxy phenol precursor.

Scheme 9 - Diol formation in the methyl ether protected catechin

As shown in Scheme 9, preparation of the methyl ether catechin began by allylation of dimethoxy phenol upon heating allyl bromide in the presence of base to produce **22**. Subsequent Claisen rearrangement using dimethylaluminum chloride produced the desired allylated phenol **23** in nearly quantative yield. Dihydroxylation of the terminal olefin with osmium tetraoxide and *N*-morpholine *N*-oxide gave the corresponding diol, **24**, in good yield.[137]

As shown in Scheme 10, several approaches were utilized in an attempt to install the toluene sulfonyl ester onto the primary alcohol **24**. Treatment of **24** with pyridine and tosyl chloride did not produce the desired primary toluene sulfonic ester **24a,** but rather the phenolic sulfonic ester **25**.[138-139] Although the phenolic toluene sulfonic ester **25** was carried into cyclization conditions, this resulted in production of a 5-membered catechin and the desired 6-membered catechin. A second approach involved treatment of **24** with diisopropylethyl amine
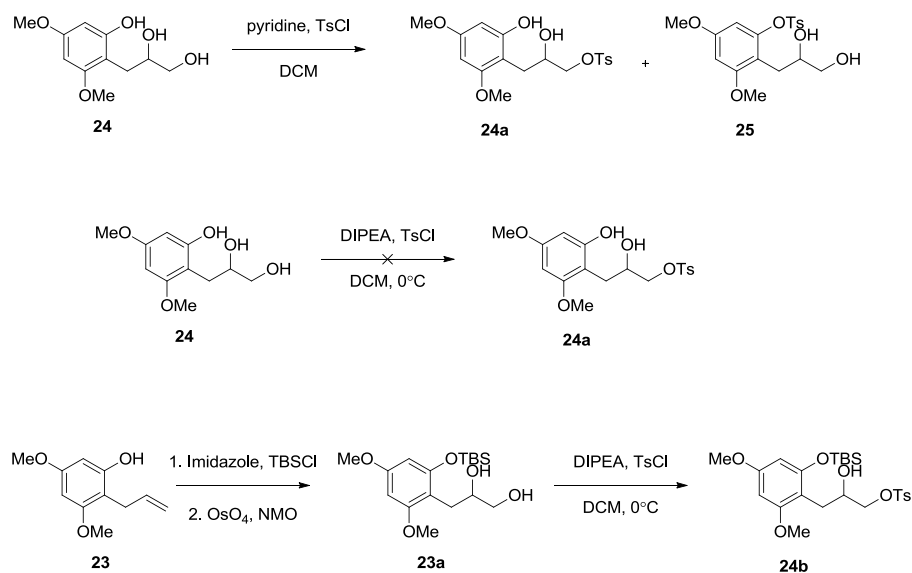
Scheme 10 - Attempts to produce the primary toluene sulfonyl ester

with tosyl chloride at 0°C. This sequence did not result in good conversion and attempts to improve the yield by performing the reaction at room temperature or for longer duration resulted in a mixture of tosylated products. Finally, a modified synthetic strategy that allowed for selective tosylation of the primary alcohol was employed, involving silyl protection of phenol **23** followed by dihydroxylation of the terminal olefin to produce **23a**. Tosylation of the primary alcohol using the procedure enlisting diisopropylethyl amine provided **24b** in poor yields. Unfortunately, this reaction sequence did not produce desired products in adequate yields and was ultimately abandoned.
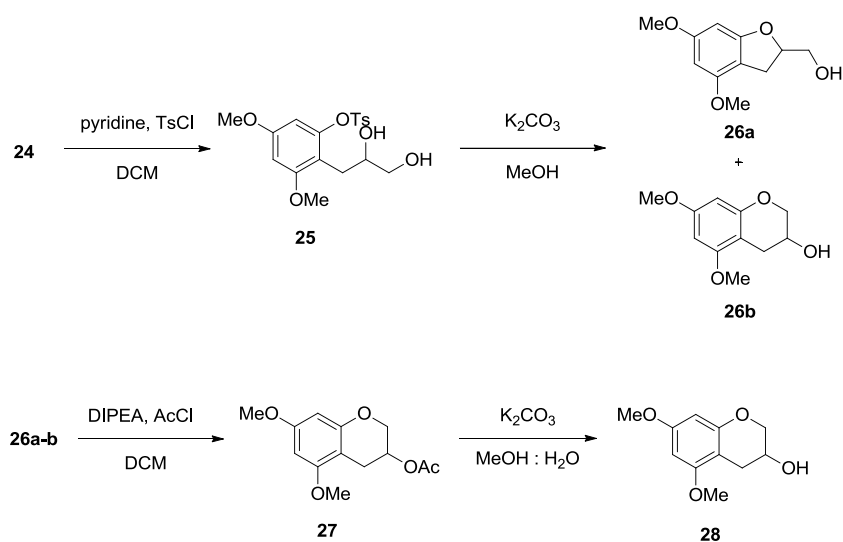
Scheme 11 - Synthesis of the methyl ether catechin

The first sequence shown in Scheme 11, was ultimately chosen due to its ability to convert all of the starting material to the desired phenolic toluene sulfonic ester **25**.[138] Next, cyclization of **25** was accomplished by treatment with base in methanol, producing a 1:1 mixture of the corresponding 5-membered catechin in addition to the desired 6-membered catechin. Unfortunately, these catechins were inseparable to be separated via column chromatography, so the secondary alcohol was acetylated to aid in separation. Acetylation was accomplished by treatment of diisopropylethyl amine and acetyl chloride at 0 °C, leading to products that could easily be separated via column chromatography to produce desired catechin **27**.[140] Solvolysis of **27**, using base in a mixture of methanol and water, produced the desired 6-membered catechin, **28**, in excellent yield.
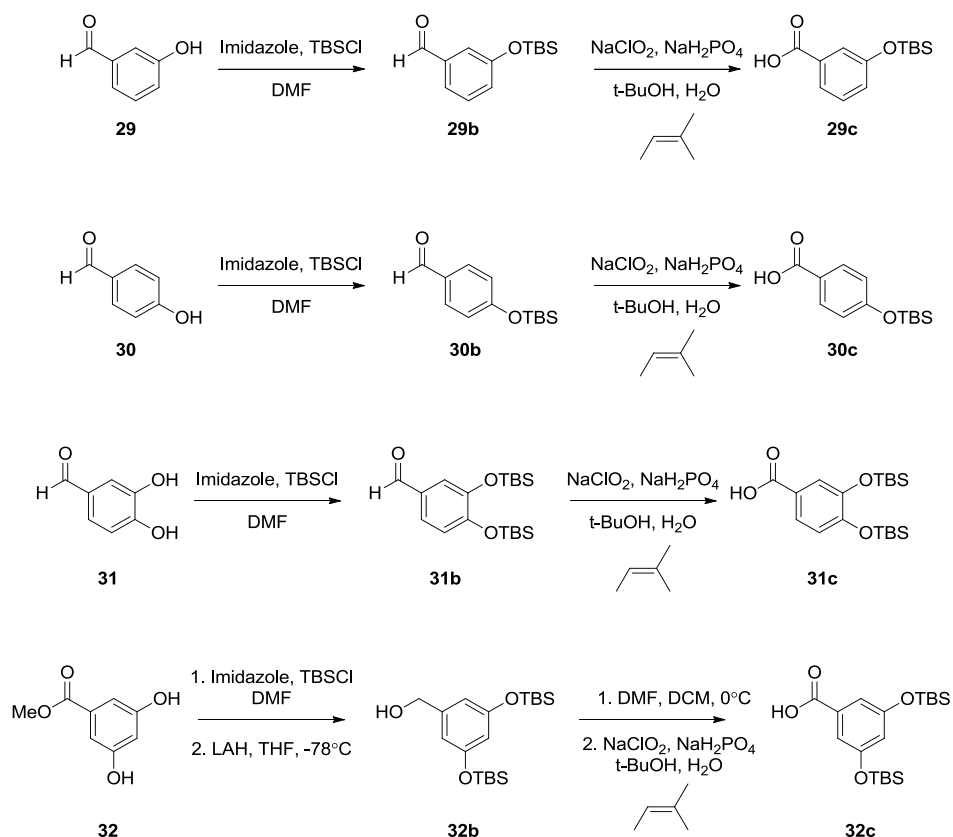
Scheme 12 - Synthesis of desired phenolic D-ring benzoic acids

The various D-rings were either commercially available benzoic acids or synthesized sequentially. D-ring methyloxy phenols were commercially available, while the phenolic analogues were synthesized as the corresponding silyl protected phenols. Synthesis of the prenylated and biaryl acids was accomplished following established procedures.[84-85] Three of the four phenolic D-ring analogues were synthesized using the same conversions, as shown in Scheme 12. Phenolic benzaldehydes **29–31** were protected as the corresponding silyl ethers, upon treatment with imidazole and *tert*-butyldimethylchlorosilane, to produce corresponding benzaldehydes **29b–31b** in good yields. The protected silyl ethers were subsequently oxidized using Pinnick conditions to afford the benzoic acids, **29c–31c**. Synthesis of the remaining
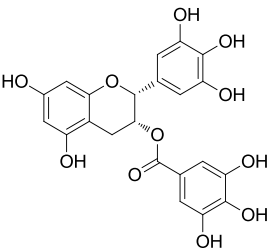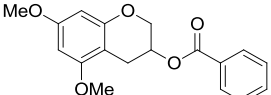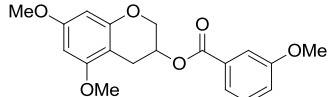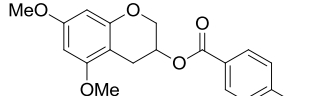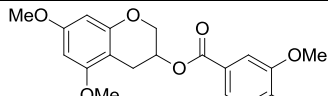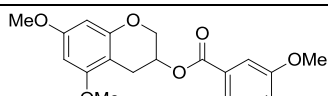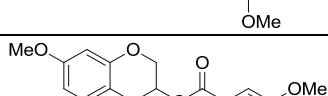
resorcinol analogue began by esterification with refluxing 3,5-dihydroxybenzoic acid in methanol and thionyl chloride to afford **32**. Protection of the phenols was accomplished using similar conditions as described above, followed by reduction of afford the ester to the corresponding primary alcohol **32b**.[141] Oxidation of the primary alcohol to the corresponding benzaldehyde was accomplished using DMP. Finally, Pinnick conditions were employed to quantitatively convert **32b** to the desired acid, **32c**.

33a = R_1 = H, R_2 = H, R_3 = H; 97%
33b = R_1 = OMe, R_2 = H, R_3 = H; 83%
33c = R_1 = H, R_2 = OMe, R_3 = H; 71%
33d = R_1 = OMe, R_2 = OMe, R_3 = H; 98%
33e = R_1 = OMe, R_2 = H, R_3 = OMe; 85%
33f = R_1 = OMe, R_2 = OMe, R_3 = OMe; 74%
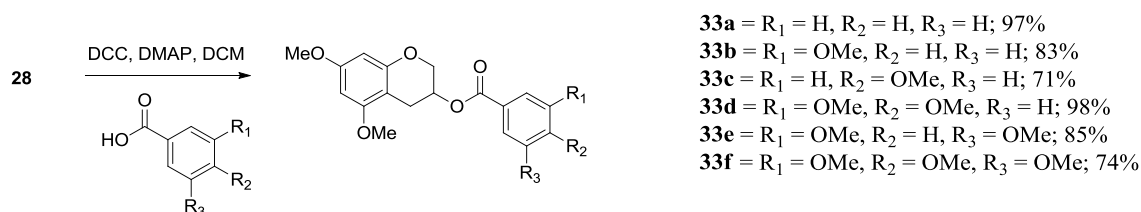
Scheme 13 - Coupling of the methyl D-ring analogues

Following preparation of the desired catechin along with the desired various D-ring derivatives, coupling of the two fragments was attempted. The secondary alcohol of the catechin was found to react with the corresponding phenolic and methoxy benzoic acids, upon activation with *N,N'*-Dicyclohexylcarbodiimide (DCC) and a catalytic amount of DMAP in excellent yields (Scheme 13). Once prepared, the resulting products were screened against MCF-7 and SKBr3 breast cancer cells for their anti-proliferative activities. The results from this screen are shown in Table 3.

Table 3 - Antiproliferative data of the methyl D-ring analogues

Analogue	Structure	MCF7 (µM)	SKBr3 (µM)
EGCG[142]		150	
33a		8.91 ± 0.81^a	14.14 ± 5.98
33b		1.89 ± 0.32	>100
33c		36.7 ± 7.83	>100
33d		10.22 ± 0.175	>100
33e		31.62 ± 1.43	>100
33f		>100	>100

^{a}Values represent mean ± standard deviation for at least two separate experiments performed in triplicate

The methyl ether analogues manifested a wide range of activities. Computer modeling indicated that substitution in the *meta* position would project along the protein and lead to favorable interactions. In agreement with this proposal, analogue **33b** exhibits an IC_{50} of approximately 2µM, which compares well to EGCG, which manifests an IC_{50} value of 150 µM. As described above, substitution at the *para* position orients the molecule towards one side of the pocket, which may allow for small substitutions at this position. Analogue **33c** increases the
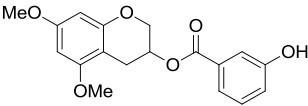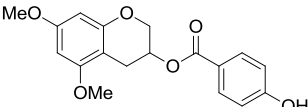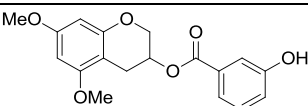
affinity for Hsp90 by taking advantage of this small space, thus increasing in the anti-proliferative activity approximately 4-fold compared to EGCG. As the model suggests, the combination of *meta* and *para* analogues into catechol substitution on the D-ring should increase interactions with the protein. However, the *para* substitution appears to push into size limitations that are incorporated at this position. Although the model suggests this combination would increase the interactions and lead to compounds possessing higher affinity for Hsp90, this was not observed. There is an approximate 5-fold reduction in the anti-proliferative activity when comparing **33b** to **33d**. Additionally, the model suggests that analogues possessing a resorcinol substitution would potentially create an inhibitor–protein steric clash, because the additional *meta* substitution projects into the protein based on the computer modeling. The resorcinol analogue **33e**, decreases affinity as predicted for Hsp90 approximately 15-fold based on the observed anti-proliferative activity. Finally, the 3,4,5-trimethoxy substituted analogue **33f** incorporates *meta* substitutions, allowing for access to the pocket that would increase affinity or ultimately project into the protein and create steric interactions with Hsp90 and decrease affinity. As discussed previously, *para* substitution may not allow for substitutions at this position, which explains the decrease in Hsp90 inhibitory activity observed for this compound.

34a = R$_1$ = OTBS, R$_2$ = H, R$_3$ = H; 96%
34b = R$_1$ = H, R$_2$ = OTBS, R$_3$ = H; 78%
34c = R$_1$ = OTBS, R$_2$ = OTBS, R$_3$ = H; 43%
34d = R$_1$ = OTBS, R$_2$ = H, R$_3$ = OTBS; 95%

35a = R$_1$ = OH, R$_2$ = H, R$_3$ = H; 72%
35b = R$_1$ = H, R$_2$ = OH, R$_3$ = H; 70%
35c = R$_1$ = OH, R$_2$ = OH, R$_3$ = H; 0%
35d = R$_1$ = OH, R$_2$ = H, R$_3$ = OH; 70%
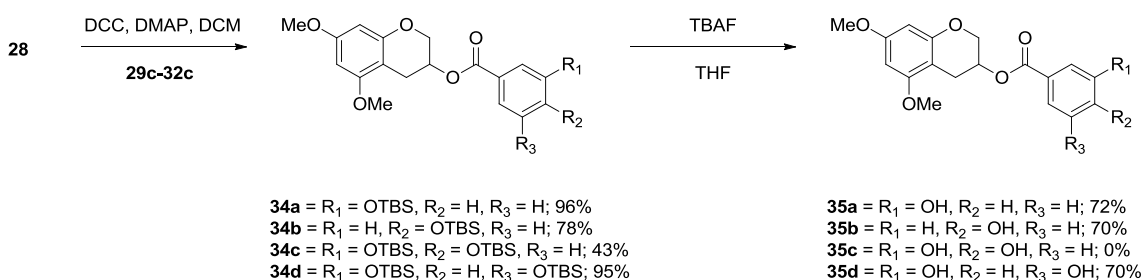
Scheme 14 - Synthesis of the phenolic derivatives of the D-ring

These initial analogues gave valuable insight into the potential binding orientation of the EGCG analogues based on our computer model. The apparent size constraints at the *para* position can be investigated through removal of this methyl ether to yield the corresponding phenol. A series of phenolic analogues, as described above, would also investigate the effect of potential hydrogen bond donors in the *meta* and *para* positions. Synthesis of the phenolic analogues was accomplished using DCC/DMAP coupling of the methyl ether catechin **28** with benzoic acids **29c–32c** in modest to excellent yields (Scheme 14). Next, silyl deprotection using TBAF produced the desired phenol. Unfortunately, the catechol derivative **35c** was unable to be collected via column chromatography, likely due to oxidation to the *ortho* quinone, which subsequently bound to the silica column. The anti-proliferative activities of the series of phenolic derivatives are found in Table 4.

Table 4 - Antiproliferative activity of the D-ring phenolic derivatives

Analogue	Structure	MCF7 (µM)
35a		38.74^a
35b		52.34
35d		>100

^{a}Values represent mean ± standard deviation for one experiment performed in triplicate

Phenolic analogues generally manifested significant decreases in activity. As described above the incorporation of a methoxy group at the *para* position may push the size constraints allowed in this position does not seem to be the determining factor. In contrast, the
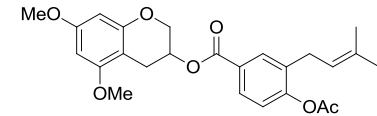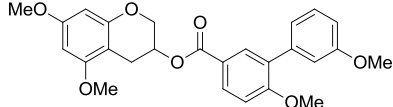
corresponding phenol **35b** revealed that removal of the methyl group at the *para* position resulted in a 2-fold decrease in Hsp90 inhibition. In a similar manner, the *meta* substitution showed a greater decrease in activity, manifesting approximately a 17-fold reduction in inhibitory activity for the free phenol **35a** versus **33b**. These phenolic modifications to the D-ring suggest that hydrogen bond donors located at either the *meta* or *para* positions are detrimental to anti-proliferative activity.
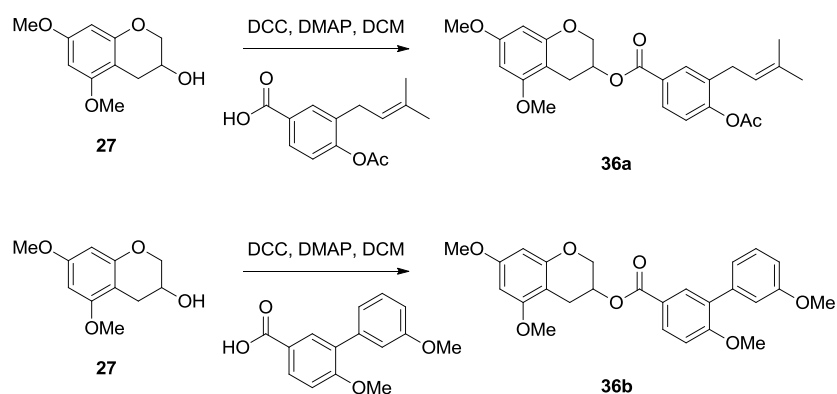
Scheme 15 - Synthesis of the novobiocin-inspired D-ring analogues

Finally, SAR for the benzamide side chain of the KU series of novobiocin analogues developed by Burlison and co-workers was incorporated into the EGCG scaffold. Computer modeling predicted that the prenylated side chain found in the natural product novobiocin would align well with the predicted orientation of EGCG analogues. The addition of the more active biaryl side chain from the KU series of compounds also suggested a favorable binding orientation with Hsp90. The syntheses of both the prenylated and the biaryl acids have been previously reported. Coupling of these two molecules was accomplished using DCC/DMAP to afford desired products in excellent yields (Scheme 15). Upon preparation of the desired compounds, they were evaluated for anti-proliferative activity (Table 5).

Table 5 - Antiproliferative activity of the KU series of inhibitors

Analogue	Structure	MCF7 (µM)
36a		51.82 ± 1.94^a
36b		>100

[a]Values represent mean ± standard deviation for at least two separate experiments performed in triplicate

Biological results of the KU series of inhibitors revealed that incorporation of the prenylated side chain maintains mid-micromolar activity and approximately a 17-fold increase in activity when compared to novobiocin. Computer modeling shows that the *meta* prenyl group could project alongside Hsp90, allowing for hydrophobic interactions that increase affinity for Hsp90. Additionally, the acetate group located in the *para* position would probe for polar contacts with the protein pocket. As described previously, computer modeling also showed a potential size constraint for substitutions at the *para* position. In comparison to the methoxy and the phenolic derivatives at this location, manifesting IC_{50} values of 36.7 and 52.3, respectfully, the acetate group is still relatively small and incorporates a hydrogen bond acceptor without limiting the size of this pocket. In a similar manner as the prenylated side chain, the biaryl D-ring analogue investigated hydrophobic interactions in the *meta* cavity, while incorporating the most active substituent tested at the *para* position. If the predicted SAR trends would be maintained from the KU series to the EGCG series, the biaryl D-ring analogue would be more active than the prenyl side chain. Unfortunately, the biaryl side chain analogue **36b** was not active at the concentrations tested, which indicates that novobiocin and EGCG have distinct binding orientations and do not directly overlap.

V.   Design of Various Catechin Cores

While previously described analogues have allowed for the development of various inhibitors to probe interactions with the D-ring of EGCG, other regions of EGCG may also improve Hsp90 inhibitory activity. Modifications of the catechin would identify the importance of the A-ring resorcinol found on EGCG. Removal of the 5- and 7-methoxy groups would give the corresponding phenyl catechin, which would explore the importance of the resorcinol functionality. Moreover, development of other catechins would allow for direct comparison to the methyl ether catechin.

A. Synthesis of the Phenyl Catechin
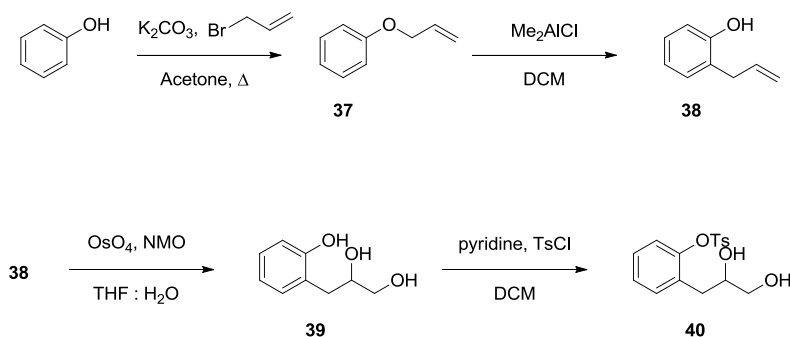
Scheme 16 - Synthesis of the phenolic intermediate

Synthesis of the phenyl catechin followed the same series of transformations as those employed in the synthesis of the methyl catechin. Starting from phenol a similar series of transformations were followed to afford the desired phenyl catechin as shown in Scheme 16. Allylation of phenol **37**, followed by the catalyzed Claisen rearrangement produced **38** in excellent yield. Dihydroxylation of the terminal olefin **39**, followed by phenolic toluene sulfonic

esterification was accomplished using the optimized conditions as described previously to give **40**.[138]
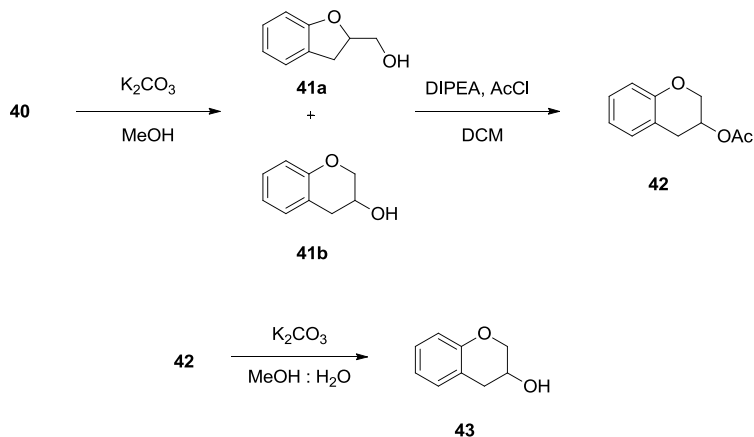
Scheme 17 - Synthesis of the phenyl catechin
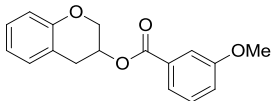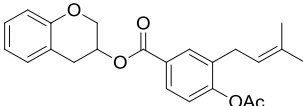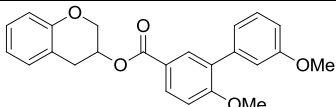
The phenolic toluene sulfonic ester was cyclized by the addition of base in methanol to produce a 1:1 mixture of the 5- and 6-membered phenyl catechins 41a–b. Unfortunately, as was the case previously, these catechins were inseparable via column chromatography and acetylation was employed to obtain the desired 6-membered catechin 42.[140] Finally, solvolysis of the protected precursor 42 produced the desired phenyl catechin 43 in excellent yield.
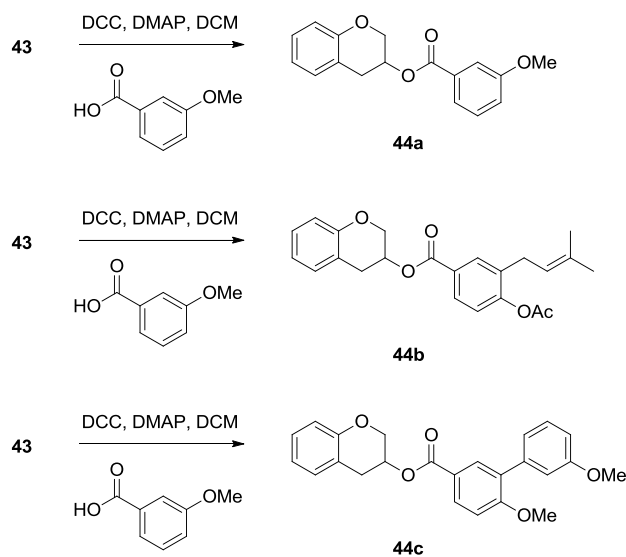
Scheme 18 - Synthesis of various phenyl catechin analogues

The various D-rings chosen, attached using standard DCC/DMAP conditions, were selected based upon multiple factors. The first benzoic acid chosen was based on the most active compound in the methyl ester series 44a, which manifested an IC$_{50}$ of 1.89 μM. Next, to further investigate whether the SAR developed for the KU series of compounds and be applied to the catechin scaffolds, both the prenylated and biaryl analogues were also synthesized producing 44b and 44c, respectfully. These molecules were evaluated against MCF-7 breast cancer cells. Data obtained from biological testing is shown in Table 6.

Table 6 - Anti-proliferative activity of phenyl catechin analogues

Analogue	Compound	MCF7 (μM)
44a		>100[a]
44b		40.55 ± 13.19
44c		>100

[a]Values represent mean ± standard deviation for at least two separate experiments performed in triplicate.

The anti-proliferative results revealed a range of activities for various analogues. Overall, it was demonstrated that removal of both methoxy ethers on the catechin is detrimental to activity. Comparison of the most active inhibitor, **33b**, which contains a methoxy *meta* to the phenyl ring, **44a**, clearly demonstrates that removal of the methoxy groups decreases activity. When the prenyl side chain is appended, in the case of **44b**, a slight increase in activity is observed, while the biaryl-containing analogue **44c** remains inactive. While these results do not seem to show a consistent trend, it is proposed that removal of the methoxy groups should eliminate interactions between the inhibitor and the protein and decrease activity. Thus, this catechin was not pursued further.

B. Western Blot analysis of 33b
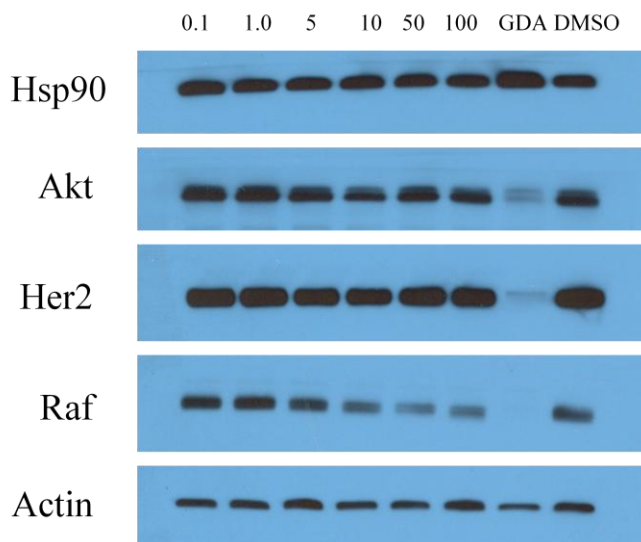
Figure 28 - Western blot analyses of Hsp90 client protein degradation assays against MCF-7 cells following treatment with EGCG analogue 33b. Concentrations (in μM) are indicated above each lane, GDA (Geldanamycin 500 nM) and DMSO were used as positive and negative controls, respectively.

To confirm that EGCG analogues were exhibiting their anti-proliferative effects through Hsp90 inhibition, analogue **33b** was evaluated for its ability to induce degradation of Hsp90 client proteins. Inhibitors that target Hsp90 demonstrate a dose-dependant degradation of client proteins at a concentration that corresponds with its IC_{50} value against the same cell line. Moreover, a hallmark of C-terminal inhibition is that the amount of Hsp90 remains constant at all concentrations tested. As seen in Figure 28, it appears as though Raf is the only client protein that is affected upon treatment with **33b** and its degradation does not occur near the measured IC_{50} value (1.89 ± 0.32 μM). This data suggests this molecule does not manifest its inhibitory activity through Hsp90 inhibition. Further analysis is needed to determine the mechanism through which **33b** manifests its anti-proliferative activity.

Development of the methyl ether and phenyl catechins has demonstrated a wide range of activities upon incorporation of D-ring analogues. Comparison of the methyl ether catechin to the phenyl catechin demonstrates the influence of substitutions to the catechin moiety, notably including a significant reduction in activity upon removal of the methoxy groups. To further explore the catechin scaffold, development of 5- and 7-phenolic catechins were pursued. It is important to note that the 7-phenolic catechin would result in the direct connectivity seen in the KU series of coumarin compounds.

C. Synthesis of a 5-hydroxy catechin
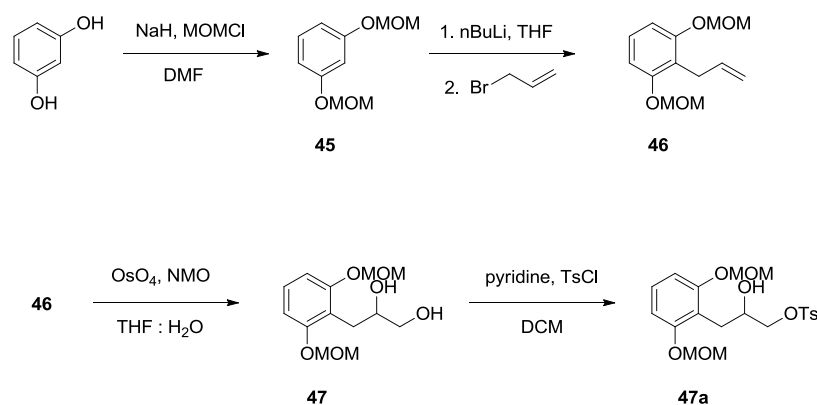
Scheme 19 - Synthesis of the primary toluene sulfonyl ester

Synthesis of a 5-hydroxy catechin was accomplished following a similar series of transformations as described for both the methyl ether and phenyl catechins. As seen in Scheme 19, resorcinol can be protected as the corresponding alkoxy ethers **45**, which allows for *ortho*-lithiation to afford the allylated resorcinol **46**. Dihydroxylation of the terminal olefin **47**, followed by toluene sulfonyl esterification of primary alcohol **47a** was accomplished in good overall yields.[138]
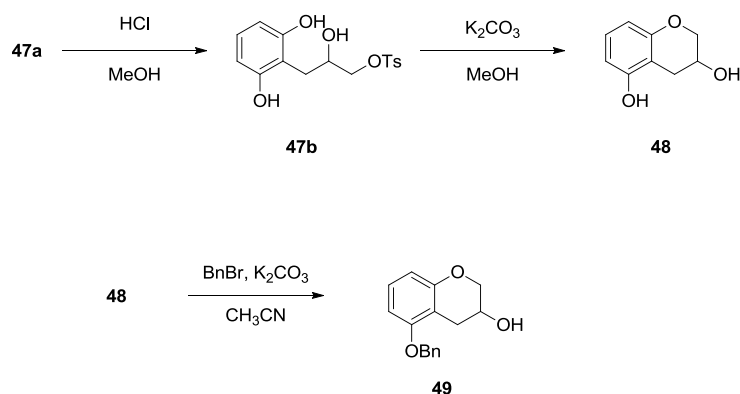
Scheme 20 - Synthesis of the protected 5-phenol catechin

Primary toluene sulfonic ester **47a** allowed cyclization to the desired 5-phenolic catechin. Next, acidic removal of the alkoxy ethers produces the phenolic resorcinol **47b** in excellent yield. Cyclization using the same conditions as described above produced the desired 5-hydroxy catechin **48** without the need for additional acetate protection during purification. Finally, selective protection of the phenol as the benzyl ether **49** was necessary to allow coupling of the catechin with the various benzoic acids.

D. Synthesis of the 7-hydroxy catechin
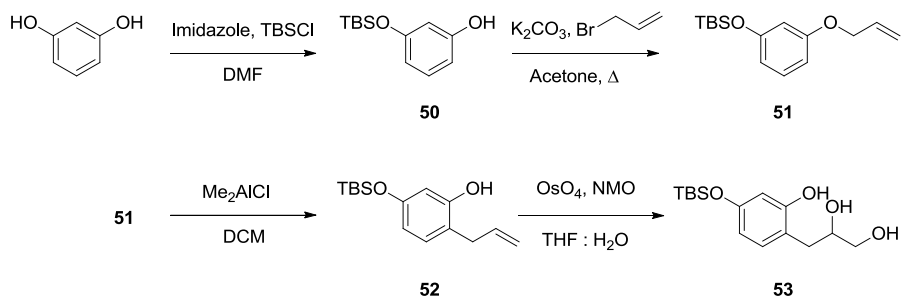
Scheme 21 - Synthesis of the dihydroxylated phenolic intermediate

Preparation of the 7-hydroxy catechin employs the same transformations that have been described for the other catechins. Although synthesis of the 7-hydroxy catechin also begins with resorcinol, selective silylation of one phenol allowed access to a different scaffold in a minimal amount of steps. Allylation of the free hydroxyl using already established conditions produces **51**, which was subsequently exposed to Claisen conditions gave the desired allylated intermediate **52.** Dihydroxylation of the terminal olefin yielded **53**, which was very similar to intermediates produced in both the phenyl and methyl catechins. Development of the 7-hydroxy catechin followed the synthetic steps previously described for the phenyl and methyl ether protected catechin.
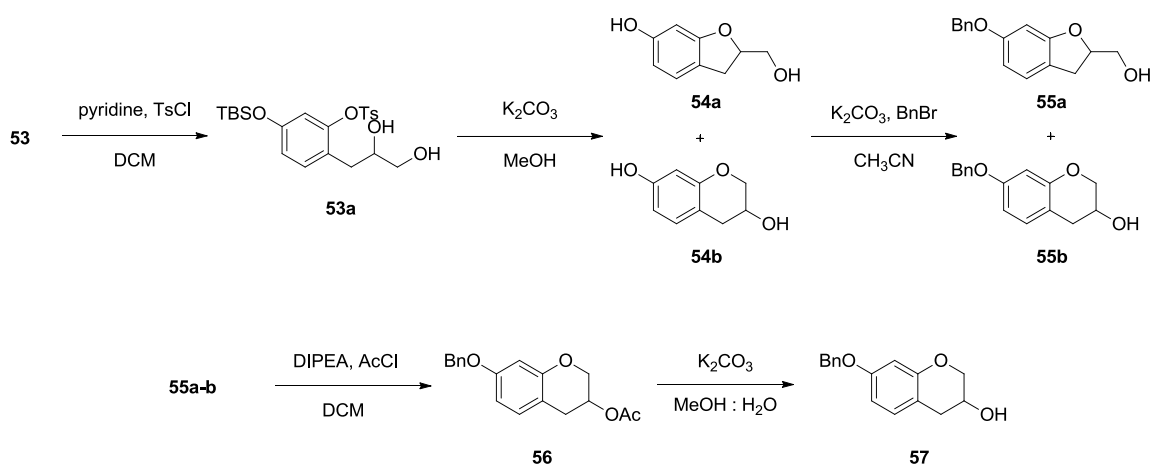
Scheme 22 - Synthesis of the desired benzyl ether protected 7-hydroxyl catechin

Synthesis of the desired 7-hydroxyl catechin proceeded with the optimized conditions described above for toluene sulfonic esterification of phenol **53**.[138] The catechin was then cyclized through addition of base to produce a 1:1 mixture of the 5- and the desired 6-membered catechins **54a–b**. Unfortunately, these cyclization conditions proceeded via removal of the silyl protecting group and produced catechins, which were not separable via column chromatography

and were thus pushed on to benzyl ether protection. Protected catechins **55a–b**, unfortunately, remained inseparable as well. Finally, acetate protection of the corresponding alcohols provided the separable 6-membered catechin **56** in overall good yield.[140] Finally, solvolysis afforded the 7-benzyl ether catechin **57** in good yield.

VI.   Conclusions

Development of the EGCG scaffold to produce compounds capable of targeting biologically relevant proteins is an area that should be pursued. Green tea has been used for centuries in the treatment of various disease states. The ability to isolate and fine tune the activity of active constituents like EGCG for the treatment of the various diseases is an exciting avenue for the development of therapeutics. Analogues containing the methyl ether catechin showed promise, manifesting a wide range of activities. However, Western blot analyses demonstrated that compounds of this type do not manifest their anti-proliferative activity through inhibition of Hsp90. In agreement with the model, the phenyl catechin showed a decrease in activity compared to the most active inhibitor. Further studies need to be carried out to explore tolerable substitutions that can be made to the EGCG scaffold without compromising its ability to inhibit Hsp90. Overall, EGCG represents a promising new scaffold upon which to build Hsp90 C-terminal inhibitors.
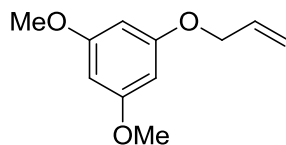
22

1-(allyloxy)-3,5-dimethoxybenzene (22): A solution of 3,5-dimethoxyphenol (1.046 grams, 6.8 mmol) was dissolved in acetone (35 mL) was treated with potassium carbonate (2.84 grams, 20.4 mmol) and allyl bromide (1.8 mL, 20.4 mmol), then the solution was heated to reflux for 12 hours. This reaction was cooled to room temperature and quenched by the addition of H_2O, extracted with EtOAc (3 x 150 mL). The combined organic fractions were washed with saturated aqueous NaCl, dried (Na_2SO_4), filtered, and concentrated. The residue was purified via column chromatography (SiO_2 30% EtOAc:Hexanes) to afford **22** (1.216g, 92%) as a colorless oil: ^{1}H NMR (500 MHz, $CDCl_3$) δ 6.13 (d, J = 2.1 Hz, 2H), 6.12 (d, J = 2.0 Hz, 1H), 6.11 − 6.03 (m, 1H), 5.44 (ddd, J = 17.2, 3.2, 1.6 Hz, 1H), 5.31 (dq, J = 10.5, 1.4 Hz, 1H), 4.52 (dt, J = 5.4, 1.5 Hz, 2H), 3.79 (s, 6H).; ^{13}C NMR (126 MHz, $CDCl_3$) δ 161.5 (2x), 160.5, 133.1, 117.8, 93.6, 93.1, 68.9, 55.3; IR (film) vmax 2999, 2939, 2839, 1600, 1475, 1458, 1423, 1205, 1193, 1154, 1064, 927, 817 cm^{-1}; HRMS (ESI+) *m/z*: [M +]+ calcd for C11H14O3, 194.0943; found, 194.0948
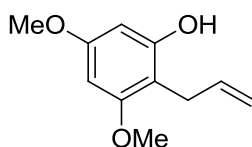
23

2-allyl-3,5-dimethoxyphenol (23): A solution of **22** (1.12 grams, 5.8 mmol) was dissolved in

DCM (30 mL) and treated dropwise with 1.0M solution of dimethylaluminum chloride (12.2 mL,

12.2 mmol) and stirred until TLC revealed complete consumption of starting material. The

reaction was quenched by the addition of 1.0 N HCl, extracted with EtOAc (3 x 150 mL). The

combined organic fractions were washed with saturated aqueous NaCl, dried (Na_2SO_4), filtered,

and concentrated. The residue was purified via column chromatography (SiO_2 20%

EtOAc:Hexanes) to afford **23** (0.997g, 89%) as a colorless oil: ^{1}H NMR (500 MHz, $CDCl_3$) δ

6.13 (d, J = 2.4 Hz, 1H), 6.11 (d, J = 2.4 Hz, 1H), 5.98 (ddt, J = 17.1, 10.0, 6.0 Hz, 1H), 5.17 –

5.09 (m, 3H), 3.80 (s, 3H), 3.79 (s, 3H), 3.44 – 3.38 (m, 2H).; ^{13}C NMR (126 MHz, $CDCl_3$) δ

159.7, 158.7, 155.9, 136.8, 115.4, 105.6, 93.7, 91.6, 55.8, 55.3, 27.0.; IR (film) vmax 3433(br),

2939, 2839, 1616, 1596, 1510, 1456, 1423, 1203, 1157, 1120, 1095, 1072, 1053, 985, 945, 912,

813 cm^{-1}; HRMS (ESI+) m/z: [M + H]+ calcd for C11H14O3H, 195.1021; found, 195.1026.
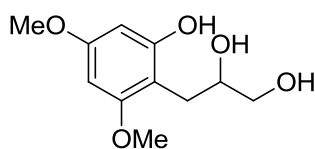
24

3-(2-hydroxy-4,6-dimethoxyphenyl)propane-1,2-diol (24): A solution of **23** (3.9 grams, 20.13

mmol) was dissolved in a (1.5 : 1.0) mixture of THF and H_2O (66 mL : 33 mL) respectively was

treated with 4-methylmorpholine N-oxide (3.53 grams, 30.2 mmol) followed by dropwise

addition of a 4% Osmium tetraoxide solution in H_2O (0.85 mL, 2.13 mmol). This was allowed to

stir for 18 hours before it was diluted with H_2O and extracted with EtOAc (3 x 250 mL). The

combined organic fractions were washed with saturated aqueous NaCl, dried (Na_2SO_4), filtered,

and concentrated. The residue was purified via column chromatography (SiO$_2$ 2% MeOH:CHCl$_3$) to afford **24** (3.99g, 87%) as a colorless oil: ^{1}H NMR (500 MHz, CDCl$_3$) δ 6.19 (d, J = 2.4 Hz, 1H), 6.10 (d, J = 2.4 Hz, 1H), 4.05 (dtd, J = 6.7, 5.6, 4.5 Hz, 1H), 3.79 (d, J = 4.3 Hz, 6H), 3.64 (dd, J = 11.2, 4.5 Hz, 1H), 3.48 (dd, J = 11.2, 6.8 Hz, 1H), 2.98 – 2.79 (m, 2H).; ^{13}C NMR (126 MHz, CDCl$_3$) δ 160.0, 158.9, 157.1, 104.8, 94.7, 91.4, 72.9, 65.2, 55.7, 55.3, 26.0.; IR (film) νmax 3359(br), 3001, 2937, 2840, 1618, 1595, 1514, 1456, 1425, 1363, 1338, 1301, 1201, 1172, 1147, 1108, 1053, 1026, 979, 933, 815 cm^{-1}; HRMS (ESI+) m/z: [M + Na]+ calcd for C11H16O5Na, 251.0895; found, 251.0893.
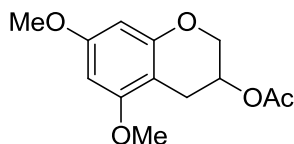
27

5,7-dimethoxychroman-3-yl acetate (27): A solution of **24** (3.95 grams, 17.3 mmol) was dissolved in DCM (80 mL) and cooled to 0°C, treated with pyridine (6.0 mL, 73.5 mmol) and allowed to stir for 5 minutes. Finally *para*-toluenesulfonyl chloride (3.61 grams, 19.0 mmol) was added and allowed to warm to room temperature after 1 hour. This was allowed to react for 12 hours and quenched by the addition of H$_2$O and extracted with EtOAc (3 x 250 mL). The combined organic fractions were washed with saturated aqueous NaCl, dried (Na$_2$SO$_4$), filtered, and concentrated. The residue was purified via column chromatography (SiO$_2$ 40% EtOAc:Hexanes) to afford crude phenolic sulfonic ester **25** (5.41g) as a yellow oil.

This oil was dissolved in MeOH (60 mL) and treated with potassium carbonate (3.146 grams, 22.7 mmol) and monitored by TLC. Once the TLC showed the consumption of starting material the solution was filtered and washed with EtOAc, dried (Na$_2$SO$_4$), filtered and concentrated. This produced an inseparable mixture of compounds **26a-b** (20% EtOAc:Hexanes), as a colorless oil (2.071g).

The mixture of compounds (1.34g, 6.36 mmol) was dissolved in DCM (30 mL) and cooled to 0°C and was treated with diisopropylethyl amine (2.22 mL, 12.7 mmol) and stirred for 5 minutes then acetyl chloride (0.46 mL, 6.36 mmol) was added dropwise and allowed to warm to room temperature over 12 hours. The reaction was quenched by the addition of H$_2$O and extracted with EtOAc (3 x 100 mL). The combined organic fractions were washed with saturated aqueous NaCl, dried (Na$_2$SO$_4$), filtered, and concentrated. The residue was purified via column chromatography (SiO$_2$ 10% EtOAc:Hexanes) to afford **27** (0.386 g, 24%) over 3 steps as a colorless oil: ^{1}H NMR (500 MHz, CDCl$_3$) δ 6.10 (d, *J* = 1.9 Hz, 1H), 6.03 (d, *J* = 2.0 Hz, 1H), 5.04 (dtd, *J* = 9.6, 7.3, 3.6 Hz, 1H), 4.33 (dd, *J* = 11.9, 3.6 Hz, 1H), 4.21 (dd, *J* = 11.9, 7.4 Hz, 1H), 3.81 (s, 3H), 3.78 (s, 3H), 3.21 (dd, *J* = 15.1, 9.6 Hz, 1H), 2.84 (dd, *J* = 15.1, 7.2 Hz, 1H), 2.13 (s, 3H); ^{13}C NMR (126 MHz, CDCl$_3$) δ 170.9, 161.8, 161.0, 156.6, 104.8, 91.3, 88.5, 81.17, 66.0, 55.6, 55.4, 29.1, 20.9; IR (film) vmax 3434(br), 2943, 2840, 2358, 1741, 1612, 1504, 1452, 1367, 1234, 1217, 1199, 1133, 1099, 1043, 983, 937, 810 cm^{-1}; HRMS (ESI+) *m/z*: [M + Na]+ calcd for C13H16O5Na, 275.0895; found, 275.0898.
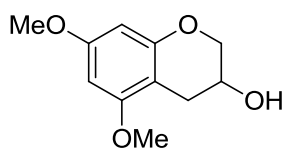
28

5,7-dimethoxychroman-3-ol (28): A solution of **27** (0.128 grams, 0.51 mmol in a (9:1) mixture of MeOH : H$_2$O (2.7 mL : 0.3 mL) was treated with potassium carbonate (0.213 grams, 1.53 mmol) and allowed to react for 4 hours. The reaction was quenched by the addition of saturated aqueous ammonium chloride and extracted with EtOAc (3 x 50 mL). The combined organic fractions were washed with saturated aqueous NaCl, dried (Na$_2$SO$_4$), filtered, and concentrated. The residue was purified via column chromatography (SiO$_2$ 30% EtOAc:Hexanes) to afford **28** (0.090g, 84%) as a colorless oil: ^{1}H NMR (500 MHz, CDCl$_3$) δ 5.98 (d, J = 2.0 Hz, 1H), 5.94 (d, J = 2.0 Hz, 1H), 4.86 (dtd, J = 10.0, 6.9, 3.3 Hz, 1H), 3.77 – 3.61 (m, 8H), 3.05 (dd, J = 15.0, 9.5 Hz, 1H), 2.76 (dd, J = 15.0, 7.0 Hz, 1H), 1.93 (s, 1H); ^{13}C NMR (126 MHz, CDCl$_3$) δ 161.7, 161.0, 156.7, 105.5, 91.2, 88.5, 84.3, 65.2, 55.6, 55.4, 28.4; IR (film) vmax 3428(br), 2937, 2840, 2358, 1623, 1612, 1504, 1452, 1429, 1357, 1217, 1199, 1134, 1099, 1045, 1008, 937, 810 cm^{-1}; HRMS (ESI+) *m/z*: [M + Na]+ calcd for C11H14O4Na, 233.0790; found, 233.0792.
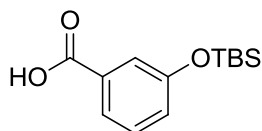
29c

3-((tert-butyldimethylsilyl)oxy)benzoic acid (29c): A solution of 3-hydroxybenzaldehyde (0.22 grams, 1.8 mmol) was dissolved in DMF (4.5 mL) and treated sequentially with imidazole (0.308 grams, 4.5 mmol) and *tert*-butyl(chloro)dimethylsilane (0.545 grams, 3.6 mmol) for 12 hours. The reaction was quenched by the addition of H$_2$O and extracted with EtOAc (3 x 50 mL). The combined organic fractions were washed with H$_2$O (3 x 50 mL), saturated aqueous NaCl, dried (Na$_2$SO$_4$), filtered and concentrated to afford **29b** as a crude colorless oil and used without further purification: ^{1}H NMR (400 MHz, CDCl$_3$) δ 9.97 (s, 1H), 7.49 (dt, J = 7.5, 1.3 Hz, 1H),

7.42 (t, *J* = 7.8 Hz, 1H), 7.34 (dd, *J* = 2.4, 1.5 Hz, 1H), 7.12 (ddd, *J* = 8.0, 2.5, 1.1 Hz, 1H), 1.01 (s, 9H), 0.24 (s, 7H).

The crude oil **29b** (0.305 grams, 1.29 mmol) was dissolved in t-BuOH (7 mL) and treated with 2-methyl-2-butene (5.0 mL, 46.4 mmol), while a separate solution of sodium chlorite (1.01 grams, 8.8 mmol) in a buffered solution of made of sodium phosphate monobasic (1.41 grams, 11.6 mmol) in H_2O (22 mL).   The oxidizing solution was added dropwise to the solution containing **29b** and allowed to react for 12 hrs. This reaction was diluted with saturated aqueous NaH_2PO_4 and extracted with DCM (3 x 50 mL), dried (Na_2SO_4), filtered, and concentrated to afford **29c** without further purification (0.3113g, 96%) as a pale yellow oil: ^{1}H NMR (500 MHz, $CDCl_3$) δ 7.74 (m, 1H), 7.59 (dd, *J* = 2.3, 1.7 Hz, 1H), 7.36 (t, *J* = 7.9 Hz, 1H), 7.11 (ddd, *J* = 8.1, 2.5, 1.0 Hz, 1H), 1.02 (s, 9H), 0.25 (s, 6H); ^{13}C NMR (126 MHz, $CDCl_3$) δ 172.0, 156.2, 130.9, 129.9, 126.2, 123.6, 121.9, 26.0 (3x), 18.6, 4.0 (2x); IR (film) vmax 3421(br), 2950, 2853, 2526, 1697, 1602, 1581, 1485, 1452, 1415, 1299, 1240, 1164, 1103, 1080, 964, 837, 783 cm^{-1}; HRMS (ESI+) *m/z*: [M + Na]+ calcd for C13H20O3SiNa, 275.1079; found, 275.1070.

30c

4-((tert-butyldimethylsilyl)oxy)benzoic acid (30c): A solution of 4-hydroxybenzaldehyde (0.226 grams, 1.85 mmol) was dissolved in DMF (4.5 mL) and treated sequentially with imidazole (0.316 grams, 4.6 mmol) and *tert*-butyl(chloro)dimethylsilane (0.560 grams, 3.7 mmol) for 12 hours. The reaction was quenched by the addition of H_2O and extracted with EtOAc (3 x 50 mL). The combined organic fractions were washed with H_2O (3 x 50 mL),

saturated aqueous NaCl, dried (Na₂SO₄), filtered and concentrated. The residue was carried on without further purification to afford **30b** as a crude colorless oil and used without further purification.

This crude benzaldehyde **30b** was dissolved in t-BuOH (2 mL) and treated with 2-methyl-2-butene (1.6 mL, 14.8 mmol), while a separate solution of sodium chlorite (0.319 grams, 2.8 mmol) in a buffered solution of made of sodium phosphate monobasic (0.444 grams, 3.7 mmol) in H_2O (7 mL). The oxidizing solution was added dropwise to the solution containing **30b** and allowed to react for 12 hrs. This reaction was diluted with saturated aqueous NaH_2PO_4 and extracted with DCM (3 x 50 mL), dried (Na₂SO₄), filtered, and concentrated to afford **30c** (0.095g, 21%) over 2 steps as a pale yellow oil without further purification: ^{1}H NMR (500 MHz, CDCl₃) δ 8.02 (m, 2H), 6.89 (m, 2H), 0.99 (s, 9H), 0.24 (s, 6H).; ^{13}C NMR (126 MHz, CDCl₃) δ 172.1, 161.0, 132.5 (2x), 122.4, 120.1 (2x), 25.7 (3x), 18.4, 4.2 (2x). IR (film) vmax 2927, 2856, 2667, 2549, 1668, 1602, 1512, 1469, 1427, 1317, 1271, 1168, 1103, 914, 862, 837, 781 cm^{-1}; HRMS (ESI+) *m/z*: [M + Na]+ calcd for C13H20O3SiNa, 275.1079; found, 275.1071.
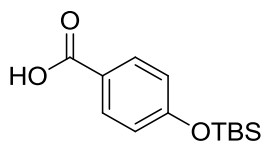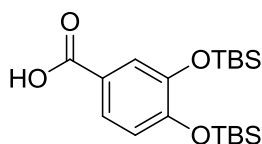

31c

3,4-bis((tert-butyldimethylsilyl)oxy)benzoic acid (31c): A solution of 3,4-hydroxybenzaldehyde (0.302 grams, 2.19 mmol) was dissolved in DMF (5.5 mL) and treated sequentially with imidazole (0.679 grams, 9.9 mmol) and *tert*-butyl(chloro)dimethylsilane (1.32 grams, 8.76 mmol) for 12 hours. The reaction was quenched by the addition of H_2O and extracted with EtOAc (3 x 50 mL). The combined organic fractions were washed with H_2O (3 x

50 mL), saturated aqueous NaCl, dried (Na$_2$SO$_4$), filtered and concentrated. The residue was carried on without further purification to afford **31b** as a crude colorless oil and used without further purification.

The crude oil **31b** was dissolved in t-BuOH (1 mL) and treated with 2-methyl-2-butene (1 mL, 7.9 mmol), while a separate solution of sodium chlorite (0.173 grams, 1.5 mmol) in a buffered solution of made of sodium phosphate monobasic (0.245 grams, 2.0 mmol) in H$_2$O (3.75 mL). The oxidizing solution was added dropwise to the solution containing **31b** and allowed to react for 12 hrs. This reaction was diluted with saturated aqueous NaH$_2$PO$_4$ and extracted with DCM (3 x 50 mL), dried (Na$_2$SO$_4$), filtered, and concentrated to afford **31c** (0.0732g, 9%) over 2 steps as a pale yellow oil without further purification: ^{1}H NMR (500 MHz, CDCl$_3$) δ 7.65 (dd, J = 8.3, 2.1 Hz, 1H), 7.61 (d, J = 2.1 Hz, 1H), 6.90 (d, J = 8.3 Hz, 1H), 1.02 (d, J = 3.3 Hz, 18H), 0.26 (d, J = 4.8 Hz, 12H).; ^{13}C NMR (126 MHz, CDCl$_3$) δ 172.0, 152.6, 146.9, 124.6, 122.9, 122.5, 120.7, 26.0 (3x), 26.0 (3x), 18.7, 18.6, 4.0 (2x), 3.9 (2x); IR (film) νmax 2954, 2929, 2858, 1687, 1596, 1574, 1514, 1433, 1392, 1293, 1253, 1124, 1103, 973, 893, 853, 781 cm^{-1}; HRMS (ESI+) *m/z*: [M +]+ calcd for C19H34O4Si2Na, 382.1996; found, 382.2004.
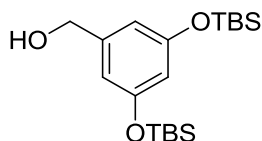
32b

(3,5-bis((tert-butyldimethylsilyl)oxy)phenyl)methanol (32b): A solution of methyl 3,5-dihydroxybenzoate(cite) (0.250 grams, 1.49 mmol) was dissolved in DMF (5.0 mL) and treated sequentially with imidazole (0.460 grams, 6.7 mmol) and *tert*-butyl(chloro)dimethylsilane (0.902

grams, 5.96 mmol) for 12 hours. The reaction was quenched by the addition of H_2O and extracted with EtOAc (3 x 50 mL). The combined organic fractions were washed with H_2O (3 x 50 mL), saturated aqueous NaCl, dried (Na_2SO_4), filtered and concentrated. The colorless oil was carried on without further purification.

A suspension of lithium aluminum hydride (0.125 grams, 3.23 mmol) was made in THF (5 mL) and cooled to 0°C. A second solution of the crude oil (0.583 grams, 1.47 mmol) was dissolved in THF (5 mL), cooled to 0°C and added dropwise to the suspension. The reaction was allowed to stir until TLC showed consumption of starting material. The reaction was quenched by the addition of H_2O and extracted with EtOAc (3 x 50 mL). The combined organic fractions were washed with H_2O (3 x 50 mL), saturated aqueous NaCl, dried (Na_2SO_4), filtered and concentrated. The residue was purified via column chromatography (SiO_2 5% EtOAc:Hexanes) to afford **32b** (0.254g, 46%) over 2 steps as a colorless oil: ^{1}H NMR (500 MHz, $CDCl_3$) δ 6.47 (d, $J = 2.2$ Hz, 2H), 6.25 (s, 1H), 4.57 (s, 2H), 0.97 (s, 18H), 0.19 (s, 12H); ^{13}C NMR (126 MHz, $CDCl_3$) δ 156.7, 143.1, 111.8, 111.2, 65.2, 25.7 (3x), 25.6 (3x), 18.2 (2x), 4.5 (4x); IR (film) νmax 3352(br), 2954, 2885, 1589, 1450, 1361, 1334, 1253, 1164, 1029, 1002, 981, 939, 831, 779 cm^{-1}; HRMS (ESI+) *m/z*: [M + Na]+ calcd for C19H36O3Si2Na, 391.2101; found, 391.2104.
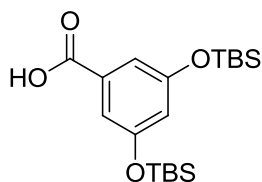
32c

3,5-bis((tert-butyldimethylsilyl)oxy)benzoic acid (32c): A solution of **32b** (0.232 grams, 0.63 mmol) was dissolved in DCM (4 mL) and treated with pyridinium chlorochromate (0.164 grams,

0.76 mmol) and allowed to react for 12 hrs. The solution was diluted with diethyl ether (10 mL) and allowed to stir for 10 min, filtered through a Celite plug (EtOAc), dried (Na$_2$SO$_4$), filtered and concentrated. The pale yellow residue was used without further purification: xx

The crude residue (0.168 grams, 0.46 mmol) was dissolved in t-BuOH (2 mL) and treated with 2-methyl-2-butene (2 mL, 16.6 mmol), while a separate solution of sodium chlorite (0.358 grams, 3.13 mmol) in a buffered solution of made of sodium phosphate monobasic (0.505 grams, 4.14 mmol) in H$_2$O (8.0 mL). The oxidizing solution was added dropwise to the solution containing crude aldehyde and allowed to react for 12 hrs. This reaction was diluted with saturated aqueous NaH$_2$PO$_4$ and extracted with DCM (3 x 50 mL), dried (Na$_2$SO$_4$), filtered, and concentrated to afford **32c** (0.1584g, 66%) over 2 steps as a pale yellow oil without further purification: ^{1}H NMR (500 MHz, CDCl$_3$) δ 7.07 (s, 1H), 6.72 (s, 1H), 6.36 (s, 1H), 0.78 (s, 9H), 0.15 (s, 6H); ^{13}C NMR (126 MHz, CDCl$_3$) δ 170.0, 157.3 (2x), 138.3, 118.4, 114.4 (2x), 25.5 (6x), 18.2 (2x), 4.2 (4x); IR (film) vmax 2956, 2858, 1704, 1589, 1458, 1382, 1336, 1255, 1170, 1031, 1006, 852, 829, 813, 781 cm^{-1} HRMS (ESI+) *m/z*: [M +]+ calcd for C19H34O4Si2Na, 382.1996; found, 382.1994.
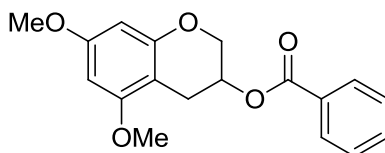
33a

5,7-dimethoxychroman-3-yl benzoate (33a): To a stirring solution of **28** (0.018 grams, 0.086 mmol) and benzoic acid (0.022 grams, 0.172 mmol) in DCM (1 mL) was added N,N'-dicyclohexylcarbodiimide (0.036 grams, 0.172 mmol) and 4-(dimethylamino)pyridine (0.001

grams, 0.008 mmol) simultaneously. This was allowed to react for 12 hours and quenched by the addition of H_2O and extracted with DCM (3 x 25 mL). The combined organic fractions were washed with saturated aqueous NaCl, dried (Na_2SO_4), filtered, and concentrated. The residue was purified via column chromatography (SiO_2 15% EtOAc:Hexanes) to afford **33a** (0.0266g, 98%) as an amorphous white solid: ^1H NMR (500 MHz, $CDCl_3$) δ 8.04 (m, 2H), 7.57 (t, $J = 7.4$ Hz, 1H), 7.43 (t, $J = 7.0$ Hz, 2H), 6.12 (d, $J = 2.2$ Hz, 2H), 5.53 (s, 1H), 4.31 (ddd, $J = 56.3, 29.2, 6.7$ Hz, 2H), 3.81 (s, 6H), 2.99 (m, 2H); ^{13}C NMR (126 MHz, $CDCl_3$) δ 166.1, 159.6, 158.8, 155.1, 133.1, 130.0, 129.8, 128.3, 100.5, 93.2, 91.8, 66.8, 66.0, 55.4, 24.9; IR (film) vmax 2937, 2840, 1716, 1620, 1593, 1498, 1450, 1353, 1315, 1287, 1217, 1201, 1178, 1142, 1128, 1110, 1070, 1056, 1026, 945, 813, 711 cm^{-1}; HRMS (ESI+) *m/z*: [M + Na]+ calcd for C18H18O5Na, 337.1052; found, 337.1058.
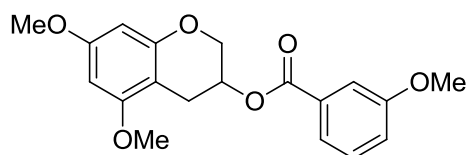
33b

5,7-dimethoxychroman-3-yl 3-methoxybenzoate (33b): To a stirring solution of **28** (0.018 grams, 0.086 mmol) and 3-methoxybenzoic acid (0.026 grams, 0.172 mmol) in DCM (1 mL) was added N,N'-dicyclohexylcarbodiimide (0.035 grams, 0.172 mmol) and 4-(dimethylamino)pyridine (0.001 grams, 0.008 mmol) simultaneously. This was allowed to react for 12 hours and quenched by the addition of H_2O and extracted with DCM (3 x 25 mL). The combined organic fractions were washed with saturated aqueous NaCl, dried (Na_2SO_4), filtered, and concentrated. The residue was purified via column chromatography (SiO_2 15% EtOAc:Hexanes) to afford **33b** (0.0246g, 83%) as an amorphous white solid: ^1H NMR (400

MHz, CDCl$_3$) δ 7.62 (m, 1H), 7.55 (dd, J = 2.6, 1.5 Hz, 1H), 7.32 (t, J = 8.0 Hz, 1H), 7.10 (ddd, J = 8.3, 2.7, 1.0 Hz, 1H), 6.11 (s, 2H), 5.51 (qd, J = 5.2, 2.2 Hz, 1H), 4.29 (m, 2H), 3.84 (s, 3H), 3.80 (s, 3H), 3.79 (s, 3H), 2.92 (m, 2H); ^{13}C NMR (126 MHz, CDCl$_3$) δ 166.0, 159.5, 158.8, 155.1, 131.3, 129.4, 122.2, 119.4, 114.3, 100.5, 93.1, 91.8, 66.8, 66.1, 55.4, 24.9; IR (film) νmax 2937, 2837, 1716, 1620, 1593, 1498, 1463, 1454, 1431, 1353, 1321, 1276, 1218, 1201, 1145, 1128, 1103, 1047, 813, 755 cm^{-1}; HRMS (ESI+) m/z: [M + Na]+ calcd for C19H20O6Na, 367.1158; found, 367.1165.

33c

5,7-dimethoxychroman-3-yl 4-methoxybenzoate (33c): To a stirring solution of **28** (0.020 grams, 0.095 mmol) and 4-methoxybenzoic acid (0.029 grams, 0.19 mmol) in DCM (1 mL) was added N,N'-dicyclohexylcarbodiimide (0.040 grams, 0.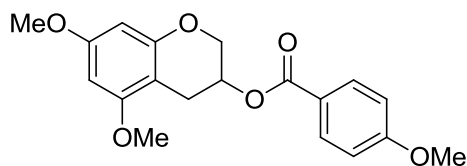19 mmol) and 4-(dimethylamino)pyridine (0.001 grams, 0.009 mmol) simultaneously. This was allowed to react for 12 hours and quenched by the addition of H$_2$O and extracted with DCM (3 x 25 mL). The combined organic fractions were washed with saturated aqueous NaCl, dried (Na$_2$SO$_4$), filtered, and concentrated. The residue was purified via column chromatography (SiO$_2$ 15% EtOAc:Hexanes) to afford **33c** (0.0232g, 71%) as an amorphous white solid: ^{1}H NMR (400 MHz, CDCl$_3$) δ 7.98 (d, J = 8.9 Hz, 2H), 6.90 (d, J = 8.9 Hz, 2H), 6.11 (s, 2H), 5.49 (qd, J = 5.1, 2.2 Hz, 1H), 4.28 (m, 2H), 3.86 (s, 3H), 3.79 (d, J = 1.8 Hz, 6H), 2.92 (m, 2H); ^{13}C NMR (126 MHz, CDCl$_3$) δ 165.8, 163.5, 159.5, 158.8, 155.1, 131.8, 129.1, 122.4, 113.6, 100.7, 93.1, 91.7, 66.9, 65.6, 55.4, 24.9; IR (film) νmax 2935, 2839, 1710, 1620, 1606, 1510, 1498, 1461, 1442, 1421, 1353, 1317, 1268, 1217, 1201,

1166, 1145, 1128, 1112, 1101, 1056, 1027, 945, 846, 811 cm^{-1}; HRMS (ESI+) *m/z*: [M + Na]+ calcd for C19H20O6Na, 367.1158; found, 367.1157.
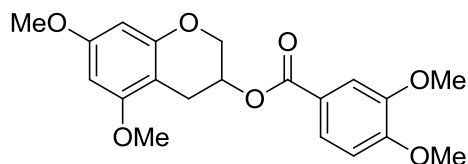
33d

5,7-dimethoxychroman-3-yl 3,4-dimethoxybenzoate (33d): To a stirring solution of **28** (0.021 grams, 0.1 mmol) and 3,4-dimethoxybenzoic acid (0.037 grams, 0.2 mmol) in DCM (2 mL) was added N,N'-dicyclohexylcarbodiimide (0.042 grams, 0.2 mmol) and 4-(dimethylamino)pyridine (0.002 grams, 0.01 mmol) simultaneously. This was allowed to react for 12 hours and quenched by the addition of H$_2$O and extracted with DCM (3 x 25 mL). The combined organic fractions were washed with saturated aqueous NaCl, dried (Na$_2$SO$_4$), filtered, and concentrated. The residue was purified via column chromatography (SiO$_2$ 15% EtOAc:Hexanes) to afford **33d** (0.0362g, 97%) as an amorphous white solid: ^{1}H NMR (400 MHz, CDCl$_3$) δ 7.66 (dd, *J* = 8.4, 2.0 Hz, 1H), 7.53 (d, *J* = 2.0 Hz, 1H), 6.85 (d, *J* = 8.5 Hz, 1H), 6.11 (s, 2H), 5.49 (qd, *J* = 5.1, 2.3 Hz, 1H), 4.27 (m, 2H), 3.93 (s, 3H), 3.92 (s, 3H), 3.80 (s, 3H), 3.79 (s, 3H), 2.93 (m, 2H^{13}C NMR (126 MHz, CDCl$_3$) δ 165.8, 159.6, 158.8, 155.1, 153.1, 148.6, 123.9, 122.5, 112.1, 110.1, 100.6, 93.1, 91.7, 66.9, 65.8, 56.0, 55.4, 55.4, 24.9; IR (film) vmax 2958, 1839, 1710, 1620, 1596, 1514, 1498, 1463, 1454, 1419, 1352, 1288, 1273, 1220, 1201, 1176, 1132, 1107, 1056, 1024, 912, 813, 763, 730 cm^{-1}; HRMS (ESI+) *m/z*: [M + Na]+ calcd for C20H22O7Na, 397.1263; found, 397.1267.
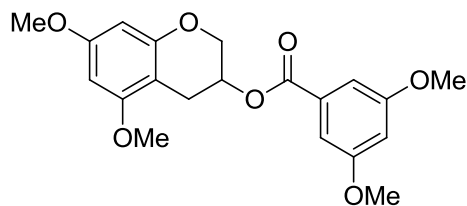
33e

5,7-dimethoxychroman-3-yl 3,5-dimethoxybenzoate (33e): To a stirring solution of **28** (0.020 grams, 0.095 mmol) and 3,5-dimethoxybenzoic acid (0.036 grams, 0.19 mmol) in DCM (1 mL) was added N,N'-dicyclohexylcarbodiimide (0.040 grams, 0.19 mmol) and 4-(dimethylamino)pyridine (0.001 grams, 0.01 mmol) simultaneously. This was allowed to react for 12 hours and quenched by the addition of H_2O and extracted with DCM (3 x 25 mL). The combined organic fractions were washed with saturated aqueous NaCl, dried (Na_2SO_4), filtered, and concentrated. The residue was purified via column chromatography (SiO_2 15% EtOAc:Hexanes) to afford **33e** (0.0301g, 85%) as an amorphous white solid: ^{1}H NMR (400 MHz, $CDCl_3$) δ 7.17 (d, *J* = 2.4 Hz, 2H), 6.64 (t, *J* = 2.4 Hz, 1H), 6.10 (s, 2H), 5.48 (dt, *J* = 5.1, 2.8 Hz, 1H), 3.82 (s, 6H), 3.80 (s, 3H), 3.79 (s, 3H), 2.92 (m, 2H); ^{13}C NMR (126 MHz, $CDCl_3$) δ 165.8, 160.6, 159.6, 158.8, 155.1, 131.9, 107.5, 105.5, 100.5, 93.1, 91.8, 66.7, 66.3, 55.6, 55.4, 24.9; IR (film) νmax 2953, 2839, 1716, 1618, 1596, 1498, 1458, 1427, 1357, 1319, 1301, 1234, 1203, 1153, 1147, 1128, 1051, 910, 813, 765, 730 cm^{-1}; HRMS (ESI+) *m/z*: [M + Na]+ calcd for C20H22O7Na, 397.1263; found, 397.1260.
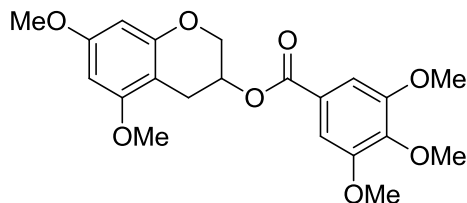
5,7-dimethoxychroman-3-yl 3,4,5-trimethoxybenzoate (33f): To a stirring solution of **28** (0.017 grams, 0.081 mmol) and 3,4,5-trimethoxybenzoic acid (0.034 grams, 0.162 mmol) in DCM (1 mL) was added N,N'-dicyclohexylcarbodiimide (0.033 grams, 0.162 mmol) and 4-(dimethylamino)pyridine (0.001 grams, 0.008 mmol) simultaneously. This was allowed to react for 12 hours and quenched by the addition of H_2O and extracted with DCM (3 x 25 mL). The combined organic fractions were washed with saturated aqueous NaCl, dried (Na_2SO_4), filtered, and concentrated. The residue was purified via column chromatography (SiO_2 30% EtOAc:Hexanes) to afford **33f** (0.0242g, 74%) as an amorphous white solid: ^{1}H NMR (400 MHz, $CDCl_3$) δ 7.28 (s, 2H), 6.11 (s, 2H), 5.49 (qd, J = 5.1, 2.8 Hz, 1H), 4.26 (m, 2H), 3.90 (s, 3H), 3.88 (s, 6H), 3.80 (s, 3H), 3.78 (s, 3H), 2.95 (m, 2H); ^{13}C NMR (126 MHz, $CDCl_3$) δ 165.7, 159.6, 158.8, 155.1, 152.9, 142.4, 125.1, 107.0, 100.6, 93.1, 91.7, 66.8, 66.3, 60.9, 56.3, 55.4, 50.9, 25.0; IR (film) vmax 2941, 2839, 1712, 1620, 1591, 1500, 1460, 1415, 1357, 1336, 1249, 1224, 1201, 1178, 1145, 1137, 1056, 1004, 972, 813 cm^{-1}; HRMS (ESI+) *m/z*: [M + Na]+ calcd for C21H24O8Na, 427.1369; found, 427.1375.

35a

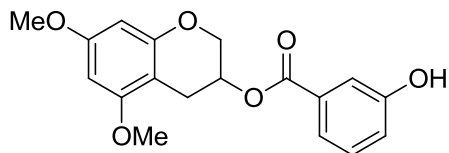**5,7-dimethoxychroman-3-yl 3-hydroxybenzoate (35a):** To a stirring solution of **28** (0.021 grams, 0.1 mmol) and benzoic acid **29c** (0.049 grams, 0.2 mmol) in DCM (1 mL) was added

N,N'-dicyclohexylcarbodiimide (0.041 grams, 0.2 mmol) and 4-(dimethylamino)pyridine (0.002 grams, 0.01 mmol) simultaneously. This was allowed to react for 12 hours and quenched by the addition of H_2O and extracted with DCM (3 x 25 mL). The combined organic fractions were washed with saturated aqueous NaCl, dried (Na_2SO_4), filtered, and concentrated. The residue was carried on without further purification.

The crude residue (0.055 grams, 0.124 mmol) was dissolved in THF (2 mL) and treated with tetrabutylammonium fluoride (0.38 mL, 0.372 mmol) and allowed to react for 12 hrs. This reaction was quenched with saturated aqueous NH_4Cl and extracted with EtOAc (3 x 50 mL), dried (Na_2SO_4), filtered, and concentrated to afford **35a** (0.0293g, 89%) over 2 steps as an amorphous white solid: ^{1}H NMR (400 MHz, CDCl₃) δ 7.60 (d, J = 7.7 Hz, 1H), 7.34 (t, J = 1.9 Hz, 1H), 7.31 (d, J = 8.0 Hz, 1H), 7.06 (m, 1H), 6.12 (d, J = 1.9 Hz, 1H), 6.06 (d, J = 2.0 Hz, 1H), 5.17 (m, 1H), 4.97 (s, 1H), 4.49 (ddd, J = 17.9, 11.8, 4.9 Hz, 2H), 3.81 (s, 3H), 3.79 (s, 4H), 3.29 (dd, J = 15.1, 9.6 Hz, 1H), 2.96 (dd, J = 15.2, 6.5 Hz, 1H); ^{13}C NMR (126 MHz, CDCl₃) δ 166.2, 161.7, 161.3, 156.7, 155.6, 131.1, 129.7, 122.3, 120.3, 116.3, 105.0, 91.3, 88.5, 81.1, 66.8, 55.6, 55.4, 29.3; IR (film) vmax 3444(br), 2954, 2856, 1718, 1625, 1602, 1508, 1463, 1452, 1361, 1266, 1217, 1199, 1161, 1141, 1097, 1047, 910, 838, 773 cm^{-1}; HRMS (ESI+) *m/z*: [M + Na]+ calcd for C18H18O6Na, 353.1001; found, 353.0993.
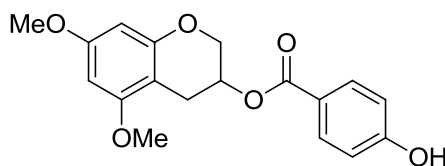

35b

5,7-dimethoxychroman-3-yl 4-hydroxybenzoate (35b): To a stirring solution of **28** (0.021 grams, 0.1 mmol) and benzoic acid **29c** (0.050 grams, 0.2 mmol) in DCM (1 mL) was added N,N'-dicyclohexylcarbodiimide (0.043 grams, 0.2 mmol) and 4-(dimethylamino)pyridine (0.003 grams, 0.01 mmol) simultaneously. This was allowed to react for 12 hours and quenched by the addition of H_2O and extracted with DCM (3 x 25 mL). The combined organic fractions were washed with saturated aqueous NaCl, dried (Na_2SO_4), filtered, and concentrated. The residue was carried on without further purification.

The crude residue (0.033 grams, 0.074 mmol) was dissolved in THF (2 mL) and treated with tetrabutylammonium fluoride (0.25 mL, 0.222 mmol) and allowed to react for 12 hrs. This reaction was quenched with saturated aqueous NH_4Cl and extracted with EtOAc (3 x 50 mL), dried (Na_2SO_4), filtered, and concentrated to afford **35b** (0.0172g, 52%) over 2 steps as an amorphous white solid: ^{1}H NMR (400 MHz, CDCl$_3$) δ 7.94 (m, 2H), 6.85 (m, 2H), 6.11 (d, J = 1.9 Hz, 1H), 6.05 (d, J = 2.0 Hz, 1H), 5.16 (m, 2H), 4.48 (qd, J = 11.8, 5.2 Hz, 2H), 3.82 (s, 3H), 3.78 (s, 3H), 3.27 (dd, J = 15.1, 9.5 Hz, 1H), 2.95 (dd, J = 15.1, 6.8 Hz, 1H).^{13}C NMR (126 MHz, CDCl$_3$) δ 166.1, 161.7, 161.2, 159.8, 156.6, 132.2, 122.4, 115.2, 104.9, 91.3, 88.5, 81.2, 66.3, 55.6, 55.4, 29.3; IR (film) vmax 3519(br), 2954, 2856, 1718, 1625, 1602, 1508, 1452, 1242, 1217, 1199, 1161, 1141, 1097, 1047, 1010, 983, 910, 838, 773 cm^{-1}; HRMS (ESI+) *m/z*: [M + Na]+ calcd for C18H18O6Na, 353.1001; found, 353.0996.
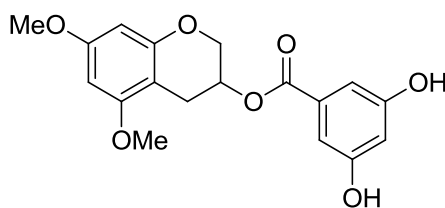
5,7-dimethoxychroman-3-yl 3,5-dihydroxyenzoate (35d): To a stirring solution of **28** (0.020 grams, 0.095 mmol) and benzoic acid **31c** (0.073 grams, 0.19 mmol) in DCM (2 mL) was added N,N'-dicyclohexylcarbodiimide (0.040 grams, 0.19 mmol) and 4-(dimethylamino)pyridine (0.002 grams, 0.01 mmol) simultaneously. This was allowed to react for 12 hours and quenched by the addition of H_2O and extracted with DCM (3 x 25 mL). The combined organic fractions were washed with saturated aqueous NaCl, dried (Na_2SO_4), filtered, and concentrated. The residue was carried on without further purification.

The crude residue (0.0445 grams, 0.077 mmol) was dissolved in THF (2 mL) and treated with tetrabutylammonium fluoride (0.25 mL, 0.232 mmol) and allowed to react for 12 hrs. This reaction was quenched with saturated aqueous NH_4Cl and extracted with EtOAc (3 x 50 mL), dried (Na_2SO_4), filtered, and concentrated to afford **35d** (0.0181g, 55%) over 2 steps as an amorphous white solid: ^{1}H NMR (400 MHz, $CDCl_3$) δ 6.96 (d, J = 2.3 Hz, 2H), 6.58 (t, J = 2.3 Hz, 1H), 6.12 (d, J = 1.9 Hz, 1H), 6.06 (d, J = 1.9 Hz, 1H), 5.54 (s, 2H), 5.15 (m, 1H), 4.45 (m, 2H), 3.81 (s, 3H), 3.78 (s, 3H), 3.28 (dd, J = 15.2, 9.6 Hz, 1H), 2.95 (dd, J = 15.2, 6.3 Hz, 1H); ^{13}C NMR (126 MHz, $CDCl_3$) δ 165.8, 161.7, 161.5, 156.8, 156.7, 131.9, 109.3 (2x), 107.5, 105.2, 91.2, 88.6, 81.0, 68.6, 67.0, 55.7, 55.4, 29.3; IR (film) vmax 3434(br), 2954, 2858, 1720, 1625, 1612, 1508, 1463, 1421, 1307, 1255, 1215, 1201, 1143, 1101, 1047, 995, 981, 898, 821, 781 cm^{-1}; HRMS (ESI+) *m/z*: [M + Na]+ calcd for C18H18O7Na, 369.0950; found, 369.0941.
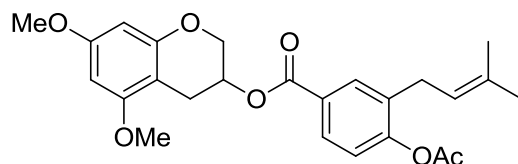
36a

5,7-dimethoxychroman-3-yl 4-acetoxy-3-(3-methylbut-2-en-1-yl)benzoate (36a): To a stirring solution of **28** (0.022 grams, 0.105 mmol) and 4-acetoxy-3-(3-methylbut-2-en-1-yl)benzoic acid(cite) (0.052 grams, 0.21 mmol) in DCM (2 mL) was added N,N'-dicyclohexylcarbodiimide (0.044 grams, 0.21 mmol) and 4-(dimethylamino)pyridine (0.002 grams, 0.01 mmol) simultaneously. This was allowed to react for 12 hours and quenched by the addition of H_2O and extracted with DCM (3 x 25 mL). The combined organic fractions were washed with saturated aqueous NaCl, dried (Na_2SO_4), filtered, and concentrated. The residue was purified via column chromatography (SiO_2 15% EtOAc:Hexanes) to afford **33a** (0.0363g, 79%) as a colorless oil: ^{1}H NMR (400 MHz, CDCl$_3$) δ 7.87 (m, 2H), 7.08 (d, J = 8.3 Hz, 1H), 6.10 (d, J = 1.9 Hz, 1H), 6.04 (d, J = 2.0 Hz, 1H), 5.18 (m, 2H), 4.49 (m, 2H), 3.80 (s, 3H), 3.77 (s, 3H), 3.26 (m, 3H), 2.95 (dd, J = 15.1, 6.7 Hz, 1H), 2.33 (s, 3H), 1.75 (s, 3H), 1.71 (s, 3H); ^{13}C NMR (126 MHz, CDCl$_3$) δ 170.0, 166.9, 164.9, 161.7, 161.5, 157.2, 156.8, 137.1, 131.9, 130.3, 128.1, 127.4, 126.3, 122.3, 121.2, 103.1, 93.5, 91.9, 80.9, 67.9, 28.7, 27.5, 25.2, 20.6, 18.6; IR (film) vmax 2958, 2931, 1762, 1720, 1625, 1610, 1504, 1452, 1369, 1280, 1259, 1201, 1164, 1143, 1103, 1047, 808, 757 cm^{-1}; HRMS (ESI+) *m/z*: [M + Na]+ calcd for C25H28O7Na, 463.1733; found, 463.1735.
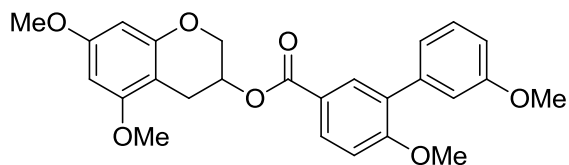
36b

5,7-dimethoxychroman-3-yl 3',6-dimethoxy-[1,1'-biphenyl]-3-carboxylate (36b): To a stirring solution of **28** (0.020 grams, 0.095 mmol) and 3',6-dimethoxy-[1,1'-biphenyl]-3-carboxylic acid(cite) (0.049 grams, 0.19 mmol) in DCM (1.5 mL) was added N,N'-dicyclohexylcarbodiimide (0.039 grams, 0.19 mmol) and 4-(dimethylamino)pyridine (0.001 grams, 0.009 mmol) simultaneously. This was allowed to react for 12 hours and quenched by the addition of H_2O and extracted with DCM (3 x 25 mL). The combined organic fractions were washed with saturated aqueous NaCl, dried (Na_2SO_4), filtered, and concentrated. The residue was purified via column chromatography (SiO_2 30% EtOAc:Hexanes) to afford **33a** (0.040g, 94%) as a colorless oil: ^{1}H NMR (500 MHz, $CDCl_3$) δ 8.03 (dd, J = 8.6, 2.3 Hz, 1H), 7.98 (d, J = 2.2 Hz, 1H), 7.36 (dd, J = 11.8, 4.5 Hz, 1H), 7.08 (m, 2H), 7.00 (d, J = 8.7 Hz, 1H), 6.93 (m, 1H), 6.10 (d, J = 2.0 Hz, 1H), 6.02 (d, J = 2.0 Hz, 1H), 5.17 (m, 1H), 4.50 (ddd, J = 18.2, 11.8, 5.1 Hz, 2H), 3.89 (s, 3H), 3.87 (s, 3H), 3.79 (s, 3H), 3.77 (s, 3H), 3.27 (dd, J = 15.1, 9.6 Hz, 1H), 2.96 (dd, J = 15.1, 6.7 Hz, 1H); ^{13}C NMR (126 MHz, $CDCl_3$) δ 166.2, 161.7, 161.3, 160.3, 159.2, 156.6, 138.8, 132.5, 131.1, 130.4, 129.1, 122.2, 122.0, 115.3, 112.9, 110.5, 104.9, 91.3, 88.4, 81.2, 66.4, 55.8, 55.6, 55.3, 29.4; IR (film) vmax 3006, 2941, 2839, 1714, 1623, 1606, 1504, 1454, 1442, 1299, 1249, 1215, 1205, 1178, 1141, 1049, 1037, 983, 810, 756 cm^{-1}; HRMS (ESI+) *m/z*: [M + Na]+ calcd for C26H26O7Na, 473.1576; found, 473.1579.
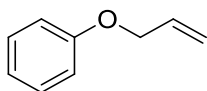
37

(allyloxy)benzene (37): A solution of phenol (0.925 g, 9.83 mmol) was dissolved in Acetone (20 mL and treated sequentially with potassium carbonate (4.08 grams, 29.5 mmol) and allyl bromide (2.6 mL 29.5 mmol). The solution was heated to reflux and allowed to react for 12

hours. This reaction was cooled to room temperature and quenched by the addition of H_2O, extracted with EtOAc (3 x 150 mL). The combined organic fractions were washed with saturated aqueous NaCl, dried (Na_2SO_4), filtered, and concentrated. The residue was purified via column chromatography (SiO_2 10% EtOAc:Hexanes) to afford **37** (0.7662g, 58%) as a colorless oil: ^{1}H NMR (400 MHz, $CDCl_3$) δ 7.31 (m, 2H), 6.97 (m, 3H), 6.09 (ddt, J = 17.2, 10.5, 5.3 Hz, 1H), 5.44 (dq, J = 17.3, 1.6 Hz, 1H), 5.31 (dq, J = 10.5, 1.3 Hz, 1H), 4.56 (dt, J = 5.3, 1.5 Hz, 2H); ^{13}C NMR (126 MHz, $CDCl_3$) δ 158.6, 133.3, 129.7, 129.4, 120.8, 117.7, 114.9, 114.5, 68.7; IR (film) vmax 3454(br), 2921, 1598, 1585, 1494, 1242, 1031, 991, 925, 881, 752 cm^{-1}; HRMS (ESI+) *m/z*: [M + H]+ calcd for C9H11O, 153.0810; found, 153.0813.
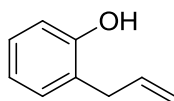
38

2-allylphenol (38): A solution of **37** (0.736 grams, 5.5 mmol) was dissolved in DCM (20 mL) and treated dropwise with 1.0M solution of dimethylaluminum chloride (6.0 mL, 6.0 mmol) and stirred until TLC revealed complete consumption of starting material. The reaction was quenched by the addition of 1.0 N HCl, extracted with EtOAc (3 x 150 mL). The combined organic fractions were washed with saturated aqueous NaCl, dried (Na_2SO_4), filtered, and concentrated. The residue was purified via column chromatography (SiO_2 30% EtOAc:Hexanes) to afford **38** (0.505g, 69%) as a colorless oil: ^{1}H NMR (400 MHz, $CDCl_3$) δ 7.08 (m, 2H), 6.85 (m, 2H), 5.95 (m, 1H), 5.01 (m, 2H), 3.25 (m, 2H); ^{13}C NMR (126 MHz, $CDCl_3$) δ 156.5, 136.3, 132.6, 127.2, 125.3, 121.0, 117.9, 115.9, 33.7; IR (film) vmax 3517(br), 3076, 2977, 1637, 1591, 1488, 1456, 1330, 1255, 1217, 1170, 916, 838, 752 cm^{-1}; HRMS (ESI+) *m/z*: [M + H]+ calcd for C9H11O, 153.0810; found, 153.0816.
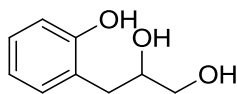
39

3-(2-hydroxy-4,6-dimethoxyphenyl)propane-1,2-diol (39): A solution of **38** (0.460 grams, 3.43 mmol) was dissolved in a (1.5 : 1.0) mixture of THF (14 mL) and H_2O (7 mL) respectively was treated with 4-methylmorpholine N-oxide (0.603 grams, 5.14 mmol) followed by dropwise addition of a 4% Osmium tetraoxide solution in H_2O (0.15 mL, 0.34 mmol). This was allowed to stir for 18 hours before it was diluted with H_2O and extracted with EtOAc (3 x 100 mL). The combined organic fractions were washed with saturated aqueous NaCl, dried (Na_2SO_4), filtered, and concentrated. The residue was purified via column chromatography (SiO_2 40% EtOAc:Hexanes) to afford **39** (0.469g, 81%) as a colorless oil: ^{1}H NMR (400 MHz, $CDCl_3$) δ 7.16 (m, 1H), 7.04 (dd, J = 7.5, 1.6 Hz, 1H), 6.88 (m, 2H), 4.03 (m, 1H), 3.69 (dd, J = 11.2, 3.2 Hz, 1H), 3.49 (m, 1H), 2.83 (m, 2H); ^{13}C NMR (126 MHz, $CDCl_3$) δ 155.4, 131.4, 128.6, 124.3, 120.5, 117.3, 65.8, 53.5, 34.9; IR (film) vmax 3341(br), 2937, 2746, 1608, 1593, 1488, 1466, 1245, 1180, 1107, 1026, 864, 754 cm^{-1}; HRMS (ESI+) *m/z*: [M + Na]+ calcd for C9H12O3Na, 191.0684; found, 191.0688.
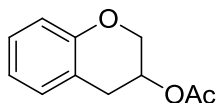
42

chroman-3-yl acetate (42): A solution of **39** (0.492 grams, 2.93 mmol) was dissolved in DCM (15 mL) and cooled to 0°C, treated with pyridine (1.1 mL, 13.2 mmol) and allowed to stir for 5

minutes. Finally *para*-toluenesulfonyl chloride (0.61 grams, 3.2 mmol) was added and allowed to warm to room temperature after 1 hour. This was allowed to react for 12 hours and quenched by the addition of H_2O and extracted with EtOAc (3 x 250 mL). The combined organic fractions were washed with saturated aqueous NaCl, dried (Na_2SO_4), filtered, and concentrated. The residue was purified via column chromatography (SiO_2 30% EtOAc:Hexanes) to afford crude phenolic sulfonic ester **40** (0.65g) as a yellow oil.

This oil was dissolved in MeOH (10 mL) and treated with potassium carbonate (0.449 grams, 3.23 mmol) and monitored by TLC. Once the TLC showed the consumption of starting material the solution was filtered and washed with EtOAc, dried (Na_2SO_4), filtered and concentrated. This produced an inseparable mixture of compounds **41a-b** (30% EtOAc:Hexanes), as a colorless oil (0.194g) .

The mixture of compounds (0.163 grams, 1.09 mmol) was dissolved in DCM (5 mL) and cooled to 0°C and was treated with diisopropylethyl amine (0.38 mL, 2.18 mmol) and stirred for 5 minutes then acetyl chloride (0.09 mL, 1.1 mmol) was added dropwise and allowed to warm to room temperature over 12 hours. The reaction was quenched by the addition of H_2O and extracted with EtOAc (3 x 25 mL). The combined organic fractions were washed with saturated aqueous NaCl, dried (Na_2SO_4), filtered, and concentrated. The residue was purified via column chromatography (SiO_2 10% EtOAc:Hexanes) to afford (0.093 g, 17%) over 3 steps as a colorless oil: ^{1}H NMR (400 MHz, CDCl$_3$) δ 7.19 (d, *J* = 7.3 Hz, 2H), 7.14 (t, *J* = 7.8 Hz, 1H), 6.88 (td, *J* = 7.4, 0.8 Hz, 2H), 6.83 (d, *J* = 8.0 Hz, 1H), 5.01 (dtd, *J* = 9.5, 7.3, 3.6 Hz, 1H), 4.36 (dd, *J* = 11.9, 3.6 Hz, 1H), 4.23 (dd, *J* = 11.9, 7.1 Hz, 1H), 3.33 (dd, *J* = 15.7, 9.5 Hz, 1H), 2.99 (dd, *J* = 15.7, 7.5 Hz, 1H), 2.12 (s, 3H); ^{13}C NMR (126 MHz, CDCl$_3$) δ 171.0, 159.2, 128.2, 127.3, 125.7, 121.0, 109.7, 80.0, 66.7, 32.0, 21.1; IR (film) vmax 3442(br), 2945, 1741, 1481,

1461, 1369, 1222, 1166, 1114, 1043, 914, 867, 752 cm^{-1}; HRMS (ESI+) *m/z*: [M + H]+ calcd for C11H13O3, 193.0865; found, 193.0867.
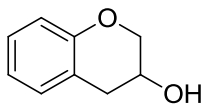
43

chroman-3-ol (43): A solution of **42** (0.0712 grams, 0.37 mmol) in a (9:1) mixture of MeOH : H$_2$O (1.8 mL : 0.2 mL) was treated with potassium carbonate (0.154 grams, 1.11 mmol) and allowed to react for 4 hours. The reaction was quenched by the addition of saturated aqueous ammonium chloride and extracted with EtOAc (3 x 50 mL). The combined organic fractions were washed with saturated aqueous NaCl, dried (Na$_2$SO$_4$), filtered, and concentrated. The residue was purified via column chromatography (SiO$_2$ 30% EtOAc:Hexanes) to afford **43** (0.441g, 79%) as a colorless oil: ^{1}H NMR (500 MHz, CDCl$_3$) δ 7.19 (dd, *J* = 7.3, 0.9 Hz, 1H), 7.14 (ddd, *J* = 8.0, 1.3, 0.7 Hz, 1H), 6.88 (td, *J* = 7.4, 0.9 Hz, 1H), 6.82 (m, 1H), 4.94 (dddd, *J* = 9.5, 7.4, 6.4, 3.2 Hz, 1H), 3.88 (ddd, *J* = 12.0, 6.9, 3.2 Hz, 1H), 3.77 (dt, *J* = 12.1, 6.1 Hz, 1H), 3.28 (dd, *J* = 15.6, 9.5 Hz, 1H), 3.04 (dd, *J* = 15.6, 7.4 Hz, 1H).; ^{13}C NMR (126 MHz, CDCl$_3$) δ 159.2, 128.1, 125.1, 120.7, 109.5, 83.0, 65.0, 31.2; IR (film) vmax 3379(br), 2925, 1596, 1481, 1461, 1325, 1230, 1097, 1047, 1014, 898, 864, 750 cm^{-1}; HRMS (ESI+) *m/z*: [M +]+ calcd for C9H10O2, 150.0681; found, 150.0686.
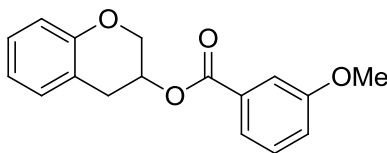
44a

chroman-3-yl 3-methoxybenzoate (44a): To a stirring solution of **43** (0.010 grams, 0.067 mmol) and 3-methoxybenzoic acid (0.021 grams, 0.134 mmol) in DCM (1 mL) was added N,N'-dicyclohexylcarbodiimide (0.029 grams, 0.134 mmol) and 4-(dimethylamino)pyridine (0.001 grams, 0.008 mmol) simultaneously. This was allowed to react for 12 hours and quenched by the addition of H_2O and extracted with DCM (3 x 25 mL). The combined organic fractions were washed with saturated aqueous NaCl, dried (Na_2SO_4), filtered, and concentrated. The residue was purified via column chromatography (SiO_2 10% EtOAc:Hexanes) to afford **44a** (0.0167g, 88%) as a colorless oil: ^{1}H NMR (400 MHz, $CDCl_3$) δ 7.96 (dd, J = 8.6, 2.2 Hz, 1H), 7.92 (d, J = 2.2 Hz, 1H), 7.36 (t, J = 8.1 Hz, 1H), 7.19 (d, J = 7.4 Hz, 1H), 7.12 (t, J = 7.7 Hz, 1H), 7.06 (m, 2H), 6.97 (d, J = 8.6 Hz, 1H), 6.92 (m, 1H), 6.84 (m, 2H), 5.14 (m, 1H), 4.55 (dd, J = 11.8, 3.8 Hz, 1H), 4.48 (dd, J = 11.8, 5.9 Hz, 1H), 3.88 (s, 3H), 3.86 (s, 3H), 3.41 (dd, J = 15.7, 9.6 Hz, 1H), 3.10 (dd, J = 15.7, 6.7 Hz, 1H); ^{13}C NMR (126 MHz, $CDCl_3$) δ 166.0, 161.0, 160.9, 131.1, 130.2, 129.6, 126.4, 122.3, 122.2, 120.4, 119.8, 118.6, 114.0, 80.2, 68.4, 55.8, 33.6; IR (film) vmax 2941, 1720, 1598, 1481, 1461, 1433, 1321, 1276, 1222, 1182, 1107, 1043, 985, 912, 873, 788, 752 cm^{-1}; HRMS (ESI+) *m/z*: [M + Na]+ calcd for C17H16O4Na, 307.0946; found, 307.0947.
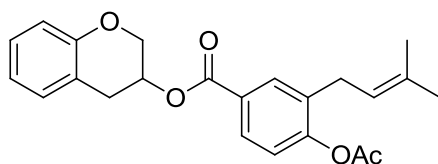
44b

5chroman-3-yl 4-acetoxy-3-(3-methylbut-2-en-1-yl)benzoate (44b): To a stirring solution of **43** (0.010 grams, 0.067 mmol) and 4-acetoxy-3-(3-methylbut-2-en-1-yl)benzoic acid(cite) (0.033 grams, 0.134 mmol) in DCM (1 mL) was added N,N'-dicyclohexylcarbodiimide (0.029 grams,

0.134 mmol) and 4-(dimethylamino)pyridine (0.001 grams, 0.007 mmol) simultaneously. This was allowed to react for 12 hours and quenched by the addition of H_2O and extracted with DCM (3 x 25 mL). The combined organic fractions were washed with saturated aqueous NaCl, dried (Na_2SO_4), filtered, and concentrated. The residue was purified via column chromatography (SiO_2 10% EtOAc:Hexanes) to afford **44b** (0.0176g, 69%) as a colorless oil: ^{1}H NMR (400 MHz, CDCl₃) δ 7.84 (d, J = 2.1 Hz, 1H), 7.80 (dd, J = 8.4, 2.2 Hz, 1H), 7.20 (d, J = 7.3 Hz, 1H), 7.15 (t, J = 7.3 Hz, 1H), 7.07 (d, J = 8.4 Hz, 1H), 6.87 (ddd, J = 16.9, 11.8, 4.4 Hz, 2H), 5.17 (m, 2H), 4.55 (dd, J = 11.8, 3.7 Hz, 1H), 4.49 (dd, J = 11.8, 5.8 Hz, 1H), 3.41 (dd, J = 15.7, 9.6 Hz, 1H), 3.25 (d, J = 7.1 Hz, 2H), 3.10 (dd, J = 15.7, 6.7 Hz, 1H), 2.33 (s, 3H), 1.75 (d, J = 1.0 Hz, 3H), 1.70 (s, 3H); ^{13}C NMR (126 MHz, CDCl₃) δ 169.9, 165.9, 161.9, 153.2, 135.1, 131.5, 130.1, 127.4, 127.1, 126.7, 123.2, 122.4, 121.3, 120.5, 119.8, 80.2, 68.5, 33.7, 28.1, 24.7, 20.3, 18.7; IR (film) vmax 3433(br), 2962, 2923, 1762, 1722, 1608, 1596, 1481, 1461, 1369, 1280, 1261, 1201, 1164, 1114, 1014, 912, 752 cm^{-1}; HRMS (ESI+) *m/z*: [M + Na]+ calcd for C23H24O5Na, 403.1521; found, 403.1514.
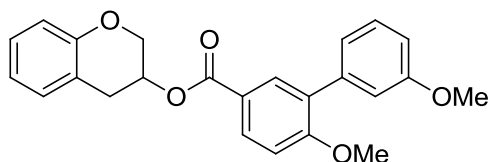
44c

chroman-3-yl 3',6-dimethoxy-[1,1'-biphenyl]-3-carboxylate (44c): To a stirring solution of **43** (0.010 grams, 0.067 mmol) and 3',6-dimethoxy-[1,1'-biphenyl]-3-carboxylic acid(cite) (0.035 grams, 0.134 mmol) in DCM (1 mL) was added N,N'-dicyclohexylcarbodiimide (0.030 grams,

0.134 mmol) and 4-(dimethylamino)pyridine (0.001 grams, 0.007 mmol) simultaneously. This was allowed to react for 12 hours and quenched by the addition of H_2O and extracted with DCM (3 x 25 mL). The combined organic fractions were washed with saturated aqueous NaCl, dried (Na_2SO_4), filtered, and concentrated. The residue was purified via column chromatography (SiO_2 30% EtOAc:Hexanes) to afford **33a** (0.0194g, 74%) as a colorless oil: ^{1}H NMR (500 MHz, CDCl$_3$) δ 7.94 (dd, J = 8.6, 2.3 Hz, 1H), 7.91 (d, J = 2.2 Hz, 1H), 7.34 (dd, J = 8.8, 7.5 Hz, 1H), 7.17 (d, J = 7.2 Hz, 1H), 7.11 (dd, J = 12.0, 4.4 Hz, 1H), 7.05 (m, 2H), 6.96 (d, J = 8.6 Hz, 1H), 6.91 (m, 1H), 6.82 (m, 2H), 5.12 (ddd, J = 13.2, 6.3, 3.3 Hz, 1H), 4.53 (dd, J = 11.8, 3.8 Hz, 1H), 4.47 (dd, J = 11.8, 6.0 Hz, 1H), 3.87 (s, 2H), 3.83 (s, 1H), 3.39 (dd, J = 15.7, 9.6 Hz, 1H), 3.09 (dd, J = 15.7, 6.7 Hz, 1H); ^{13}C NMR (126 MHz, CDCl$_3$) δ 166.2, 160.3, 159.3, 138.7, 132.5, 131.1, 130.4, 129.1, 128.2, 125.9, 124.8, 122.1, 120.6, 115.3, 112.8, 110.6, 109.5, 80.0, 66.5, 55.8, 55.3, 32.2; IR (film) νmax 3434(br), 2941, 1714, 1604, 1481, 1461, 1438 1311, 1239, 1205, 1178, 1137, 1116, 1035, 875, 752 cm^{-1}; HRMS (ESI+) *m/z*: [M + Na]+ calcd for C24H22O5Na, 413.1365; found, 413.1374.
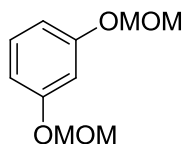
45

1,3-bis(methoxymethoxy)benzene (45): A suspension of sodium hydride (5.8 grams, 143.2 mmol) in DMF (30 mL) was made at 0°C and resorcinol (3.95 grams, 143.2 mmol) dissolved in DMF (10 mL) was added dropwise to the suspension. Finally, MOMCl (24.0 mL, 143.2 mmol) was added at 0°C and allowed to warm to room temperature overnight. The reaction was quenched by the addition of H_2O and extracted with EtOAc (3 x 150mL). The combined organic

fractions were washed with saturated aqueous NaCl, dried (Na$_2$SO$_4$), filtered, and concentrated. The residue was purified via column chromatography (SiO$_2$ 10% EtOAc:Hexanes) to afford **45** as a pale yellow oil (7.166g, 99%): ^{1}H NMR (500 MHz, CDCl$_3$) δ 7.19 (t, J = 8.2 Hz, 1H), 6.74 (t, J = 2.3 Hz, 1H), 6.71 (d, J = 2.3 Hz, 1H), 6.69 (d, J = 2.3 Hz, 1H), 5.16 (s, 4H), 3.48 (s, 6H); ^{13}C NMR (126 MHz, CDCl$_3$) δ 158.3, 130.0, 109.6, 105.0, 94.5, 56.0; IR (film) vmax 3310(br), 2943, 2895, 1647, 1592, 1471, 1443, 1399, 1319, 1257, 1150, 1112, 1084, 1042, 995, 773, 665 cm^{-1}; HRMS (ESI+) *m/z*: [M + H]+ calcd for C10H15O4, 199.0970; found, 199.0969.
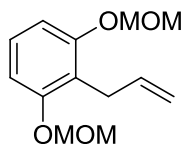
46

2-allyl-1,3-bis(methoxymethoxy)benzene (46): To a stirring solution of **45** (1.16 grams, 5.86 mmol) in THF (30mL) was cooled to 0°C and treated dropwise with a 2.5M solution of n-butyl lithium (2.8 mL, 7.0 mmol) and allowed to warm to room temperature over 30 min. Allyl bromide (0.53 mL, 5.9 mmol) was added to the stirring solution and allowed to react for 2 hrs and quenched by the addition of H$_2$O and extracted with EtOAc (3 x 100 mL). The combined organic fractions were washed with saturated aqueous NaCl, dried (Na$_2$SO$_4$), filtered, and concentrated. The residue was purified via column chromatography (SiO$_2$ 5% EtOAc:Hexanes) to afford **46** (0.729g, 52%) as yellow oil: ^{1}H NMR (500 MHz, CDCl$_3$) δ 7.13 (t, J = 8.3 Hz, 1H), 6.81 (s, 1H), 6.79 (s, 1H), 5.99 (ddt, J = 17.0, 10.0, 6.1 Hz, 1H), 5.21 (s, 4H), 4.99 (ddd, J = 13.6, 12.1, 2.0 Hz, 2H), 3.49 (s, 6H); ^{13}C NMR (126 MHz, CDCl$_3$) δ 155.8, 136.8, 127.2, 118.3, 114.2, 107.9, 94.4, 56.1, 27.7; IR (film) vmax 3440(br), 2954, 2900, 1637, 1595, 1469, 1440, 1402, 1321, 1255, 1153, 1114, 1081, 1041, 995, 921, 777, 663 cm^{-1}; HRMS (ESI+) *m/z*: [2M + Na]+ calcd for C26H36O8Na, 499.2308; found, 499.2330.
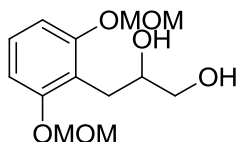
47

3-(2,6-bis(methoxymethoxy)phenyl)propane-1,2-diol (47): A solution of **46** (0.69 grams, 2.9 mmol) was dissolved in a (1.5 : 1.0) mixture of THF (10 mL) and H_2O (5 mL) respectively was treated with 4-methylmorpholine N-oxide (0.511 grams, 4.35 mmol) followed by dropwise addition of a 4% Osmium tetraoxide solution in H_2O (0.12 mL, 0.29 mmol). This was allowed to stir for 18 hours before it was diluted with H_2O and extracted with EtOAc (3 x 100 mL). The combined organic fractions were washed with saturated aqueous NaCl, dried (Na_2SO_4), filtered, and concentrated. The residue was purified via column chromatography (SiO_2 2% MeOH:DCM) to afford **47** (0.469g, 87%) as a yellow oil: ^{1}H NMR (400 MHz, $CDCl_3$) δ 7.15 (t, J = 8.4 Hz, 1H), 6.83 (s, 1H), 6.81 (s, 1H), 5.23 (s, 4H), 3.97 (td, J = 5.8, 3.9 Hz, 1H), 3.61 (ddd, J = 11.8, 8.3, 3.6 Hz, 1H), 3.52 (m, 7H), 2.99 (qd, J = 13.4, 6.6 Hz, 2H), 2.65 (d, J = 5.8 Hz, 1H), 2.41 (dd, J = 8.2, 5.1 Hz, 1H); ^{13}C NMR (126 MHz, $CDCl_3$) δ 156.2, 128.0, 115.8, 108.2 (2x), 94.7 (2x), 72.1, 66.0, 56.3, 27.3; IR (film) νmax 3436, 2933, 1595, 1467, 1255, 1182, 1153, 1105, 1078, 1051, 1022, 919, 779 cm^{-1}; HRMS (ESI+) *m/z*: [M + Na]+ calcd for C13H20O6Na, 295.1158; found, 295.1148.
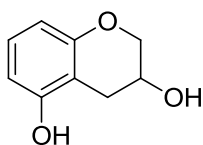
48

chroman-3,5-diol (48): A solution of **47** (4.82 grams, 17.7 mmol) was dissolved in DCM (90 mL) and cooled to 0°C, treated with pyridine (6.5 mL, 76.6 mmol) and allowed to stir for 5 minutes. Finally *para*-toluenesulfonyl chloride (3.78 grams, 19.5 mmol) was added and allowed to warm to room temperature after 1 hour. This was allowed to react for 12 hours and quenched by the addition of H_2O and extracted with EtOAc (3 x 250 mL). The combined organic fractions were washed with saturated aqueous NaCl, dried (Na_2SO_4), filtered, and concentrated. The residue was purified via column chromatography (SiO_2 40% EtOAc:Hexanes) to afford crude phenolic sulfonic ester **47a** (6.01g, 80%) as a yellow oil:

A solution of **47a** (6.01 grams, 14.1 mmol) was dissolved in MeOH (70 mL) and treated with an aqueous 6.0M solution of hydrochloric acid (17.5 mL) and allowed to react for 12 hours and quenched by pouring the reaction mixture in a saturated aqueous hydrogen bicarbonate solution and extracted with EtOAc (3 x 250 mL). The combined organic fractions were washed with saturated aqueous NaCl, dried (Na_2SO_4), filtered, and concentrated. The residue was purified via column chromatography (SiO_2 40% EtOAc:Hexanes) to afford **47b** (3.52g, 74%) as a pale yellow oil:

To a solution of **47b** (0.184 grams, 0.544 mmol) was dissolved in MeOH (4 mL) and treated with potassium carbonate (0.122 grams, 0.87 mmol) and monitored by TLC. Once the TLC showed the consumption of starting material the solution was filtered and washed with saturated aqueous NaCl, dried (Na_2SO_4), filtered and concentrated. This residue was purified via column chromatography (SiO_2, 30% EtOAc:Hexanes), as a colorless oil (0.194g) EtOAc (3 x 250 mL). The combined organic fractions were washed with saturated aqueous NaCl, dried (Na_2SO_4), filtered, and concentrated. The residue was purified via column chromatography (SiO_2 40% EtOAc:Hexanes) to afford **48** (0.075g, 83%) as a pale yellow oil: ^{1}H NMR (500 MHz,

Acetone) δ 8.24 (s, 1H), 6.83 (t, $J = 8.1$ Hz, 1H), 6.35 (dd, $J = 8.0$, 1.0 Hz, 1H), 6.24 (dd, $J = 8.2$,

0.8 Hz, 1H), 4.15 (d, $J = 4.7$ Hz, 1H), 4.08 (ddd, $J = 6.6$, 3.8, 1.5 Hz, 1H), 4.04 (ddd, $J = 10.4$,

2.9, 1.7 Hz, 1H), 3.75 (ddd, $J = 10.4$, 7.1, 1.1 Hz, 1H), 2.92 (ddd, $J = 16.6$, 5.4, 1.5 Hz, 1H), 2.52

(dd, $J = 16.7$, 6.7 Hz, 1H); ^{13}C NMR (126 MHz, Acetone) δ 157.0, 156.3, 127.6, 109.1, 108.4,

107.4, 70.4, 63.2; IR (film) vmax 3338, 2931, 1620, 1595, 1492, 1454, 1381, 1342, 1278, 1147,

1097, 1012, 961, 827, 733, 698 cm^{-1}; HRMS (ESI+) *m/z*: [M + Na]+ calcd for C9H10O3Na,

189.0528; found, 189.0532.
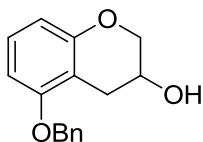
49

5-(benzyloxy)chroman-3-ol (49). To a solution of **48** (0.0154 grams, 0.093 mmol) was

dissolved in CH$_3$CN (2 mL) and treated sequentially with benzyl bromide (0.011 mL, 0.095

mmol) and potassium carbonate (0.013 grams, 0.095 mmol) and allowed to react for 12 hrs. The

reaction was quenched by the addition of H$_2$O and extracted with EtOAc (3 x 25 mL). The

combined organic fractions were washed with saturated aqueous NaCl, dried (Na$_2$SO$_4$), filtered,

and concentrated. The residue was purified via column chromatography (SiO$_2$ 30%

EtOAc:Hexanes) to afford **49** (0.016 g, 66%) as a colorless oil: ^{1}H NMR (400 MHz, CDCl$_3$) δ

7.35 (m, 5H), 6.98 (t, $J = 8.0$, 2.3 Hz, 1H), 6.37-6.34 (d, $J = 8.1$, 2H), 5.04 (s, 2H), 4.82 (m, 1H),

3.77 (m, 1H), 3.68 (m, 1H), 3.17 (m, 1H), 2.90 (m, 1H), 1.91 (s, 1H); ^{13}C NMR (126 MHz,

CDCl$_3$) δ 161.3, 157.4, 137.1, 129.5, 128.7 (2x), 127.8, 125.8 (2x), 114.1, 109.5, 103.0, 83.7,

70.0, 65.1, 29.2; IR (film) vmax 3353(br), 2923, 2871, 1593, 1496, 1471, 1452, 1379, 1340,

1265, 1238, 1174, 1108, 1056, 972, 767, 737, 696 cm^{-1}; HRMS (ESI+) *m/z*: [M + Na]+ calcd for

C16H16O3Na, 279.0997; found, 279.0987.
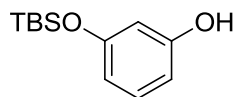
50

3-((tert-butyldimethylsilyl)oxy)phenol (50): A solution of resorcinol (0.526 grams, 4.78 mmol)

was dissolved in DMF (8 mL) and treated sequentially with imidazole (0.491 grams, 7.2 mmol)

and *tert*-butyl(chloro)dimethylsilane (0.71 grams, 4.78 mmol) and allowed to react for 12 hours.

The reaction was quenched by the addition of H$_2$O and extracted with EtOAc (3 x 50 mL). The

combined organic fractions were washed with H$_2$O (3 x 50 mL), saturated aqueous NaCl, dried

(Na$_2$SO$_4$), filtered and concentrated. The residue was purified via column chromatography (SiO$_2$

10% EtOAc:Hexanes) to afford **50** (0.469 g, 44%) as a pale yellow oil: ^{1}H NMR (500 MHz,

CDCl$_3$) δ 7.07 (t, *J* = 8.1 Hz, 1H), 6.43 (dd, *J* = 8.1, 2.3 Hz, 2H), 6.35 (t, *J* = 2.3 Hz, 1H), 4.71 (s,

1H), 0.98 (s, 9H), 0.20 (s, 6H); ^{13}C NMR (126 MHz, CDCl$_3$) δ 157.1, 156.6, 130.1, 112.9, 108.5,

107.7, 25.8 (3x), 18.3, 4.3 (2x); IR (film) vmax 3429(br), 2956, 2858, 1604, 1593, 1492, 1471,

1361, 1294, 1257, 1170, 1145, 981, 948, 783 cm^{-1}; HRMS (ESI+) *m/z*: [M + Na]+ calcd for

C12H20O2SiNa, 247.1130; found, 247.1134.
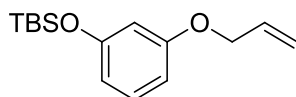
51

(3-(allyloxy)phenoxy)(tert-butyl)dimethylsilane (51): A solution of **50** (0.43 grams, 1.9

mmol) was dissolved in acetone (10 mL) was treated with potassium carbonate (0.80 grams, 5.7

mmol) and allyl bromide (0.5 mL, 5.7 mmol), then the solution was heated to reflux for 12 hours. This reaction was cooled to room temperature and quenched by the addition of H_2O, extracted with EtOAc (3 x 75 mL). The combined organic fractions were washed with saturated aqueous NaCl, dried (Na_2SO_4), filtered, and concentrated. The residue was purified via column chromatography (SiO_2 5% EtOAc:Hexanes) to afford **51** (0.462g, 92%) as a pale yellow oil: ^1H NMR (500 MHz, $CDCl_3$) δ 7.11 (t, J = 8.1 Hz, 1H), 6.53 (m, 1H), 6.44 (m, 1H), 6.34 (d, J = 2.3 Hz, 1H), 6.05 (m, 1H), 5.41 (ddd, J = 17.3, 2.6, 1.6 Hz, 1H), 5.28 (m, 1H), 4.51 (ddt, J = 8.6, 5.3, 1.5 Hz, 2H), 0.98 (s, 9H), 0.20 (s, 6H); ^{13}C NMR (126 MHz, $CDCl_3$) δ 159.8, 156.7, 133.3, 129.6, 120.8, 117.7, 112.8, 107.0, 68.8, 25.7 (3x), 18.2, 4.4 (2x); IR (film) vmax 2947, 2891, 1611, 1589, 1514, 1460, 1425, 1359, 1297, 1253, 1172, 1112, 997, 835, 784cm^{-1}; HRMS (ESI+) *m/z*: [M + Na]+ calcd for C15H24O2SiNa, 287.1443; found, 287.1435.
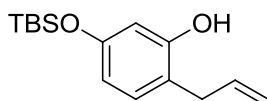
52

2-allyl-5-((tert-butyldimethylsilyl)oxy)phenol (52): A solution of **51** (0.45 grams, 1.7 mmol) was dissolved in DCM (10 mL) and treated dropwise with 1.0M solution of dimethylaluminum chloride (1.9 mL, 1.9 mmol) and stirred until TLC revealed complete consumption of starting material. The reaction was quenched by the addition of 1.0 N HCl, extracted with EtOAc (3 x 50 mL). The combined organic fractions were washed with saturated aqueous NaCl, dried (Na_2SO_4), filtered, and concentrated. The residue was purified via column chromatography (SiO_2 5% EtOAc:Hexanes) to afford **52** (0.1604g, 36%) as a colorless oil: ^1H NMR (500 MHz, $CDCl_3$) δ 6.92 (d, J = 8.1 Hz, 1H), 6.38 (dd, J = 8.1, 2.4 Hz, 1H), 6.35 (d, J = 2.4 Hz, 1H), 6.00 (ddd, J =

15.8, 12.0, 7.9 Hz, 1H), 5.16 (m, 1H), 5.13 (t, J = 1.6 Hz, 1H), 4.90 (s, 1H), 3.34 (m, 2H), 0.97 (s, 9H), 0.19 (s, 6H); ^{13}C NMR (126 MHz, CDCl$_3$) δ 155.5, 154.8, 136.8, 130.7, 117.9, 116.3, 112.6, 108.0, 34.7, 25.7 (3x), 18.2, 4.4 (2x); IR (film) vmax 2957, 2929, 2894, 2858, 1614, 1591, 1514, 1469, 1463, 1425, 1361, 1294, 1255, 1230, 1170, 1112, 997, 867, 833, 781 cm^{-1}; HRMS (ESI+) *m/z*: [M + Na]+ calcd for C15H24O2SiNa, 287.1443; found, 287.1449.
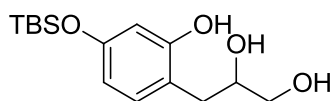
53

3-(4-((tert-butyldimethylsilyl)oxy)-2-hydroxyphenyl)propane-1,2-diol (53): A solution of **52** (0.132 grams, 0.50 mmol) was dissolved in a (1.5 : 1.0) mixture of THF and H$_2$O (1.65 mL : 0.75 mL) respectively was treated with 4-methylmorpholine *N*-oxide (0.090 grams, 0.75 mmol) followed by dropwise addition of a 4% Osmium tetraoxide solution in H$_2$O (0.05 mL, 0.01 mmol). This was allowed to stir for 18 hours before it was diluted with H$_2$O and extracted with EtOAc (3 x 50 mL). The combined organic fractions were washed with saturated aqueous NaCl, dried (Na$_2$SO$_4$), filtered, and concentrated. The residue was purified via column chromatography (SiO$_2$ 40% EtOAc:Hexanes) to afford **55** (0.1167g, 78%) as a pale yellow oil: ^{1}H NMR (500 MHz, CDCl$_3$) δ 6.84 (d, J = 8.2 Hz, 1H), 6.42 (d, J = 2.5 Hz, 1H), 6.34 (dd, J = 8.1, 2.4 Hz, 1H), 4.00 (m, 1H), 3.68 (dd, J = 11.1, 3.3 Hz, 1H), 3.47 (dd, J = 11.1, 7.7 Hz, 1H), 2.79 (dd, J = 14.8, 3.8 Hz, 1H), 2.72 (dd, J = 14.8, 7.0 Hz, 1H), 0.97 (s, 9H), 0.18 (s, 6H); ^{13}C NMR (126 MHz, CDCl$_3$) δ 156.0, 155.9, 131.6, 117.2, 112.3, 109.0, 73.6, 65.7, 34.4, 25.7 (3x), 18.2, 4.4 (2x); IR (film) vmax 3315(br), 2954, 2929, 2851, 1618, 1579, 1508, 1471, 1425, 1361, 1296, 1255, 1170,

1110, 1024, 979, 939, 873, 838, 783 cm^{-1}; HRMS (ESI+) *m/z*: [M + Na]+ calcd for C15H26O4SiNa, 321.1498; found, 321.1500.
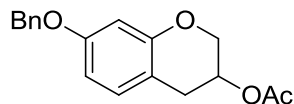
56

7-(benzyloxy)chroman-3-yl acetate (56): A solution of **53** (1.773 grams, 5.95 mmol) was dissolved in DCM (25 mL) and cooled to 0°C, treated with pyridine (2.2 mL, 26.8 mmol) and allowed to stir for 5 minutes. Finally *para*-toluenesulfonyl chloride (1.246 grams, 6.5 mmol) was added and allowed to warm to room temperature after 1 hour. This was allowed to react for 12 hours and quenched by the addition of H$_2$O and extracted with EtOAc (3 x 100 mL). The combined organic fractions were washed with saturated aqueous NaCl, dried (Na$_2$SO$_4$), filtered, and concentrated. The residue was purified via column chromatography (SiO$_2$ 20% EtOAc:Hexanes) to afford crude phenolic sulfonic ester **53a** (2.06g) as a yellow oil.

This oil (2.12 grams, 4.69 mmol) was dissolved in MeOH (20 mL) and treated with potassium carbonate (1.04 grams, 7.5 mmol) and monitored by TLC. Once the TLC showed the consumption of starting material the solution was filtered and washed with EtOAc, dried (Na$_2$SO$_4$), filtered and concentrated. This produced an inseparable mixture of compounds **54a-b** (40% EtOAc:Hexanes), as a colorless oil (0.2042g).

This oil (0.469 grams, 2.82 mmol) was dissolved in CH$_3$CN (12 mL) and treated sequentially with benzyl bromide (0.33 mL, 2.82 mmol) and potassium carbonate (0.389 grams,

0.2.82 mmol) and allowed to react for 12 hrs. The reaction was quenched by the addition of H_2O and extracted with EtOAc (3 x 50 mL). The combined organic fractions were washed with saturated aqueous NaCl, dried (Na_2SO_4), filtered, and concentrated. The residue was purified via column chromatography (SiO_2 30% EtOAc:Hexanes) to afford an inseperable mixture of compounds **55a-b** (0.21 g, 66%) as a colorless oil.

The mixture of compounds **55a-b** (0.21 grams, 0.82 mmol) was dissolved in DCM (5 mL) and cooled to 0°C and was treated with diisopropylethyl amine (0.29 mL, 1.64 mmol) and stirred for 5 minutes then acetyl chloride (0.06 mL, 0.82 mmol) was added dropwise and allowed to warm to room temperature over 12 hours. The reaction was quenched by the addition of H_2O and extracted with EtOAc (3 x 50 mL). The combined organic fractions were washed with saturated aqueous NaCl, dried (Na_2SO_4), filtered, and concentrated. The residue was purified via column chromatography (SiO_2 10% EtOAc:Hexanes) to afford **56** (0.1012 g, 41%) as a colorless oil: ^{1}H NMR (500 MHz, CDCl$_3$) δ 7.38 (m, 5H), 7.06 (m, 1H), 6.51 (dd, J = 7.4, 1.8 Hz, 2H), 5.03 (m, 3H), 4.35 (dd, J = 11.9, 3.5 Hz, 1H), 4.22 (dd, J = 11.9, 7.2 Hz, 1H), 3.26 (dd, J = 15.3, 9.4 Hz, 1H), 2.92 (ddd, J = 15.3, 7.4, 0.7 Hz, 1H), 2.13 (s, 3H). ^{13}C NMR (126 MHz, CDCl$_3$) δ 170.9, 160.4, 159.6, 137.0, 128.6 (2x), 127.9, 127.5 (2x), 124.9, 117.9, 107.3, 97.4, 81.0, 70.3, 66.0, 31.4, 20.9; IR (film) vmax 2933, 2358, 2341, 1735, 1622, 1585, 1506, 1454, 1373, 1238, 1163, 1132, 1116, 1024, 966, 738, 696 cm^{-1}; HRMS (ESI+) *m/z*: [M + Na]+ calcd for C18H18O4Na, 321.1103; found, 321.1108.
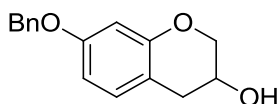
57

7-(benzyloxy)chroman-3-ol (57): A solution of **56** (0.094 grams, 0.315 mmol in a (9:1) mixture of MeOH : H_2O (1.8 mL : 0.2 mL) was treated with potassium carbonate (0.133 grams, 0.945 mmol) and allowed to react for 4 hours. The reaction was quenched by the addition of saturated aqueous ammonium chloride and extracted with EtOAc (3 x 50 mL). The combined organic fractions were washed with saturated aqueous NaCl, dried (Na_2SO_4), filtered, and concentrated. The residue was purified via column chromatography (SiO_2 40% EtOAc:Hexanes) to afford **60** (0.0691g, 86%) as a colorless oil: ^1H NMR (400 MHz, $CDCl_3$) δ 7.39 (m, 6H), 7.05 (d, $J = 8.0$ Hz, 1H), 6.51 (d, $J = 2.2$ Hz, 1H), 6.48 (dd, $J = 3.9, 2.2$ Hz, 1H), 5.04 (s, 2H), 4.95 (m, 1H), 3.85 (m, 1H), 3.75 (dt, $J = 12.0, 6.0$ Hz, 1H), 3.20 (dd, $J = 15.2, 9.4$ Hz, 1H), 2.95 (dd, $J = 15.1, 7.3$ Hz, 1H), 1.90 (t, $J = 6.4$ Hz, 1H); ^{13}C NMR (126 MHz, $CDCl_3$) δ 160.6, 159.6, 137.0, 129.4 (2x), 128.9, 127.9 (2x), 111.2, 107.2, 97.2, 70.3, 70.0, 66.9, 55.4, 29.7; IR (film) vmax 3512, 3438, 3359, 2923, 1622, 1595, 1494, 1452, 1380, 1344, 1278, 1186, 1147, 1095, 1010, 962, 948, 825, 736, 696 cm^{-1}; HRMS (ESI+) *m/z*: [M + Na]+ calcd for C16H16O3Na, 279.0997; found, 279.0982.

Anti-proliferation Assay

MCF-7 and SKBr3 cells were maintained in a 1:1 mixture of Advanved DMEM/F12 (Gibco) supplemented with non-essential amino acids, L-glutamine (2 mM), streptomycin (500 μg/mL), penicillin (100 units/mL), and 10% FBS. Cells were grown to confluence in a humidified atmosphere (37°C, 5% CO_2), seeded (2000/well, 100 μL) in 96-well plates, and allowed to attach overnight. Each compound or GDA at varying concentrations in DMSO (1% DMSO final concentration) was added, and cells were returned to the incubator for 72 hours. At 72 hours, the number of viable cells was determined using an MTS/PMS cell proliferation kit (Promega) per the manufacturer's instructions. Cells incubated in 1% DMSO were used as 100%

proliferation, and values were adjusted accordingly. IC$_{50}$ values were calculated from separate experiments performed in triplicate using GraphPad Prism.

Western Blot Analysis

MCF-7 cells were cultured as described above and treated with various concentrations of drug, GDA in DMSO (1% DMSO final concentration), or vehicle (DMSO) for 24 h. Cells were harvested in cold PBS and lysed in RIPA lysis buffer containing 1 mM PMSF, 2 mM sodium orthovanadate, and protease inhibitors on ice for 1 h. Lysates were clarified at 14000g for 10 min at 4° C. Protein concentrations were determined using the Pierce BCA protein assay kit per the manufacturer's instructions. Equal amounts of protein (20 μg) were electrophoresed under reducing conditions, transferred to a nitrocellulose membrane, and immunoblotted with the corresponding specific antibodies. Membranes were incubated with an appropriate horseradish peroxidase-labeled secondary antibody, developed with a chemiluminescent substrate, and visualized.

References:

(1)   Chaudhury, S.; Welch, T. R.; Blagg, B. S. J. *ChemMedChem* **2006**, *1*, 1331.

(2)   Bishop, S. C.; Burlison, J. A.; Blagg, B. S. J. *Curr. Cancer Drug Targ.* **2007**, *7*, 369.

(3)   Powers, M. V.; Workman, P. *FEBS Lett.* **2007**, *581*, 3758.

(4)   Hanahan, D.; Weinberg, R. A. *Cell* **2000**, *100*, 57.

(5)   Zhang, H.; Burrows, F. *J. Mol. Med.* **2004**, *82*, 488.

(6)   Ali, M. M.; Roe, S. M.; Vaughan, C. K.; Meyer, P.; Piper, P. W.; Prodromou, C.; Pearl, L. H. *Nature* **2006**, *440*, 1013.

(7)   Donnelly, A.; Blagg, B. S. J. *Curr. Med. Chem.* **2008**, *15*, 2702.

(8)   Peterson, L. B.; Blagg, B. S. J. *Future Med. Chem.* **2009**, *1*, 267.

(9)   Csermely, P.; Schnaider, T.; Soti, C.; Prohaszka, Z.; Nardai, G. *Pharmacol. Ther.* **1998**, *79*, 129.

(10)   Pearl, L. H.; Prodromou, C. *Annu. Rev. Biochem* **2006**, *75*, 271.

(11)   Young, J. C.; Obermann, W. M. J.; Hartl, F. U. *J. Biol. Chem.* **1998**, *273*, 18007.

(12)   Chen, S.; Sullivan, W. P.; Toft, D. O.; Smith, D. F. *Cell Stress Chaperones* **1998**, *3*, 118.

(13)   Prodromou, C.; Roe, S. M.; O'Brien, R.; Ladbury, J. E.; Piper, P. W.; Pearl, L. H. *Cell* **1997**, *90*, 65.

(14)   Dutta, R.; Inouye, M. *Trends Biochem. Sci.* **2000**, *25*, 24.

(15)   Huai, Q.; Wang, H.; Liu, Y.; Kim, H.; Toft, D. O.; Ke, H. *Structure* **2005**, *13*, 579.

(16)   Meyer, P.; Prodromou, C.; Hu, B.; Vaughan, C. K.; Roe, S. M.; Panaretou, B.; Piper, P. W.; Pearl, L. H. *Molecular Cell* **2003**, *11*, 647.

(17)   Soti, C.; Nagy, E.; Giricz, Z.; Vigh, L.; Csermely, P.; Ferdinandy, P. *Br. J. Pharmacol.* **2005**, *146*, 769.

(18)   Csermely, P. *Trends Biochem. Sci.* **1997**, *22*, 147.

(19)   Lindquist, S. L.; Craig, E. A. *Annu. Rev. Genet.* **1988**, *22*, 631.

(20)   Hohfeld, J.; Jentsch, S. *EMBO J.* **1997**, *16*, 6209.

(21) Sondermann, H.; Scheufler, C.; Schneider, C.; Hohfeld, J.; Hartl, F. U.; Moarefi, I. *Science* **2001**, *291*, 1553.

(22) Murphy, P. J. M.; Kanelakis, K. C.; Galigniana, M. D.; Morishima, Y.; Pratt, W. B. *J. Biol. Chem.* **2001**, *276*, 30092.

(23) Forsythe, H. L.; Jarvis, J. L.; Turner, J. W.; Elmore, L. W.; Holt, S. E. *J. Biol. Chem.* **2001**, *276*, 15571.

(24) Kosano, H.; Stensgard, B.; Charlesworth, M. C.; McMahon, N.; Toft, D. O. *J. Biol. Chem.* **1998**, *273*, 32973.

(25) Prodromou, C.; Panaretou, B.; Chohan, S.; Siligardi, G.; O'Brien, R.; Ladbury, J. E.; Roe, S. M.; Piper, P. W.; Pearl, L. H. *EMBO J.* **2000**, *19*, 4383.

(26) Connell, P.; Ballinger, C. A.; Jiang, J.; Wu, Y.; Thompson, L. J.; Hohfeld, J.; Patterson, C. *Nat. Cell Biol.* **2001**, *3*, 93.

(27) Ballinger, C. A.; Connell, P.; Wu, Y.; Hu, Z.; Thompson, L. J.; Yin, L.; Patterson, C. *Mol. Cell. Biol.* **1999**, *19*, 4535.

(28) Workman, P. *Cancer Lett.* **2004**, *206*, 149.

(29) Taldone, T.; Gozman, A.; Maharaj, R.; Chiosis, G. *Curr. Opin. Pharmacol.* **2008**, *8*, 370.

(30) Muchowski, P. J. *Neuron* **2002**, *35*, 9.

(31) Muchowski, P. J.; Wacker, J. L. *Nat. Rev. Neurosci.* **2005**, *6*, 11.

(32) Adams, J.; Elliott, P. J. *Oncogene* **2000**, *19*, 6687.

(33) Chiosis, G.; Huezo, H.; Rosen, N.; Mimnaugh, E.; Whitesell, L.; Neckers, L. *Mol. Cancer Ther.* **2003**, 123.

(34) Solit, D. B.; Zheng, F. F.; Drobnjak, M.; Munster, P. N.; Higgins, B.; Verbel, D.; Heller, G.; Tong, W.; Cardon-Cordo, C.; Agus, D. B.; Scher, H. I.; Rosen, N. *Clin. Cancer Res.* **2002**, *8*, 986.

(35) Agnew, E. B.; Wilson, R. H.; Morrison, G.; Neckers, L.; Takimoto, C. H.; Grem, J. L. *Proc. Am. Assoc. Cancer Res.* **2002**, *43*, 1349.

(36) Xu, W.; Neckers, L. *Clin. Cancer Res.* **2007**, *13*, 1625.

(37) Jolly, C.; Morimoto, R. I. *J. Natl. Cancer Inst.* **2000**, *92*, 1564.

(38) de Duve, C.; de Barsy, T.; Poole, B.; Trouet, A.; Tulkens, P.; Van Hoff, F. *Biochem. Pharmacol.* **1974**, *23*, 2495.

(39)   Altan, N.; Chen, Y.; Schindler, M.; Simon, S. M. *J. Exp. Med.* **1998**, *187*, 1583.

(40)   Kokkonen, N.; Rivinoja, A.; Kauppila, A.; Suokas, M.; Kellokumpu, I.; Kellokumpu, S. *J. Biol. Chem.* **2004**, *279*, 39982.

(41)   Warrick, J. M.; Chan, H. Y. E.; Gray-Board, G. L.; Chai, Y.; Paulson, H. L.; Bonini, N. M. *Nat. Genet.* **1999**, *23*, 425.

(42)   Yan, Y.; Wang, C. *Curr. Alzheimer Res.* **2008**, *5*, 548.

(43)   Alonso, A. C.; Zaidi, T.; Novak, M.; Grundle-Iqbal, I.; Iqbal, K. *Pro. Natl. Acad. Sci. USA* **2001**, *98*, 6923.

(44)   Neckers, L. *J. Biosci.* **2007**, *32*, 517.

(45)   Zou, J.; Guo, Y.; Guettouche, T.; Smith, D. F.; Voellmy, R. *Cell* **1998**, *94*, 471.

(46)   Shamovsky, I.; Nudler, E. *Cell. Mol. Life Sci.* **2008**, *65*, 855.

(47)   Dickey, C. A.; Eriksen, J.; Kamal, A.; Burrows, F.; Kasibhatla, S.; Eckman, C. B.; Hutton, M.; Petrucelli, L. *Curr. Alzheimer Res.* **2005**, *2*, 231.

(48)   Dou, F.; Netzer, W. J.; Tanemura, K.; Li, F.; Hartl, F. U.; Takashima, A.; Gouras, G. K.; Greengard, P.; Xu, H. *Pro. Natl. Acad. Sci. USA* **2003**, *100*, 721.

(49)   Dickey, C. A.; Kamal, A.; Lundgren, K.; Klosak, N.; Bailey, R. M.; Dunmore, J.; Ash, P.; Shoraka, S.; Zlatkovic, J.; Eckman, C. B.; Patterson, C.; Dickson, D. W.; Nahman, N. S.; Hutton, M.; Burrows, F.; Petrucelli, L. *J. Clin. Invest.* **2007**, *117*, 648.

(50)   Ansar, S.; Burlison, J. A.; Hadden, K. M.; Yu, X. M.; Desino, K. E.; Bean, J.; Neckers, L.; Audus, K. L.; Michaelis, M. L.; Blagg, B. S. J. *Bioorg. Med. Chem. Lett.* **2007**, *17*, 1984.

(51)   Agrawal, M.; Garg, R. J.; Cortes, J.; Quintas-Cardama, A. *Curr. Hematol. Malig. Rep.* **2010**, *5*, 70.

(52)   Sausville, E. A.; Tomaszewski, J. E.; Ivy, P. *Curr. Cancer Drug Targ.* **2003**, *3*, 377.

(53)   Driggers, E. M.; Hale, S. P.; Lee, J.; Terrett, N. K. *Nat. Rev. Drug Disc.* **2008**, *7*, 608.

(54)   DeBoer, C.; Meulman, P. A.; Wnuk, R. J.; Peterson, D. H. *J. Antibiot.* **1970**, *23*, 442.

(55)   Omura, S.; Iwai, Y.; Takahashi, Y.; Sadakane, N.; Nakagawa, A.; Otwa, H.; Hasegawa, Y.; Ikai, T. *J. Antibiot.* **1979**, *32*, 255.

(56)   Andrus, M. B.; Meredith, E. L.; Simmons, B. L.; Sekhar, B. B. V. S.; Hicken, E. J. *Org. Lett.* **2002**, *4*, 3549.

(57)   Hadden, K. M.; Lubbers, D. J.; Blagg, B. S. J. *Curr. Top. Med. Chem* **2006**, *6*, 1173.

(58)   Jove, R.; Hanafusa, H. *Ann. Rev. Cell Biol.* **1987**, *3*, 31.

(59)   Whitesell, L.; Shifrin, S. D.; Schwab, G.; Neckers, L. *Cancer Res.* **1992**, *52*, 1721.

(60)   Whitesell, L.; Mimnaugh, E.; De Costa, B.; Myers, C. E.; Neckers, L. *Proc. Natl. Acad. Sci. USA* **1994**, *91*, 8324.

(61)   Stebbins, C. E.; Russo, A. A.; Schneider, C.; Rosen, N.; Hartl, F. U.; Pavletich, N. P. *Cell* **1997**, *89*, 239.

(62)   Schnur, R. C.; Corman, M. L. *J. Org. Chem.* **1994**, *59*, 2581.

(63)   Dikalov, S.; Landmesser, U.; Harrison, D. G. *J. Biol. Chem.* **2002**, *277*, 25480.

(64)   Supko, J. G.; Hickman, R. L.; Grever, M. R.; Malspeis, L. *Cancer Chemother. Pharmacol.* **1995**, *36*, 305.

(65)   Roe, S. M.; Prodromou, C.; O'Brien, R.; Ladbury, J. E.; Piper, P. W.; Pearl, L. H. *J. Med. Chem.* **1999**, *42*, 260.

(66)   Dikalov, S.; Rumyantseva, G. V.; Piskunov, A. V.; Weiner, L. M. *Biochemistry* **1992**, *31*, 8947.

(67)   Tian, Z.; Liu, Y.; Zhang, D.; Wang, Z.; Dong, S. D.; Carreras, C. W.; Zhou, Y.; Rastelli, G.; Santi, D. V.; Myles, D. C. *Bioorg. Med. Chem.* **2004**, *12*, 5317.

(68)   Delmotte, P.; Delmotte-Plaque, J. *Nature* **1953**, *171*, 344.

(69)   Schulte, T. W.; Akinaga, S.; Soga, S.; Sullivan, W. P.; Stensgard, B.; Toft, D. O.; Neckers, L. *Cell Stress Chaperones* **1998**, *3*, 100.

(70)   Sharma, S. V.; Agatsuma, T.; Nakano, H. *Oncogene* **1998**, *16*, 1639.

(71)   Geng, X.; Yang, Z.; Danishefsky, S. J. *Synlett* **2004**, *8*, 1325.

(72)   Prodromou, C.; Nuttall, J. M.; Millson, S. H.; Roe, S. M.; Sim, T.; Tan, D.; Workman, P.; Pearl, L. H.; Piper, P. W. *ACS Chem. Biol.* **2009**, *4*, 289.

(73)   Soga, S.; Neckers, L.; Schulte, T. W.; Shiotsu, Y.; Akasaka, K.; Narumi, H.; Agatsuma, T.; Ikuina, Y.; Murakata, C.; Tamaoki, T.; Akinaga, S. *Cancer Res.* **1999**, *59*, 2931.

(74)   Agatsuma, T.; Ogawa, H.; Akasaka, K.; Asai, A.; Yamashita, Y.; Mizukami, T.; Akinaga, S.; Saitoh, Y. *Bioorg. Med. Chem.* **2002**, *10*, 3445.

(75)   Ikuina, Y.; Amishiro, N.; Miyata, M.; Narumi, H.; Ogawa, H.; Akiyama, T.; Shiotsu, Y.; Akinaga, S.; Murakata, C. *J. Med. Chem.* **2003**, *46*, 2534.

(76)   Yamamoto, K.; Garbaccio, R. M.; Stachel, S. J.; Solit, D. B.; Chiosis, G.; Rosen, N.; Danishefsky, S. J. *Angew. Chem. Int. Ed.* **2003**, *42*, 1280.

(77)   Allan, R. K.; Mok, D.; Ward, B. K.; Ratajczak, T. *J. Biol. Chem.* **2006**, *281*, 7161.

(78)   Reece, R. J.; Maxwell, A. *Crit. Rev. Biochem. Mol. Biol.* **1991**, *26*, 335.

(79)   Laurin, P.; Ferroud, D.; Schio, L.; Klich, M.; Dupuis-Hamelin, C.; Mauvais, P.; Lassaigne, P.; Bonnefoy, A.; Musicki, B. *Bioorg. Med. Chem. Lett.* **1999**, *9*, 2875.

(80)   Ali, J. A.; Jackson, A. P.; Howells, A. J.; Maxwell, A. *Biochemistry* **1993**, *32*, 2717.

(81)   Marcu, M. G.; Schulte, T. W.; Neckers, L. *J. Natl.Cancer Inst.* **2000**, *92*, 242.

(82)   Marcu, M. G.; Chadli, A.; I., B.; Catelli, M.; Neckers, L. *J. Biol. Chem.* **2000**, *275*, 37181.

(83)   Yu, X. M.; Shen, G.; Neckers, L.; Blake, H.; Holzbeierlein, J.; Cronk, B.; Blagg, B. S. J. *J. Am. Chem. Soc.* **2005**, *127*, 12778.

(84)   Burlison, J. A.; Neckers, L.; Smith, A. B.; Maxwell, A.; Blagg, B. S. J. *J. Am. Chem. Soc.* **2006**, *128*, 15529.

(85)   Burlison, J. A.; Avila, C.; Vielhauer, G.; Lubbers, D. J.; Holzbeierlein, J.; Blagg, B. S. J. *J. Org. Chem.* **2008**, *73*, 2130.

(86)   Palermo, C. M.; Hernando, J. I. M.; Dertinger, S. D.; Kende, A. S.; Gasiewicz, T. A. *Chem. Res. Toxicol.* **2003**, *16*, 865.

(87)   Yang, C. S.; Miliakal, P.; Meng, X. *Ann. Rev. Pharmacol. Toxicol.* **2002**, *42*, 25.

(88)   Schmidt, J. V.; Bradfield, C. A. *Annu. Rev. Cell Dev. Biol.* **1996**, *12*, 55.

(89)   Whitlock, J. P. *Chem. Res. Toxicol.* **1993**, *6*, 754.

(90)   Palermo, C. M.; Westlake, C. A.; Gasiewicz, T. A. *Biochemistry* **2005**, *44*, 5041.

(91)   Ding, T.; Wang, X.; Cao, X. *Chin. J. Chem.* **2006**, *24*, 1618.

(92)   Li, L.; Chan, T. H. *Org. Lett.* **2001**, *3*, 739.

(93)   Wan, S. B.; Landis-Piwowar, K. R.; Kuhn, D. J.; Chen, D.; Dou, Q. P.; Chan, T. H. *Bioorg. Med. Chem.* **2005**, *13*, 2177.

(94)   Massey, A. J. *J. Med. Chem.* **2010**, *53*, 7280.

(95)   Taldone, T.; Zatorska, D.; Patel, P. D.; Zong, H.; Rodina, A.; Ahn, J. H.; Moulick, K.; Guzman, M. L.; Chiosis, G. *Bioorg. Med. Chem.* **2011**, *19*, 2603.

(96)   Day, J. E.; Sharp, S. Y.; Rowlands, M. G.; Aheme, W.; Lewis, W.; Roe, S. M.; Prodromou, C.; Pearl, L. H.; Workman, P.; Moody, C. J. *Chemistry* **2010**, *16*, 10366.

(97)   Sekiguchi, H.; Muranaka, K.; Osada, A.; Ichikawa, S.; Matsuda, A. *Bioorg. Med. Chem.* **2010**, *18*, 5732.

(98)   Obermann, W. M. J.; Sondermann, H.; Russo, A. A.; Pavletich, N. P.; Hartl, F. U. *J. Cell Bio.* **1998**, *143*, 901.

(99)   Hadden, K. M.; Blagg, B. S. J. *J. Org. Chem.* **2009**, *74*, 4697.

(100)   Hills, I. D.; Holloway, M. K.; Leon, P.; Nomland, A.; Zhu, H.; Graham, S. L.; Stachel, S. J. *Bioorg. Med. Chem. Lett.* **2009**, *19*, 4993.

(101)   Clevenger, R. C.; Blagg, B. S. J. *Org. Lett.* **2004**, *6*, 4459.

(102)   Sreedhar, A. S.; Kalmar, E.; Csermely, P.; Shen, Y.-F. *FEBS Lett.* **2004**, *562*, 11.

(103)   Sreedhar, A. S.; Csermely, P. *Pharmacol. Ther.* **2004**, *101*, 227.

(104)   Kamal, A.; Thao, L.; Sensintaffar, J.; Zhang, L.; Boehm, M. F.; Fritz, L. C.; Burrows, F. *Nature* **2003**, *425*, 407.

(105)   Neckers, L. *Curr. Med. Chem.* **2003**, *10*, 733.

(106)   Immormino, R. M.; Metzger, L. E.; Reardon, P. N.; Dollins, D. E.; Blagg, B. S. J.; Gewirth, D. T. *J. Mol. Biol.* **2009**, *388*, 1033.

(107)   Dollins, D. E.; Warren, J. J.; Immormino, R. M.; Gewirth, D. T. *Molecular Cell* **2007**, *28*, 41.

(108)   Soldano, K. L.; Jivan, A.; Nicchitta, C. V.; Gewirth, D. T. *J. Biol. Chem.* **2003**, *279*, 48330.

(109)   Ty, N.; Kaffy, J.; Arrault, A.; Thoret, S.; Pontikis, R.; Dubois, J.; Morin-Allory, L.; Florent, J. *Bioorg. Med. Chem. Lett.* **2009**, *19*, 1318.

(110)   Upadhayaya, R. S.; Shinde, P. D.; Sayyed, A. Y.; Kadam, S. A.; Bawane, A. N.; Poddar, A.; Plashkevyvh, O.; Foldesi, A.; Chattopadhyaya, J. *Org. Biomol. Chem.* **2010**, *8*, 5661.

(111)   Duerfeldt, A. S.; Brandt, G. E. L.; Blagg, B. S. J. *Org. Lett.* **2009**, *11*, 2353.

(112)   Lu, J.; Ma, J.; Xie, X.; Chen, B.; She, X.; Pan, X. *Tetrahedron: Asymmetry* **2006**, *17*, 1066.

(113)   Tatsuta, K.; Furuyama, A.; Yano, T.; Suzuki, Y.; Ogura, T.; Hosokawa, S. *Tetrahedron Letters* **2008**, *49*, 4036.

(114)   Still, W. C.; Gennari, C. *Tetrahedron Letters* **1983**, *24*, 4405.

(115)   Charette, A. B.; Prescott, S.; Brochu, C. *J. Org. Chem.* **1995**, *60*, 1081.

(116)   Charette, A. B.; Juteau, H. *J. Am. Chem. Soc.* **1994**, *116*, 2651.

(117)   Gunanathan, C.; Ben-David, Y.; Milstein, D. *Science* **2007**, *317*, 790.

(118)   Zhang, J.; Leitus, G.; Ben-David, Y.; Milstein, D. *J. Am. Chem. Soc.* **2005**, *127*, 10840.

(119)   Hoemann, M. Z.; Agrios, K. A.; Aube, J. *Tetrahedron* **1997**, *53*, 11087.

(120)   El-Faham, A.; Funosas, R. S.; Prohens, R.; Albericio, F. *Chem. Eur. J.* **2009**, *15*, 9404.

(121)   Rech, J. C.; Floreancig, P. E. *Org. Lett.* **2005**, *7*, 5175.

(122)   Kazi, A.; Wang, Z.; Kumar, N.; Falsetti, S. C.; Chan, T.; Dou, Q. P. *Anticancer Res.* **2004**, *24*, 943.

(123)   Furuta, T.; Hirooka, Y.; Abe, A.; Sugata, Y.; Ueda, M.; Murakami, K.; Suzuki, T.; Tanaka, K.; Kan, T. *Bioorg. Med. Chem. Lett.* **2007**, *17*, 3095.

(124)   Dodo, K.; Minato, T.; Noguchi-Yachide, T.; Suganuma, M.; Hashimoto, Y. *Bioorg. Med. Chem.* **2008**, *16*, 7975.

(125)   Anderson, J. C.; Headley, C.; Stapleton, P. D.; Taylor, P. W. *Bioorg. Med. Chem. Lett.* **2005**, *15*, 2633.

(126)   Larsen, C. A.; Dashwood, R. H.; Bisson, W. H. *Pharmacol. Res* **2010**, *62*, 457.

(127)   Matts, R. L.; Dixit, A.; Peterson, L. B.; Sun, L.; Voruganti, S.; Kalyanaraman, P.; Hartson, S. D.; Blagg, B. S. J. *ACS Chem. Biol.* **2011**, *Submitted*.

(128)   Perdew, G. *J. Biol. Chem.* **1988**, *263*, 13802.

(129)   Rowlands, J. C.; Gustafsson, J.-A. *Crit. Rev. Toxicol.* **1997**, *27*, 109.

130)   Coumailleau, P.; Poellinger, L.; Gustafsson, J.-A.; Whitelaw, M. L. *J. Biol. Chem.* **1995**, *270*, 25291.

(131)   Whitelaw, M. L.; Gustafsson, J.-A.; Poellinger, L. *Mol. Cell. Biol.* **1994**, *14*, 8343.

(132)   Yin, Z.; Henry, E. C.; Gasiewicz, T. A. *Biochemistry* **2009**, *48*, 336.

(133)   Jia, Y.; Alayash, A. I. *Free Radic. Biol. Med.* **2008**, *45*, 659.

(134)   Cao, D.; Zhang, Y.; Zhang, H.; Zhong, L.; Qian, X. *Rapid Commun. Mass Spectrom.* **2009**, *23*, 1147.

(135)   Arakawa, H.; Maeda, M.; Okubo, S.; Shimamura, T. *27* **2004**, 277.

(136)   Mazzulli, J. R.; Armakola, M.; Dumoulin, M.; Parastatidis, I.; Ischiropoulos, H. *J. Biol. Chem.* **2007**, *282*, 31621.

(137)   Jackson, S. K.; Kerr, M. A. *J. Org. Chem.* **2007**, *72*, 1405.

(138)   Jew, S.; Kim, H.; Park, H. *Arch. Pharm. Res.* **1997**, *20*, 144.

(139)   Brimble, M. A.; Elliott, R. J. R. *Tetrahedron* **2002**, *58*, 183.

(140)   Ishihara, K.; Kurihara, H.; Yamamoto, H. *J. Org. Chem.* **1993**, *58*, 3791.

(141)   Solorio, D. M.; Jennings, M. P. *J. Org. Chem.* **2007**, *72*, 6621.

(142)   Tran, P.; Kim, S.-A.; Choi, H. S.; Yoon, J.-H.; Ahn, S.-G. *BMC Cancer* **2010**, *10*, 1.